# Mitogen-inducible-gene-6 is an endogenous inhibitor of HGF/Met-induced cell migration and neurite growth

**Dissertation**

**der Fakultät für Biologie der Ludwig-Maximilians-Universität München**

**Vorgelegt von**

**Guido Pantè**

**München 2005**

**Dissertation eingereicht am 22.03.2005**

**Tag der mündlichen Prüfung: 21.07.2005**

**Erstgutachter: PD Dr. Rüdiger Klein**

**Zweitgutachter: PD Dr. Mark Hübener**

Hiermit erkläre ich, dass ich die vorliegende Dissertation selbständig und ohne unerlaubte Hilfe angefertigt habe. Sämtliche Experimente sind von mir selbst durchgeführt, ausser wenn explizit auf Dritte verwiesen wird. Ich habe weder andersweitig versucht, eine Dissertation oder Teile einer Dissertation einzureichen bzw. einer Prüfungskommission vorzulegen, noch eine Doktorprüfung durchzuführen.

München, den 22.03.2005

1. Gutachter: Dr Rüdiger Klein
2. Gutachter: Dr Mark Hübener

*A Matteo*

The work presented in this thesis has been submitted the 2nd of February 2005 for publication in the Journal of Cell Biology.

**Mitogen-inducible-gene-6 is an endogenous inhibitor of HGF/Met-induced cell migration and neuronal differentiation**

Guido Pante, Jane Thompson, Fabienne Lamballe, Tomoko Iwata, Francis A. Barr, Alun M. Davies, Flavio Maina, Rüdiger Klein

# Table of contents

**TABLE OF CONTENTS ..... I**

**ABBREVIATION ..... V**

**SUMMARY ..... 1**

**INTRODUCTION ..... 2**

CELL COMMUNICATION AND SURFACE RECEPTOR PROTEINS ..... 2

*Receptor tyrosine kinases and signal transduction ..... 3*

*RTKs and their paradigm: do all the pathways lead to the same outcome? ..... 4*

*The two faces of RTKs: involvement in physiological and pathological processes ... 6*

NEGATIVE RECEPTOR SIGNALING ..... 8

*Irreversible inhibitory signals ..... 8*

Cbl ubiquitin ligase ..... 9

*Reversible negative signaling ..... 11*

Protein tyrosine phosphates ..... 11

RTK inhibition by protein tyrosine phosphatases ..... 12

RTK signaling inhibition by protein tyrosine posphatases ..... 14

*Negative signaling via adaptor proteins: ..... 15*

APS, SH2-B, Lnk ..... 15

SLAP (Src-Like-Adaptor-Protein) ..... 17

Grb2 ..... 18

*Negative signaling via Feedback loops ..... 20*

Limiting the duration of a signal ..... 22

Spatial control of the signal by negative feedback loop ..... 24

MET AND HGF ..... 26

Met signaling during development ..... 28

Met and HGF in pathological conditions ..... 30

Met-mediated branching morphogenesis ..... 30

Met-mediated cytoskeleton rearrangement: Rho GTP-binding proteins ..... 32

**RESULTS ..... 35**

MLP29, C2C12 and Trophoblast stem cells activate Map kinase, Akt and Gab1 upon HGF stimulation ..... 35

MLP29 proliferate and scatter upon HGF stimulation ..... 38

Microarray analysis of HGF-stimulated MLP29 cells ..... 38
Microarray data validation by northern blot analysis ..... 44
Met/HGF transcriptionally regulates the newly identified target genes in cells of different origin ..... 46
MIG6 is specifically up-regulated by HGF stimulation ..... 48
mig6 and met receptor tyrosine kinase transcripts are co-expressed *in-vivo* ..... 50
Mig6 overexpression inhibits HGF-dependent MLP29 cell migration ..... 53
Mig6 is a physiological suppressor of Met-mediated cell migration ..... 57
Endogenous Mig6 inhibits HGF-mediated cell migration independently of cell proliferation ..... 60
Overexpression of Mig6 suppresses HGF/Met-mediated cortical neuron migration ..... 62
Mig6 suppresses HGF/Met-mediated neuronal differentiation ..... 65
The CRIB-domain of MIG6 is required and sufficient to inhibit HGF-mediated cell migration ..... 69
Mig6 antagonizes Met signaling possibly by binding to a Rho family GTPase ..... 73

**DISCUSSION ..... 75**

Transcriptional profile of HGF-stimulated MLP29 ..... 75
Mig6 induction by external signals ..... 76
Mig6 modulates a variety of cellular responses ..... 77
Mig6 negatively regulates HGF-mediated neurite extensions and branching but not survival of sympathetic neurons ..... 79
Mig6 and Met are partially coexpressed in the somites and in the developing muscles ..... 80
Mig6 acts distally from Met via interaction with Rho family GTPases ..... 81

CONCLUDING REMARKS ..... 83

**MATERIALS AND METHODS ..... 85**

MATERIALS ..... 85
Plasmids ..... 85
Chemicals, enzymes and commercial kits ..... 86
Media and standard solutions ..... 86

Media and supplements for primary culture ..... 86
*Buffers and solutions* ..... *87*
Northern blot ..... 87
Microarray ..... 88
Genotyping PCR ..... 88
SiRNA ..... 88
*In-situ* hybridization ..... 88
Whole mount *in-situ* hybridization ..... 89
Embryo powder ..... 89
*Antibodies* ..... *90*
Primary antibodies ..... 90
Secondary antibodies ..... 91
METHODS ..... 91
*Molecular biology* ..... *91*
Cloning and generation of *in-situ* and northern blot probes ..... 92
Northern blot ..... 93
Microarray production and probe labeling ..... 94
Microarray hybridization ..... 95
Microarray analysis ..... 95
Tail DNA preparation and genotyping PCR ..... 96
*Yeast methods* ..... *97*
Strains, growth and media ..... 97
Yeast transformation (frozen cell method) ..... 98
*Biochemistry* ..... *99*
Western blotting ..... 99
Recombinant protein purification ..... 99
Pull down ..... 100
Immunization of the rabbit ..... 101
Antigen purification of the antibody ..... 101
*Cell cultures* ..... *102*
MLP29 and C2C12 cell lines ..... 102
Cortical neuron culture and electroporation ..... 102
SCGs cultures ..... 103

Trophoblast Stem (TS) cells culture ..... 104
Plasmid transfection and Boyden chamber assay ..... 104
SiRNA transfection and Boyden chamber assay ..... 105
BrdU assay ..... 106
Immunofluorescence ..... 106
*Mouse work* ..... *107*
*Histology* ..... *107*
Cryostat sections and *in-situ* hybridization ..... 107
Whole mount *in-situ* hybridization ..... 108
Cryosections of gelatin embedded whole mount *in-situ* hybridization ..... 109
Antibody staining on cryostat sections ..... 109
**ACKNOWLEDGEMENTS ..... 110**
**REFERENCES ..... 112**
***CURRICULUM VITAE* ..... 128**

# Abbreviation

| | |
|---|---|
| **Ack** | activated Cdc42 associated kinase |
| **Cdc42** | cell division cycle protein 42 |
| **CRIB** | Cdc42/Rho interacting binding |
| **CSFR1** | colony-stimulating factor receptor 1 |
| **DMSO** | dimethyl sulfoxide |
| **DSP** | dual-specific phosphatase |
| **EGF** | epidermal growth factor |
| **EGFR** | epidermal growth factor receptor |
| **Endo** | endophillin |
| **EPO** | erythropoietin |
| **EPOR** | erythropoietin receptor |
| **ERK1/2** | extracellular-signal related/regulated kinase 1/2 |
| **FGF2** | fibroblast growth factor 2 |
| **G3PDH** | glyceraldehyde-3-phosphate dehydrogenase |
| **GAB1** | Grb2-associated binder1 |
| **Grb2** | Grow factor receptor-bound protein 2 |
| **HGF/SF** | hepatocyte growth factor/scatter factor |
| **IGF-I** | insulin growth factor-like I |
| **INFR** | interferonγ receptor |
| **IP** | inositolphosphate |
| **JAK** | just another kinase, janus kinase |
| **Kek-1** | kekkon-1 |
| **KSR** | kinase suppressor of Ras |
| **Map kinase** | mitogen activated protein kinase |
| **MDCK cells** | madine-darby canine kidney cells |
| **Mig6** | mitogen inducible gene 6 |
| **MKP** | Map kinase phosphatase |
| **MNK** | Map kinase-interacting kinase |
| **MSP** | macrophage-stimulating protein |

| | |
|---|---|
| **NGF** | nerve growth factor |
| **P90RSK** | 90kDa ribosomal S6 kinase |
| **PAK** | p21-activated protein kinase |
| **PDGF** | platelet-derived growth factor |
| **PIs** | inositol phospholipids |
| **PI3 kinase** | phosphatidylinositide-3'-kinase |
| **PKA** | protein kinase A |
| **PKC** | protein kinase C |
| **PLCγ** | Phospholipase Cγ |
| **PP1** | protein tyrosine phosphatase 1 |
| **PP2A** | phospho-protein phosphatase 2A |
| **PTP** | protein tyrosine phosphatase |
| **PTEN** | phosphatase and tensin homologue deleted on chromosome 10 |
| **PTP1B** | protein tyrosine phsphatase 1B |
| **PYK2** | proline-rich tyrosine kinase 2 |
| **Ralt** | receptor-associated late transducer |
| **RTK** | receptor tyrosine kinase |
| **SCF** | stem cell factor |
| **SH2,3** | Src-homology domain 2,3 |
| **SHC** | SH2-containing collagen-related protein |
| **SHP1-2** | SH2-containing phosphatase 1-2 |
| **SLAP** | Src-like-adapter-protein |
| **SOCS** | suppressor of cytokine signaling |
| **Sos** | son of sevenless |
| **Spry** | sprouty |
| **Ssr2** | signal sequence receptor beta |
| **STAT3** | signal transducer and activator of transcription 3 |
| **TK** | tyrosine kinase |
| **TKB** | tyrosine kinase binding |
| **tPA** | tissue-type plasminogen activator |
| **TS cells** | trophoblast stem cells |

# Summary

Hepatocyte Growth Factor (HGF) is a pleiotropic factor acting on cells expressing the Met receptor tyrosine kinase. HGF/Met signaling has been described in detail and it is known to control cell migration, growth and differentiation in several embryonic organs and to be implicated in human cancer. Conversely, little is known about the transcriptional targets that lead to Met-mediated biological functions. Also, little is known about the physiological mechanisms that attenuate Met signaling.

This work provides the results of a screen for genes transcriptionally regulated by Met in several cell lines and addresses the functions of the highly inducible gene Mig6 (Mitogen-inducible-gene6, also called Gene 33 and RALT). By the use of Met loss of function mutant mice Met is shown to be the major inducer of mig6 in hepatocytes and lungs of E13.5 embryos. Mig6 is shown in turn to negatively regulate HGF/Met-induced cell migration. The effect is observed by Mig6 overexpression and reversed by Mig6 siRNA knock down experiments indicating that endogenous Mig6 is part of a mechanism that inhibits Met signaling. Mig6 functions in cells of hepatic origin and in neurons suggesting a role for Mig6 in different cell lineages. Mechanistically, Mig6 requires an intact Cdc42/Rho interactive binding (CRIB) domain to exert its inhibitory action suggesting that Mig6 acts at least in part distally from Met possibly by sequestering Rho-like GTPases. Because Mig6 is also induced by HGF stimulation, this work provides evidence that Mig6 is part of a negative feedback loop that attenuates Met functions in different contexts and cell types.

# Introduction

## Cell communication and surface receptor proteins

Multicellularity was a relatively late evolutionary innovation presumably because of the difficulties of developing the necessary intercellular communication mechanisms (Bruce Alberts, 2002). Cells must communicate in a complex way in order to control their behaviors for the benefit of the organism as a whole. Communication depends, in many cases, on extracellular signaling molecules which are produced by cells to signal to their neighbors or to other cells further away. It also depends upon systems of proteins within each cell that enable the signaling in a cell-specific manner. These proteins include cell surface receptor proteins and a variety of intracellular signaling proteins which propagate the signal inside of the cell's appropriate compartments. Depending on the organism, signaling molecules may include peptides, amino-acids, nucleotides, steroids, fatty acid derivates, or dissolved gas such as nitric oxide. Most of these signaling molecules are released into the extracellular space by exocytosis. Others freely diffuse from the cellular membrane to the extracellular space.

Regardless of the nature of the signaling molecules, the target cells respond through a specific receptor, which binds the signaling molecules and initiates a signaling cascade inside the cell, resulting in a specific alteration of the behavior of the target cell. In many cases the receptors are transmembrane proteins that upon binding of their specific ligands become activated and generate the signaling cascade responsible for a specific biological function.

Cell surface receptors can be divided into three main groups, each of which transduces the signal in different ways. Ion-channel linked receptors can transduce the signal by opening or closing the channel upon ligand binding, allowing passage of ions. The G-protein coupled receptor indirectly activates or inactivates membrane-bound enzymes or ion-channels via GTP-binding proteins (G-proteins). Enzyme linked surface receptors either act directly as enzymes or are coupled to an enzyme. Generally these

enzymes are protein kinases which phosphorylate specific target molecules that initiate the signal transduction cascade that drives the cell to a specific cellular response.

**Receptor tyrosine kinases and signal transduction**

The most abundant members of the enzyme-linked surface receptors with an intrinsic enzymatic activity are the Receptor Tyrosine Kinases (RTK). These receptors share a general characteristic structure: they are integral membrane proteins, spanning the cellular membrane once, with the N-terminal of the protein on the extra cellular side of the membrane, and the C-terminal part on the cytoplasmic side. The cytoplasmic part of these receptors also shares the enzymatic activity: they are tyrosine kinases. Many tyrosine kinases were first identified in the early 1980's as cellular counterparts of viral oncogenes, whose isolation was made possible by the transforming activity of their constitutively active products (Snyder and Bishop, 1984). During the following ten years together with the cloning and characterization of several RTKs, it was established that the pre-requisite for RTK activation and the consequent initiation of the signal transduction pathways was ligand-induced stabilization of receptor-dimers (Ullrich and Schlessinger, 1990). Dimer formation results in a conformational change of the tyrosine kinase domain, leading to a substantial increase of substrate (the receptor itself) concentration and to its phosphorylation (a process referred to as *auto-phosphorylation*) (Mohammadi et al., 1996a; Mohammadi et al., 1996b). The auto-phosphorylation event results in the initiation of the signaling cascade.

On the other hand as early as the 1990's it became clear that the receptors mediate the activation of the signal transduction via the phosphorylation of specific tyrosine residues outside of the kinase domain. Together with the discovery of the SH2 domain as a phospho-tyrosine binding modules it became clear that specific phospho-tyrosine residues act as high affinity-docking sites for SH2-containing cytoplasmic molecules relocating them to the plasma membrane (Koch et al., 1991). This recruitment, often followed by activation *via* tyrosine phosphorylation, brings the effectors in the optimal position in order to generate secondary messengers and to start the signal transduction cascade from membrane-anchored proteins. Many signaling molecules also contain other

protein-modules that allow them to interact specifically with other proteins as part of the signaling process. These modules include the SH3 domain which binds to proline-rich motifs allowing protein-protein interactions between intracellular proteins. The presence of SH2 together with SH3 domains in many signaling molecules is one of the mechanisms by which additional signaling partners can be indirectly recruited to the receptor, thus assembling multi-molecular complexes capable to initiate intricate signaling pathways. Since the identification of the SH2 domain, shortly followed by the SH3-domain discovery, searches for other conserved domains have yelded many additional contributors to the complex mechanisms of signal transduction. These networks of protein-protein interactions allow for rapid, spatially controlled and reversible activation of signaling pathways downstream of RTKs.

**RTKs and their paradigm: do all the pathways lead to the same outcome?**

As mentioned above many signal transduction mechanisms transmit information from the extra cellular space, or an intracellular compartment, to the nucleus, where they influence gene expression and thus biological response. There is a spectrum of RTK-activated intracellular signaling pathways, some driven by adaptor proteins and some driven by enzymes. Different RTKs mediate a broad spectrum of biological functions ranging from proliferation, cell motility, and differentiation, to protection from apoptosis. However, different RTKs despite their distinct biological effect nevetheless stimulate similar arrays of downstream pathways (Fig.1). Several studies *in vitro*, in flies and vertebrates have addressed the question of how different RTKs, even sharing similar activated signaling pathways, can drive a receptor-specific outcome (Tan and Kim, 1999) (Simon, 2000). *In vitro* studies of the tyrosine kinase receptor for Platelet-Derived Growth Factor (PDGF receptor) suggested that the pathways downstream of the receptor are in fact redundant in terms of what gene they can activate (Fambrough et al., 1999). In other words, individual effectors activated by the receptor are extensively cross-talking, resulting in the transcriptional activation of broadly overlapping sets of genes.

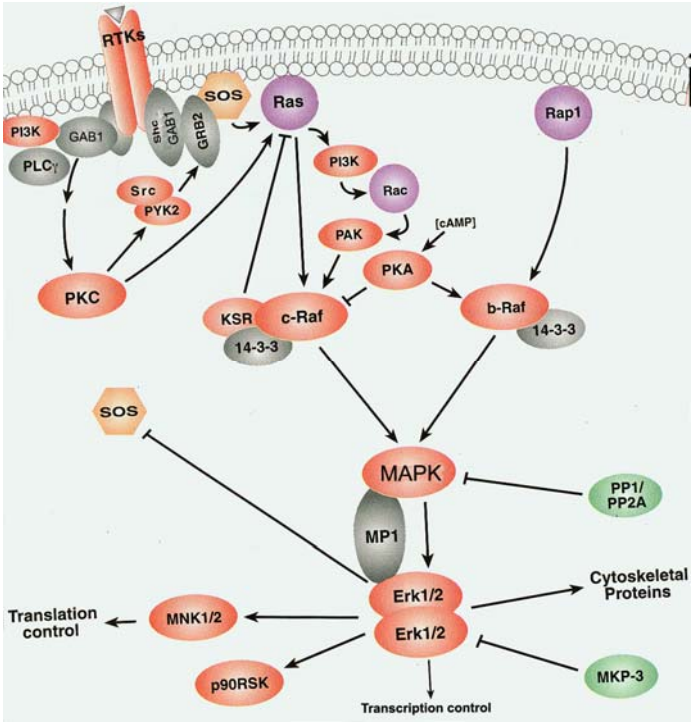


*(Technology, 2002)*

**Figure 1. RTKs use similar signal transduction cascades.**

*RTKs stimulate similar arrays of downstream signaling pathways via the recruitment of either adaptor proteins, such as Grb2, Shc and GAB1, or molecules with enzymatic activity such as PLCγ, Src and PI3 kinase. The activation of RTK-mediated signaling leads to translational and transcriptional regulation and/or cytoskeletal protein modification resulting in the control of a broad spectrum of biological functions.(modified from*

However, experiments performed in the whole animal, expressing signaling mutant forms of the RTK Met, suggested that the activation of specific, non redundant, effectors is required for receptor-mediated biological functions (Maina et al., 2001). These studies concluded that each individual receptor superimposes, above a generic threshold signaling level, different qualitative signals to achieve specific biological functions. The results from the *in-vitro* and *in-vivo* data are difficult to compare, due to the use of two different RTKs and systems. In the case of PDGF studies, Fambrough and co-workers assayed, in ligand saturating conditions, immediate-early gene expression by transcriptional profile. In contrast the studies on Met receptor used a classical *in-vivo* phenotypical analysis. Nonetheless the experiments performed on the whole organism suggest that signaling pathways are not completely redundant at the phenotypic level (Maina et al., 2001).

**The two faces of RTKs: involvement in physiological and pathological processes**

Another extensively studied aspect of RTK signaling is how, during development, a signal that in one context causes a cell to proliferate, in another can cause differentiation and in a third apoptosis. Obviously, for a cell's fate, not only the qualitative difference between various activated pathways is important, but it is also important for a cell to have precise developmental characteristics in order to properly respond to a signal. In general during development, the outcome of the signaling event is not only determined by the signal itself but also by the developmental state of the cell receiving it. This developmental state consists of the various cellular targets (such as transcription factors, cytoskeletal proteins, etc.) that are primed to respond to the signal. Whether they are primed depends on the cellular developmental history. Despite these differences in cellular competence during the development of an organism, signaling events nevertheless have to be precisely regulated in space, time and strength. A signal that is produced at the wrong time and place can lead to serious developmental defects. Signals must furthermore be robust enough to ensure that the cell receives them at a high enough level in order to respond. Finally, the signals must operate in cells and tissues of different origins and with different kinetic properties. Spatial and temporal precision, robustness and versatility of a signal represent stringent requirements for intracellular signals.

There is striking evidence from animal models that deregulated RTKs can drive pathological phenotypes. Experimentally, there are two classical approaches used in order to investigate whether receptor-mediated signaling is required or sufficient for a particular biological function: the first is the inactivation of the receptor/signaling (loss of function) and the second is its over-activation (gain of function). The loss of function approach has shown that RTKs are necessary to mediate a broad range of cellular responses ranging from proliferation, differentiation, and migration to protection from apoptosis. Conversely, gain of function experiments indicate that all the naturally occurring receptor-mediated events during development and adulthood, when de-regulated by uncontrolled receptor-mediated signaling, can give rise to pathological conditions.

In this thesis I will describe the work on the RTK Met and its specific ligand, Scatter Factor/Hepatocyte Growth Factor (SF/HGF), as a representative example of a large body of literature on a variety of RTKs.

The scatter factors receptors have been shown to be required to mediate important processes during embryonic development, but their signaling, when deregulated, can also give rise to serious pathological disorders. Scatter factor ligands include Hepatocyte Growth Factor (HGF), which acts trough Met receptor tyrosine kinase, and Macrophage-Stimulating Protein (MSP) which is the specific ligand for Ron receptor tyrosine kinase which shares extensive homologies with Met. Scatter factors are the main mediators of a complex process called invasive growth. This process combines cell proliferation with cell-cell dissociation and movement, extracellular matrix degradation and survival. Experiments carried out using loss of function mutants of either HGF or Met demonstrated that this ligand-receptor pair plays a key role during placenta and liver development (Uehara et al., 1995) (Maina et al., 1996) (Bladt et al., 1995) (Schmidt et al., 1995). Phenotypic analysis of the mutants furthermore revealed an essential role for HGF and Met during cell migration and polarization (Brand-Saberi et al., 1996). Not surprisingly, the events that are modulated by scatter factors in normal cells are the same as those that foster the aberrant tendency of malignant tumors to start invasive growth. Transgenic animals expressing mutant constitutively active Met receptor develop mammary hyperplasia and metastatic carcinomas (Jeffers et al., 1998; Liang et al., 1996). More strikingly, the simple overexpression of the wild-type form of Met receptor in hepatocytes results in hepatocellular carcinomas (Wang et al., 2001). Accordingly, mice overexpressing HGF are characterized by the appearance of a broad array of metastatic neoplasms (Takayama et al., 1997a; Takayama et al., 1997b) (Otsuka et al., 1998).

Variation in space and time, strength and duration, of a given receptor-mediated signal are clearly important parameters by which a cell is driven to either respond physiologically in controlling development, or aberrantly in driving disease-associated processes. In order to avoid errors, cells have developed mechanisms which ensure that appropriate parameters of a signal are received and maintained for the correct time. Thus the generation, tuning, and termination of a signal must be viewed as integrated processes that orchestrate in time and space the correct output of any given signal.

## Negative receptor signaling

As discussed above, even if some receptors convey inhibitory signals, many of them also mediate "positive" signals, either in a physiological or in an aberrant manner, involved in cell stimulation. In order to avoid errors in signaling, cells have developed mechanisms which counterbalance "positive" receptor-outputs to ensure that appropriate thresholds of receptor signaling is achieved and maintained for the correct length of time. These mechanisms are defined as "negative" signals.

In most cases a receptor induces simultaneously "positive" and "negative" signals that appear to be functionally connected. A delicate balance between positive and negative signaling appears to be critical for normal cell homeostasis, and its deregulation is often implicated in developmental abnormalities and human diseases.

### Irreversible inhibitory signals

Negative signaling results in the attenuation of signal transmission via a very complex chain of events occurring at various cellular levels, and can be categorized as reversible and irreversible.

Irreversible inhibition of signaling is most commonly mediated by activation-dependent protein degradation. Degradation of signaling proteins fulfill two different purposes: it terminates the signal by removing activated protein, and it generates a latency period in the cell before the next signaling events can be transmitted again. While many cytoplasmic signaling molecules are locally targeted for destruction in the proteasome, RTKs are also removed from the membrane's surface via endocytosis and degraded in the lysosomal compartment. Many of the steps required for degradation of signaling molecules depend on protein ubiquitination, an evolutionary conserved modification, where a small protein, ubiquitin, is covalently bound to specific lysine residues on the target protein by families of enzymes called ubiquitin ligases (Pickart, 2001). Proteins can be modified either by the addition of a single ubiquitin molecule (mono-ubiquitination) or by the addition of a chain of ubiquitins (poly-ubiquitination) and also by the addition of several single ubiquitin molecules (multi-ubiquitination). The

general consensus is that monoubiquitination is sufficient to drive internalization and endosomal sorting of the cell membrane receptor, whereas poly-ubiquitinied proteins are recognized by the proteasome which mediates protein unfolding and degradation (Hicke, 2001) (Weissman, 2001).

**Cbl ubiquitin ligase**

Several ubiquitine ligases have been implicated in tyrosine kinase receptor ubiquitination. However, the Cbl family plays the most relevant role in ligand-induced receptor tyrosine kinase ubiquitination and therefore down regulation (Thien and Langdon, 2001). Cbl is an ubiquitine ligase that can be divided into distinct domains. Each domain interacts with multiple signal transducers, giving the molecule a multiadaptor characteristic as well (Fig.2A). Cbl contains a tyrosine kinase binding domain that interacts with activated tyrosine kinases of the receptor and non-receptor type; a RING domain which is responsible for the ubiquitine ligase activity; and a proline rich region critical for SH3-containing protein interaction. Cbl also contains tyrosine residues, that upon phosphorylation, can bind with SH2-containing proteins. Several RTKs such as EGFR, ErbB2, and Met are ubiquitinated upon binding to Cbl (Thien and Langdon, 2001) (Joazeiro and Weissman, 2000). However, more recent studies suggested that Cbl action is not limited to RTK ubiquitination. Cbl appears to play an active role in ligand-induced RTK endocytosis, contributing to RTK down-regulation via both modes. This has been described in two studies in which Cbl was shown to regulate RTK endocytosis by binding to a multiprotein complex (Soubeyran et al., 2002) (Petrelli et al., 2002). One member of this complex, CIN85, has been proposed to act as a scaffolding protein. CIN85 is able to recruit signaling molecules into receptor-associated protein complexes critical for RTK trafficking (Dikic, 2002). Moreover, CIN85 was found to be constitutively associated with endophilins, a family of proteins that mediate the negative curvature of the plasma membrane, which is a critical step during endocytosis. The model proposed by these studies is that CIN85 *via* its SH3 domain is recruited to the receptor-associated Cbl.

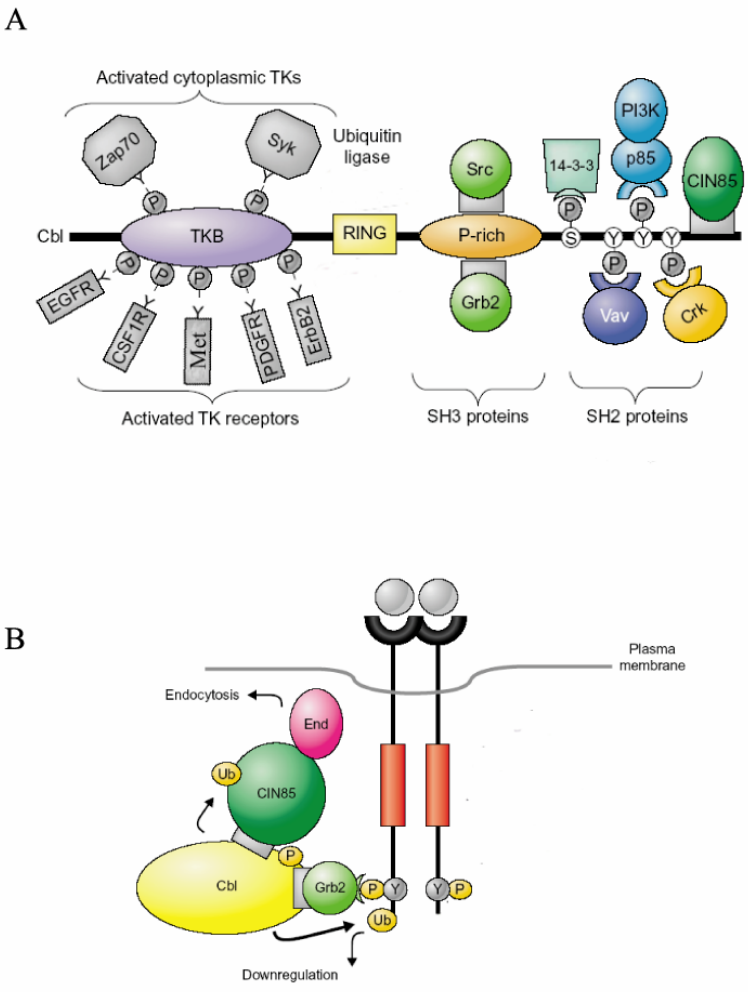


**Figure 2. Cbl, a ubiquitin ligase and a multiadapator protein.** *The Cbl protein can be divided into distinct domains and each of them interacts with multiple signal transducers (A). The amino-terminal portion contains the tyrosine Kinase Binding (TKB) domain that interacts with activated Ttyrosine Kinases (TKs) of the receptor and non-receptor type. The RING-finger domain is responsible for Cbl enzymatic activity. A polyproline-rich region (P-rich) is critical for interaction with SH3-containing proteins such as Grb2 or Src. The Cbl carboxyl terminus contains several tyrosine residues (Y) that, upon phosphorylation (P), interact with SH2-domain-containing proteins. It also contains a serine residue (S) that, when phosphorylated, binds to 14-3-3 protein. The binding site for the SH3 domains of CIN85 is found in the distal carboxyl terminus of Cbl. CSFR1, colony-stimulating factor receptor. Cbl promotes receptor endocytosis and down regulation of activated RTKs (B). Once that Cbl is directly or indirectly recruited to the active RTK, the CIN85–endophilin (End) complex binds to the receptor-associated Cbl via SH3 interaction. Cbl controls from one side the endocytic process by recruiting CIN85-endophilin complex in the proximity of the receptor and from the other side the ubiquitination of RTKs and receptor-associated proteins. P, phosphate; Ub, ubiquitin. (modified from (Dikic and Giordano, 2003)*

The binding stability between CIN85 and Cbl was found to be increased by ligand-induced Cbl phosphorylation. By these processes the receptor is then functionally associated with endocytosis-regulating molecules. Disrupting the Cbl-CIN85-endophilin complex, without affecting Cbl ubiquitin ligase activity, was sufficient to inhibit RTK endocytosis and degradation. Interestingly Cbl was found also to mediate EGF-induced ubiquitination of CIN85, which was important for EGF receptor degradation (Haglund et al., 2002). The binding of Cbl to activated RTKs thus control from one side the endocytic process by recruiting CIN85-endophilin complex in the proximity of the receptor and from the other side the ubiquitination of RTKs and receptor-associated proteins (Fig. 2B). The Cbl-mediated mechanisms are therefore more likely to dampen the signal transduction by removing the active receptor from the cell membrane rather than fine tuning the receptor-mediated signaling.

**Reversible negative signaling**

Transient inhibition tunes signal transduction by temporarily interfering with the strength and duration of the signal. Multiple mechanisms can contribute to reversible inhibition such as steric hindrance, compartmentalization of effectors, post-translational modification or inhibition of catalytic activity. Some of these mechanisms result in dampening of the entire RTK-mediated signal, directly affecting the receptors ability to transmit signals. Others appear to negatively regulate specific pathways downstream of RTKs, therefore resulting in the fine tuning of the final signaling output.

**Protein tyrosine phosphates**

Dephosphorylation of protein tyrosine kinases by protein phosphates is probably one of the most intensively studied mechanisms of RTK negative regulation. It is well recognized that Protein Tyrosine Phosphatases (PTPs) play a specific and active role in determining the levels of phospho-tyrosine within the cell and in the regulation of physiological processes (Mustelin, 2002) (Tonks and Neel, 1996) (Tonks, 1996). Recent

work has identified 107 genes that encode members of the protein tyrosine phosphatase family (Alonso et al., 2004). All PTPs have a conserved catalytic domain with phosphor-tyrosine-specific phosphohydrolase activity responsible for the selective removal of phosphate groups from tyrosine residues located in specific phosphorylated proteins. Based upon the amino acid sequences of their catalytic domains, the PTP can be classified into four separate families each of which present a range of substrate specificity.

Due to the complexity of the subject I will limit the description of PTPs to some of the better studied class I PTPs and their involvement in RTKs negative signaling. The class I, in fact, constitutes by far the largest family; it contains the 38 well-known and characterized PTPs and the "dual-specific" phosphatases which are the most divergent class of phosphatases in terms of substrate specificity. The "classical" PTPs can be further divided into transmembrane, Receptor-like Protein Tyrosine Phosphatases (RPTP) and non transmembrane protein tyrosine phosphatases. Even if the class I PTPs are the better studied and characterized member of the tyrosine phosphatase family, one common features among all the PTPs is the presence of combinations of modular domains (Alonso et al., 2004). Many of these domains are responsible of protein-protein interaction or phospholipids binding modules, although many of the domains' functions are still poorly characterized. The domains found in PTPs include modules that bind specific domains or motifs in other protein (phosphorylated or not), cellular membranes, the cytoskeleton, or specific phospholipids. It is interesting to note that the domains found in protein tyrosine kinases are substantially different from the ones found in PTPs. These differences in structure between protein tyrosine kinase and PTPs can reflect the need to regulate the two classes of enzymes in a temporally and spatially distinct and often reciprocal manner.

**RTK inhibition by protein tyrosine phosphatases**

Only two human non-receptor PTPs (SHP1 and SHP2) have SH2 domains organized in a tandem fashion, while no PTP contains SH3 domain. The presence of a SH2 domain in SHP1 and 2 suggested that these enzymes could be targets for recruitment by RTKs in order to switch-off signaling, presumably by dephosphorylation. Thus the

involvement of SHP1 and 2 in negative signaling was intensively studied. However, SHP2 phosphatase and its *Drosophila Melanogaster* homologue *Corkscrew* have been implicated in positive rather then negative signals by RTK (Perkins et al., 1992). On the other hand, a well characterized functional interplay between a PTP and RTK is elegantly demonstrated by the use of a naturally occurring SHP1 and Kit RTK loss of function mutant mice. Upon ligand stimulation SHP1 is recruited, via its SH2 domain, by Kit RTK (Yi and Ihle, 1993). Kit RTK is encoded by the *Dominant White Spotting (W)* locus in the mouse, while SHP1 by the *motheaten (me)* gene. Both mutants are characterized by haematologic defects, since SHP1 and Kit expression is mainly confined to haematopoietic tissues. Homozygosity for mutations in both *W* and *me* ameliorates aspects of both phenotypes, demonstrating that Kit RTK plays a role in the pathology of the *me* phenotype and, conversely, that SHP1 negatively regulates Kit signaling *in-vivo* (Paulson et al., 1996). Moreover, the negative signaling by SHP1 and its recruitment by the erythropoietin (EPO) receptor has been shown to be essential for the receptor physiological function. EPO receptor is devoid of intrinsic kinase activity but it can signal via phosphorylation by the non-receptor protein tyrosine kinase JAK2. The recruitment of SHP1 to the receptor appears to be essential in order for termination of EPO-mediated proliferation signals via dephosphorylation of JAK2 (Klingmuller et al., 1995). Similarly, PTPs have been shown to play a major role in removing phosphate groups on auto-phosphorylation sites of RTKs located either in the kinase activation loop, therefore inhibiting the kinase activity, or in receptors docking sites, therefore inactivating specific signal transduction pathways (Hunter, 1995). As for RTKs, the most convincing evidence of the roles played by PTPs is arising from studies where the loss of a specific PTP is analyzed. For example the function of PTP1B (non-receptor tyrosine phosphatase, class I) has been investigated by destructing the gene in mice (Elchebly et al., 1999) (Klaman et al., 2000). These studies provided evidence that PTP1B is essential to negatively regulate the Insulin RTK signaling. The phosphorylation level of the Insulin Receptor, upon ligand stimulation, was found to be prolonged in the liver of mice lacking PTP1B compared to wild type mice. Moreover, these mice were found to be more sensitive to Insulin treatment in respect to wild types as measured by glucose uptake assays. Interestingly, the effects of the absence of PTP1B were found to be tissue specific

since the glucose uptake was found to be affected in the muscles but not in the adipose tissue of the mutant mice.

Recent work provided images of spatial and temporal interaction between the non-receptor tyrosine phosphatase PTP1B and activated RTKs (Haj et al., 2002). This study illustrated how inactivation of RTKs can be spatially controlled by intracellular PTPs. Upon ligand activation, the RTKs are internalized to the endosomes, where they undergo limited dephosphorylation by PTP1B present in the endoplasmic reticulum. PTP1B therefore has been shown to specifically provide spatial limits on RTK activity.

Finally, PTPs not only play a critical role in negatively regulating ligand-activated kinases, but it has further been demonstrated, by exposing cells to PTP inhibitors, that they are critical in maintaining the ligand-independent RTKs activation at low levels (Jallal et al., 1992).

**RTK signaling inhibition by protein tyrosine posphatases**

As mentioned before, the "dual-specific" phosphatases (DSPs) of the Class I phosphatases are the most divergent group of phosphatases in terms of substrate specificity (Alonso et al., 2004). 11 of the 61 DSPs encoded by the human genome are specific for the mitogen-activated kinase (Map kinase) Erk, JNK and p38 kinase (Keyse, 1998) (Saxena and Mustelin, 2000). These are all critical signaling pathways activated by most RTKs. Map kinase phosphatases are all characterized by dual phosphothreonine and phosphor-tyrosine specificity and the presence of a Map kinase targeting motif (Alonso et al., 2003; Bordo and Bork, 2002). These enzymes contribute in regulating specific signals downstream of RTK-activated signaling pathways.

Finally, another well characterized sub-class of PTPs is represented by the phosphatase and tensin homologue (PTEN) genes. These enzymes specifically dephosphorylate inositol phospholipids (PIs). The PIs, membrane-associated phospholipids known to regulate many biological processes, play a crucial role in the RTKs-mediated signal transduction. Different PIs are localized in distinct plasma or endosomal membrane compartments and are involved in the regulation of membrane dynamics by their ability to interact with signaling molecules containing PI-binding

domains. The cellular levels of PIs vary as a consequence of stimuli-dependent phosphatidyl-inositol kinases and phosphatases whose enzymatic balance maintains a correct threshold of PIs-mediated signaling. PTEN is a ubiquitously expressed phosphatase specific for the 3' position of the inositol ring. It has a tumor suppressor activity, indicating its important role in growth inhibition pathways. Furthermore, PTEN loss of function mutant mice die embryonically, while high tumor frequency is observed in heterozygosis (Suzuki et al., 1998). These findings show PTEN to specifically down-regulate the RTK-mediated phosphatidyl-inositol kinases activation pathway.

Although the role of PTPs in the regulation of signal transduction is still under intense investigation, taken together the available data indicate that PTPs play an important role in regulating the level of tyrosine phosphorylation in the cell opposing their enzymatic activity to the protein tyrosine kinases one, thus controlling specific RTK-mediated biological functions through negative signaling.

**Negative signaling via adaptor proteins:**

**APS, SH2-B, Lnk**

Over the past years a number of adaptor proteins have been identified as part of the RTKs inhibitory machinery. These molecules contain several protein-protein interaction domains that are generally responsible for the recruitment of inhibitory molecules (such as Cbl) to the proximity of the receptor, therefore coupling the receptors with their own inhibitory pathways. APS, SH2B and Lnk form a conserved family of adaptor proteins, whose members share several conserved domains such as a proline-rich putative SH3 binding motif, a plextrine homology domain (PH domain), several potential tyrosine phosphorylation sites and a SH2 domain which suggest a role in kinase-mediated signaling. This role is supported by the evidence that these adaptors specifically bind to activated RTKs (Riedel et al., 1997) becoming substrate for receptor-mediated tyrosine phosphorylation (Ahmed et al., 1999; Kotani et al., 1998). Mice lacking Lnk show increased B-cell production due to over-proliferation of the B-cell precursors in response

to Stem Cell Factor (SCF), the specific ligand for Kit RTK (Takaki et al., 2003). Thus Lnk negatively modulates c-Kit RTK and plays a critical role in B-cell and haematopoietic development via a mechanism that is still not clear. In contrast, despite the significant structural homologies in the members of the family, SH2-B has been shown to be required *in-vivo* for proper development of the gonadal organs possibly by positively regulating the Insulin Growth Factor-like receptor (IGF-I) (Ohtsuka et al., 2002). The third member of the family, APS, has been shown to associate with and to be phosphorylated by several receptors including the Insulin Receptor and the receptor for Nerve Growth Factor (NGF), TrkA (Moodie et al., 1999) (Qian et al., 1998). Loss of function mutant mice for APS displayed an increased number of a B-cell subset resulting in over-production of a specific antibody. Even if the molecular mechanisms by which the members of the family work are poorly understood, several studies suggested that at least APS exerts its inhibitory function through the recruitment of Cbl in the proximity of the activated receptor, thus promoting ligand-dependent receptor ubiquitination (Ahmed et al., 2000) (Wakioka et al., 1999).

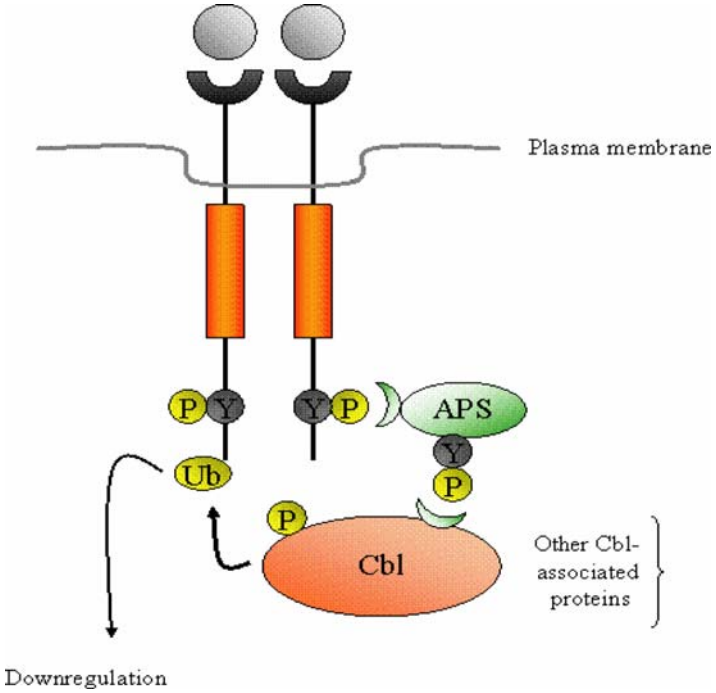


**Figure 3 Aps recruit Cbl to the activated insulin receptor.**
*Potential signaling complexes generated by APS after stimulation with Insulin. Aps recruits Cbl and Cbl-associated proteins to the active Insulin receptor. This results in the ligand-dependent ubiquitination and degradation of the receptor.P, phosphate. Ub, ubiquitin.*

**SLAP (Src-Like-Adaptor-Protein)**

SLAP provides another example of an adapter protein involved in negative regulation of specific RTKs. It has been named due to the high similarity of its SH2 domain to the one of Src family kinases. The Src-family kinases are non-receptor tyrosine kinases recruited and activated by a number of RTKs. Upon ligand stimulation several RTKs transmit via Src recruitment and activation, critical proliferative signals. SLAP contains an SH2 domain, an SH3 domain and a 100 amino acid unique C-terminal tail. By overexpression studies SLAP was found to inhibit PDGF-RTK-mediated proliferative signal, while depletion of the protein, via antibody microinjection, resulted in over-proliferation upon Platelet-Derived Growth Factor (PDGF) or serum stimulation (Roche et al., 1998). Since SLAP and Src share the same tyrosine docking site on PDGF receptor and co-localize in cells and since the SH2 domain of SLAP was found to be required for SLAP inhibition of PDGF-RTK-mediated proliferative signals, SLAP was thought to act via competing with Src for the binding to the activated receptor (Fig.4). However, investigating SLAP inhibition of PDGF-mediated proliferative response in an excess of Src kinase condition, this model appeared to be not completely correct (Manes et al., 2000). The picture that is emerging from this data is that SLAP is recruited to the activated receptor via its SH2 domain and competes partially with Src kinase for the association with the receptor. On the other hand SLAP SH3 domain is able to bind specific Src effectors, sequestering them from further interactions and signaling, and this may explain why in the presence of Src excess SLAP is still able to inhibit proliferation downstream PDFG receptor (Fig.4). Therefore this model proposes that SLAP acting via its SH2 domain competes with Src for the binding of activated receptor. It also acts via its SH3 domain, sequestering specific Src effectors and thus inhibiting specific signaling pathways activated by the receptor through Src recruitment.

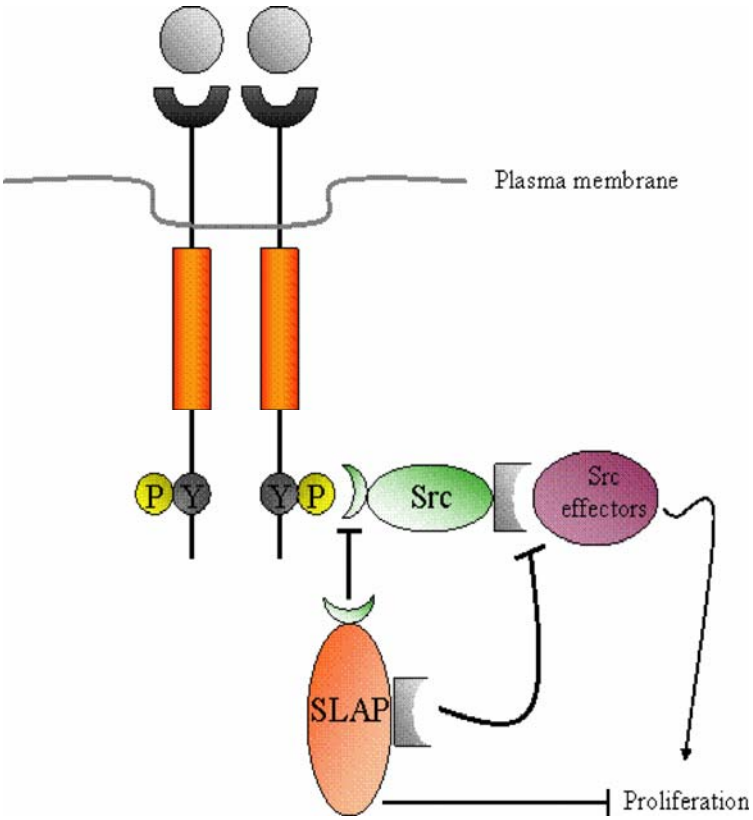


**Figure 4. SLAP inhibits PDGF-mediated proliferative signals.**

*SLAP is recruited in the proximity of the activated PDGFRr and competes, via its SH2 domain, with Src for the binding to phosphorylated tyrosines. The SH3 domain of SLAP, on the other hand, sequesters Src-specific effectors resulting in the inhibition of Src-specific signaling pathway.*

**Grb2**

The mechanism of stimulation-dependent receptor ubiquitination has been also proposed to be mediated by the adaptor protein Grb2. Grb2 contains one SH2 domain through which it binds to several RTK specific phospho-tyrosines and two SH3 domains that link the receptor-Grb2 complex to downstream effectors. The most widely studied among Grb2 interactors is the Ras Guanine Nucleotide Exchanger Sos. The ligand-dependent recruitment of Grb2 by RTKs leads to the activation of Sos/Ras pathway that in turn activates various other signaling proteins to relay the signal downstream along several pathways. The SH3 domain of Grb2 can also bind Cbl ubiquitin ligase therefore indirectly recruiting Cbl to activated RTKs such as Met or EGFR (Waterman et al., 2002)

(Peschard et al., 2001; Peschard et al., 2004). Additional evidence that Grb2-Cbl interaction is important for negative regulation of RTKs is provided by genetic studies in the nematode *C.elegans*, where SLI-1, the orthologue of Cbl, is able to restore the phenotype due to loss of function mutation in LET-23 gene (orthologue of EGFR), and for this function SEM-5, the orthologue of Grb2, is required (Yoon et al., 1995). Since Cbl and Sos form exclusive complexes with Grb2, Cbl may compete with Grb2 for Sos binding, thus further inhibiting Ras activation.

Grb2 is also able to bind other signaling inhibitors such as Ack and SOCS (Hopper et al., 2000) (De Sepulveda et al., 1999). Acks (Activated Cdc42-associated tyrosine Kinase) are a non receptor tyrosine kinase family whose function in mammalian cells remains elusive. Acks contain several domains including a SH3 domain a CRIB domain (Cdc42/Rho Interacting Binding) and a number of potential Map kinase phosphorylation sites. A genetic study in the nematode *C.elegans* suggested that sem5 (the orthologous of Grb2) inhibits LET23-(orthologous of EGFR) mediated biological function via the recruitment of inhibitors such as Ark-1, the Ack orthologue (Hopper et al., 2000).

Furthermore Grb2 is able to bind SOCS (Suppressor Of Cytokine Signaling), another adaptor protein that has been shown to be involved in negative receptor signaling. Forcing the expression of SOCS in haematopoietic cells result in a strong and specific decrease of Kit RTK-mediated proliferation, while cell survival was not affected (De Sepulveda et al., 1999). One of the particular characteristics of the model proposed by these studies is that SOCS has also been shown to be transcriptionally up-regulated by the Kit ligand. Thus, Grb2 appears to recruit SOCS, an inducible switch, to the active receptor leading to the negative modulation of proliferative signals in favor of cell survival signals.

Taken together these data picture Grb2 as an adaptor protein able to integrate both positive and negative signals by activating Ras pathway via Sos and by attenuating RTK signaling via the recruitment of different negative regulators (Fig.5).

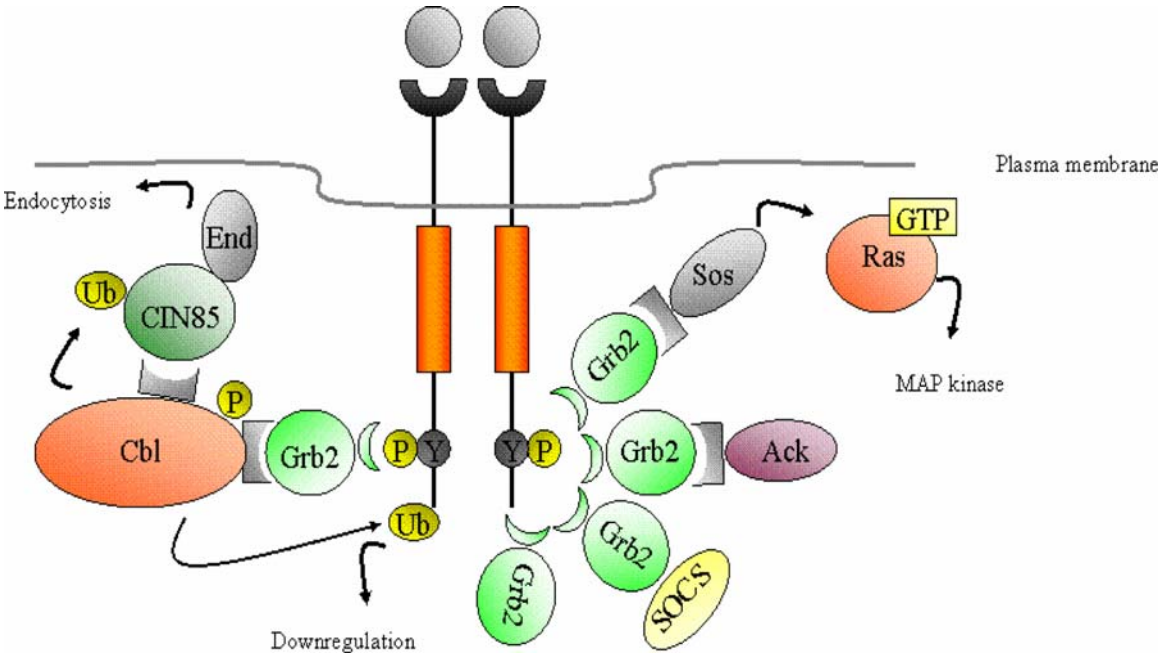


**Figure 5. Multiple functions of Grb2.**

*The adaptor protein Grb2 may serve as a regulated scaffold for the binding of other signaling proteins that include both positive (Sos) and negative (Ack, SOCS, Cbl) regulators. Grb2 can link RTKs with activation of Ras/MAPK pathway via its association with Sos, while it promotes receptor ubiquitination and endocytosis by binding to the Cbl-CIN85-endophilin (End) complex. Grb2 can also recruits Ack to further attenuate signaling pathways. Furthermore, Grb2 can recruit SOCS, which transcription is activated by the receptor itself, to the active receptor. This leads to the negative modulation of proliferative signals in favor of cell survival signals. P, phosphate, Ub, ubiquitine*

## Negative signaling via Feedback loops

Several of the adapters found to be involved in negative regulation of RTKs signaling are expressed in the context of transcriptional responses activated by the RTK itself. In other words the RTK mediates the transcriptional activation of negative

regulators of the RTK itself. This mechanism is used by the cells to adjust receptors output in response of monitoring their own activity. These events are defined as feed-back loops. Recently it has become clear that the principles of feedback, both positive and negative, are indeed widely used to produce the signaling properties required for a proper overall signaling output that is necessary in physiological processes. Negative feedback loop occurs when for example a signal induces the expression of its own inhibitor; it serves to dampen and/or to limit the signal. Positive feedback occurs when a signal induces more of itself, or another molecule that amplifies the original signal and it serves to stabilize, amplify, or prolong the signaling. The widespread use of feedbacks and the variety of its consequences make it an important principle of regulating signals from RTKs.

Negative feedback loops are used in several processes. For the purpose of this thesis I will describe some examples that well illustrate the strategies in which feed back loops participate, pointing-out the relevance of known negative feedbacks during physiological processes and their relevance in diseases. Thus, I will particularly focus on experimental demonstration of the involvement of negative feedback loops that are either directly acting on RTKs or in the proximity of their signal transduction rather then describing the better studied and characterized negative feedbacks in the context of transcription factor regulation (Smolen et al., 2000).

The most common use of negative feedback is to limit the duration of a signal. In a straightforward model it occurs when a signal induces its own negative regulator so that when a given signal reaches a certain threshold the signal is terminated. Feedback loops are also involved during development when a receptor/ligand has to exert its biological function in a limited space, close to the source of the signal, without affecting more distant cells. In this case the negative feed back loop is involved in spatial control of a signal. On the other side pattern formation is an event during development where positive and negative feedback must integrate their information in order for the cells to respond properly. The establishments of left and right asymmetry, anterior/posterior compartment boundaries, dorso/ventral axes are all critical events during development controlled by the coordinated integration of positive and negative feedback loops.

**Limiting the duration of a signal**

There are several examples of such a use of negative feedback loops; interferon signaling describes well the importance of these negative signaling events in physiological processes.

The interferon family consist of two main groups: the type I interferons include interferonα and interferonβ, whereas interferonγ is the only type II interferon (Billiau, 1996). Interferonγ acts by binding to and inducing the multimerization of a cell surface transmembrane receptor composed by IFNGR1 and IFNGR2 (Hemmi et al., 1994) (Novick et al., 1994). This results in the activation of the signaling pathways that drives the expression of a variety of genes involved in activation of macrophages, antiviral and antiproliferative responses (Boehm et al., 1997). The Interferonγ is a key player in coordinating resistance to infections (Boehm et al., 1997; De Maeyer-Guignard et al., 1993) but its actions are not always beneficial since the infections might elicit in the host responses of sufficient magnitude to become life threatening. Experiments by which the Interferonγ levels were experimentally elevated in neonatal mice showed the potentially toxic effect of interferonγ signaling, including fatty degeneration of the liver (Toyonaga et al., 1994) (Gresser, 1982). The genes that are transcriptionally regulated by the active receptor include a family of molecules that can terminate the signal (Starr et al., 1997) (Endo et al., 1997). These molecules such as SOCS are involved in negative feedback loops. The physiological importance of this feedback mechanism is well exemplified by the characterization of SOCS function *in vivo*. SOCS1 loss of function mutant mice die perinatally by a complex neonatal disease, exhibiting excessive responses to Interferonγ signaling (Brysha et al., 2001). Although the mechanisms by which SOCS1 is able to inhibit interferon signaling are not completely clear, there is evidence indicating that in this context, SOCS acts as a pseudo-JAK substrate targeting the active JAK kinase for degradation, therefore terminating the signal. In these studies SOCS1 appears to be an inducible key modulator of Interferonγ actions allowing the benefic effects of this cytokine to occur without the risk of associated pathological responses.

Another example of such a negative feed-back loop is represented by Mig6 (Mitogen Inducible Gene 6) adaptor protein. Mig6 shows in its protein sequence

extensive homologies with the non receptor tyrosine kinase Ack which was found, as mentioned before, to inhibit EGFR-mediated biological function in *C. Elegans*. Mig6 was isolated as a protein interacting with ErbB2 and was shown to be induced by ErbB ligands (Fiorentino et al., 2000). The predicted structure of this molecule consists of several conserved domains. Among these the CRIB domain, a putative SH3 binding motif, a putative clathrin binding motif and a nuclear localization signal (Makkinje et al., 2000). Overexpression studies suggested that Mig6 is a selective inhibitor of ErbB2 proliferative responses (Fiorentino et al., 2000) (Hackel et al., 2001) as part of a negative feedback loop. Accordingly, Mig6-specific siRNA transfection or micro-injection of anti-Mig6 antibodies into growth factor-stimulated fibroblasts enhanced the mitogenic activity of ErbB2 receptor suggesting that Mig6 is part of a physiological negative feedback mechanism of ErbB receptors (Fiorini et al., 2002; Xu et al., 2005). The mode by which Mig6 is able to inhibit receptor-mediated proliferative responses is not clearly understood, however due to its ability to bind ErbB2 and EGFR, Mig6 was proposed to interfere with the signaling as a receptor-proximal inhibitor (Hackel et al., 2001) (Fiorentino et al., 2000). The ability of Mig6 to interfere with ErbB2 biological function has been proposed to depend on the direct binding observed between Mig6 and several receptor-proximal signaling molecules such as Grb2. Furthermore, upon ectopic expression of Mig6 in murine fibroblasts ErbB2-mediated map kinase activation was found to be altered. Interestingly, under these conditions, Map kinase activation was found to be affected by Mig6 overexpression at the late (3-9 hours upon ligand stimulation), but not the early time point of ligand activation (Fiorentino et al., 2000). However, more recent overexpression data using a mutant version of Mig6 lacking the ErbB binding region suggested that Mig6 can antagonize mitogenic signals further downstream of activated ErbB receptors (Anastasi et al., 2003). Thus, the mode of action of Mig6 has been proposed to be a scaffold/adaptor protein able to recruit and interfere with the time course and strength of activation of several signaling molecules critical for receptor-mediated proliferative response.

**Spatial control of the signal by negative feedback loop**

The biological significance of the negative feedback loop was demonstrated in studies on the cell fate mediated by EGFR and its antagonist *Argos*. *Argos* is a soluble molecule that carries a modified EGF domain and is able to bind the extracellular domain of DER (EGFR orthologue in *drosophila*) as a pseudo-ligand. *Argos* is then able to compete with *Spitz*, the main activator of DER, for receptor binding. The binding of *Argos* to DER receptor results in receptor inactivation. Therefore *Argos* is an extracellular inhibitor of DER (Freeman, 1997). It has been shown that *Argos* expression is dependent on DER activation, therefore forming a negative feed-back loop (Fig.6A). The roles of DER, *spitz* and *Argos* have been extensively investigated in several organisms. The best picture of spatial control mediated by this negative feed back loop is certainly arising from studies conducted in the *drosophila* eye (Freeman, 1998). The fly eye is formed by 750 facets, or "ommatidia". Each ommatidium contains the same set of specified cells and presents the same internal structure that develops from a monolayer epithelium called the eye immaginal disk. DER is essential for the formation of all the cells in the ommatidium. This is supported by two observations: the first is that *Spitz* (the main activator of DER) is required for the formation of all the photoreceptors, the second is that *Argos* (the *Spitz* antagonist) loss of function leads to over-recruitment of photoreceptors and consistent with this, its overexpression leads to a reduction in their number. In the early ommatidium, active *Spitz* is produced in the three earliest and centrally located cells (Fig.6B,C). This leads to DER activation in the neighboring and undifferentiated cells. The neighboring cells are in this way determined for differentiation. Each cell that is activated by *Spitz* ligand up-regulate *Argos*. *Argos* is then secreted and has the ability to diffuse further away compared to the secreted *Spitz* (Freeman et al., 1992), thus blocking more remote cells from responding to the ligand. *Argos* is however, unable to inhibit the effect of *Spitz* in cells that are exposed to high concentration of ligand (cells close to the source of *Spitz*) or to cells that are already committed to differentiation (Freeman, 1998). This mechanism is therefore limiting the effective range of *Spitz* action and thereby the number of cells that are recruited to the developing eye (Fig. 6 B,C).

Interestingly the EGF receptor action can be inhibited by different inhibitory molecules. The inhibitors *Argos*, *Sprouty* and *Kekkon* are all regulated by EGFR taking part in negative feedback loop. Importantly it appears that these different negative EGFR regulators have all different biological functions (Fig. 6A). For example *Argos* is a secreted EGFR extracellular inhibitor that can act at long range distances (Freeman et al., 1992) (Schweitzer et al., 1995), *Sprouty* is a more general intracellular signaling inhibitor that can act downstream several RTKs (Casci et al., 1999) and *Kekkon* is a EGFR specific transmembrane inhibitor that act only locally on the cell that expresses it (Ghiglione et al., 1999). Accordingly the loss of function mutants of *Argos*, *Sprouty* and *Kekkon* in *Drosophila* show different phenotypes. This evidence supports the idea that different negative regulators are not redundant but rather specific in regulating different receptor-mediated biological functions.

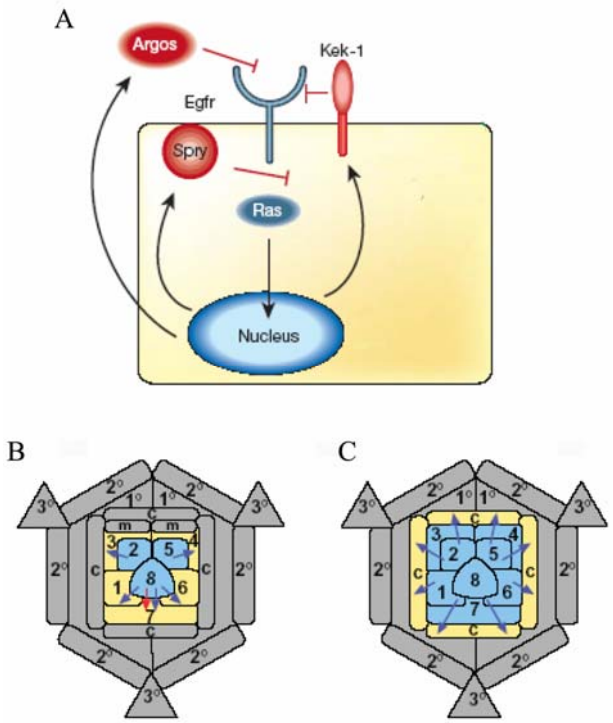


**Figure 6. Multiple feedback loops regulate the *Drosophila* EGF receptor.** *There are three known feedback inhibitors (shown in red) of the fly EGF receptor (Egfr), which signals through Ras: Sprouty (Spry), Kekkon-1 (Kek-1) and Argos (A). Each of which have different biological functions. (B,C) A model of ommatidial development. Ommatidia of increasing maturity are shown from left to right; (B) the recruitment of photoreceptors and (C) cone cells. Blue cells are the source of Spitz and they are able to recruit the neighboring yellow cells at each stage, but are unable to trigger the more remote grey cells, which are inhibited by Argos. Argos is expressed by each cell as it is determined. Because of its long range of action (see text), it may be more accurate to think of it usually forming a 'sea' of inhibitor surrounding all the developing ommatidia (Modified from Freeman et al.,2000 and Freeman et al.,1997).*

## Met and HGF

Met Receptor tyrosine Kinase was first identified as an oncogene (Cooper et al., 1984). This proto-oncogene was found to be a receptor tyrosine kinase but the ligand was not known (Park et al., 1986). Independently, two different experimental approaches identified a potent motogenic factor (Scatter Factor, S.F.) (Stoker et al., 1987) and a factor that was strongly promoting mitogenesis in hepatocytes (Hepatocyte Growth Factor, HGF) (Nakamura et al., 1989). These factors were found to be the same molecule, which is referred to as HGF/SF (Gherardi and Stoker, 1990). Then further studies identified HGF/SF as the high affinity ligand for Met receptor tyrosine kinase (Bottaro et al., 1991). HGF/SF, together with the Macrophage Stimulating Protein (MSP), belongs to the Plasminogen family of proteins. Plasminogen is a circulating pro-enzyme that is responsible, in its active form, for the lysis of blood clots. The Plasminogen family members are characterized by the presence of at least one domain known as the kringle domain, a serine protease domain and an activation domain located between the kringle domain and the serine protease domain. HGF and MSP are unique members of the plasminogen family since they lack catalytic serine protease activity due to mutations in essential amino-acids. Like the plasminogen, HGF and MSP are synthesized and secreted as a single chain, mainly inactive precursors; they are further proteolitically converted into their active, disulphide-linked heterodimers in the extracellular matrix. Once secreted, the conversion from the inactive single-chain to the active two-chain heterodimer is effected by several serine proteases present in the extracellular matrix.

HGF has also been shown to bind heparan-sulfate-proteoglycans with high affinity, which limits the diffusion of the factor *in-vivo* (Schwall et al., 1996) (Hartmann et al., 1998). The biological activity of HGF depends solely on its receptor Met, which like HGF, is a disulphide-linked heterodimer. The mature form of the receptor molecule is composed by one short extracellular $\alpha$ chain and a longer transmembrane $\beta$ chain. The $\beta$ chain presents a transmembrane domain, a tyrosine kinase domain, and a unique bidentate docking site which comprises two tyrosines that are essential for the Met-mediated biological functions (Maina et al., 1996) (Ponzetto et al., 1994). The bidentate docking site contains in fact two tandem tyrosines in a degenerate motif, which when

auto-phosphorylated by the active receptor, bind different SH2-containing molecules such as PI3 kinase, Grb2 and the multiadaptor Gab1 (Furge et al., 2000). *In-vivo* mutations in the two tyrosines lead to an embryonic lethal phenotype resembling that of the HGF/Met null mutants, indicating that the overall biological effects mediated by the receptor is mainly transduced by this multifunctional docking site. Several cytokines and growth factors can induce cell proliferation, differentiation, motility, protection from apoptosis and in some circumstances they may contribute to the onset and maintenance of invasive growth. However, the disruption of growth constrain, acquisition of a motile phenotype, resistance to programmed cell death and the orchestration of several steps during this processes are optimally accomplished by HGF (Fig.7).

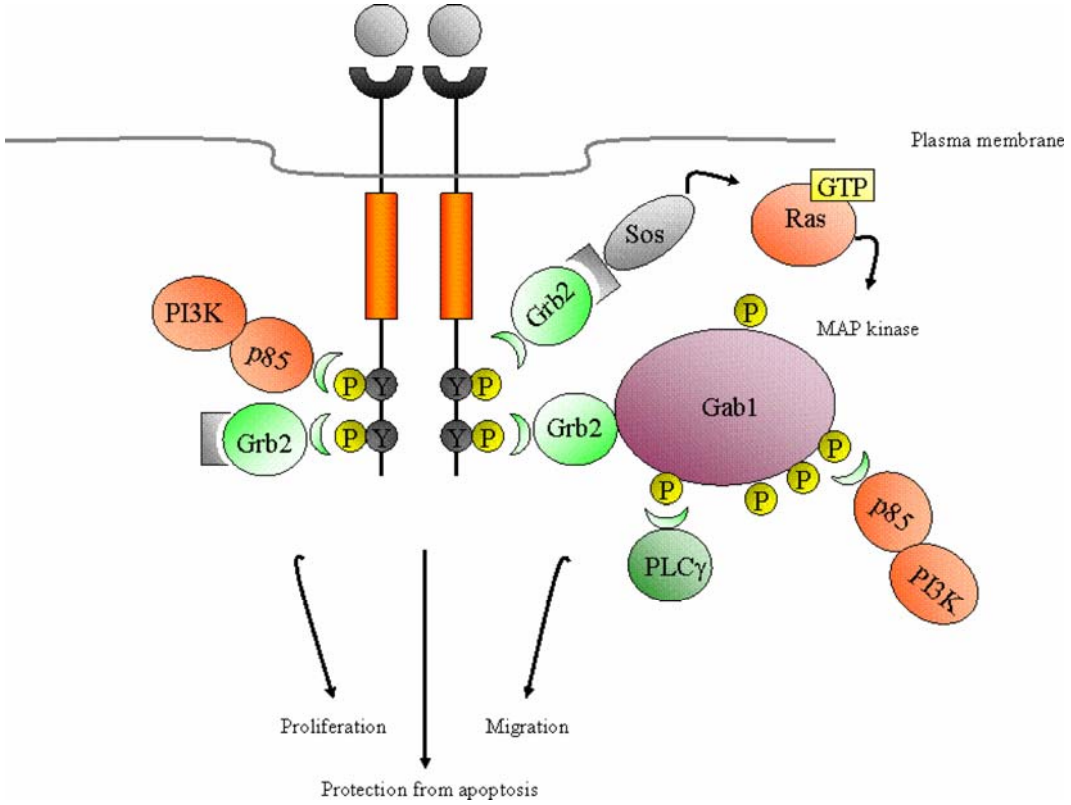


**Figure 7. Biological functions mediated by the bidentate docking site of the Met receptor.**
*Met receptor bidentate docking site contains two tyrosines embedded in a degenerate motif which, upon phosphorylation, can bind an array of signaling molecules such as Grb2, the p85 subunit of PI3K and the multiadaptor Gab1. The two tyrosines are essential in order to mediate the entire array of Met biological function*

**Met signaling during development**

The phenotype analysis of HGF and Met mutant mice has shown that this ligand-receptor couple plays essential roles in controlling several processes during mammalian development (Schmidt et al., 1995); (Bladt et al., 1995; Uehara et al., 1995); (Maina et al., 1996; Maina et al., 2001). These studies suggested that the function and the responses evoked by HGF/Met are complex and therefore they are not restricted to a single step during development. Met and HGF are expressed in a variety of organs during development. They provide essential signals for the survival and proliferation of hepatocytes and placental trophoblasts. Consistently the liver of null mutant of both HGF and Met is considerably reduced in size due to a decreased proliferation and increase in apoptosis of hepatocytes (Fig.8C,D). The loss of function mutant embryos of both Met and HGF die in uterus due to a defect in placental development (Fig.8A,B). However, these genetic studies showed a striking role for HGF and Met in regulating cellular motility. During development cells often migrate over long distances to their final target where they differentiate to form organs and tissues. These precursor cells initiate invasive growth by budding off from their primitive place of origin to migrate along chemotractant gradients and eventually differentiate to specify the architecture of a newly formed organ. For example, an important class of skeletal muscle is derived from long-range migratory progenitors. The muscle progenitors delaminate (a phenomenon referred to as epithelial-mesenchimal transition) from an epithelial structure called dermomyotome which forms part of the developing somite. In mice, precursors of the limb, diaphragm, and the tip of tongue muscles migrate from the dermomyotome to their final location where they differentiate to form skeletal muscles. Null mutant mice for HGF or Met are completely devoid of muscle in the limb, diaphragm and tip of the tongue, highlighting the essential role played by Met and HGF in driving this "physiologically occurring" invasive growth (Fig8E-H). This phenotype was demonstrated to arise from a lack of epithelial-mesenchimal transition which results in a defect in the delamination of muscle precursors from the dermomyotome and secondly from a deficiency in cell migration.

Invasive growth plays also a relevant role during the development of the central and peripheral nervous system. The precisely controlled directional movement of axons and neurites following attraction or repulsive signals that guide them towards the target is crucial for the formation of the adult brain. Not surprisingly, HGF, secreted by the limb mesenchyme, was found to be a chemo attractant factor for motor neurons. The limb mesenchyme derived from wild type, but not from HGF-null mutants, was found to be able to induce axonal outgrowth from spinal cord culture. Consistent with this *in-vitro* observation, axons emerging from limb-innervating motoneurons of Met and HGF null mutant embryos show a significant decrease in neurite length (Fig.8I,J). Finally, not only does Met and HGF induce motoneurons axonal outgrowth but they also induce differentiation, survival and axonal outgrowth of sensory and sympathetic neurons *in-vivo* (Maina et al., 1998).

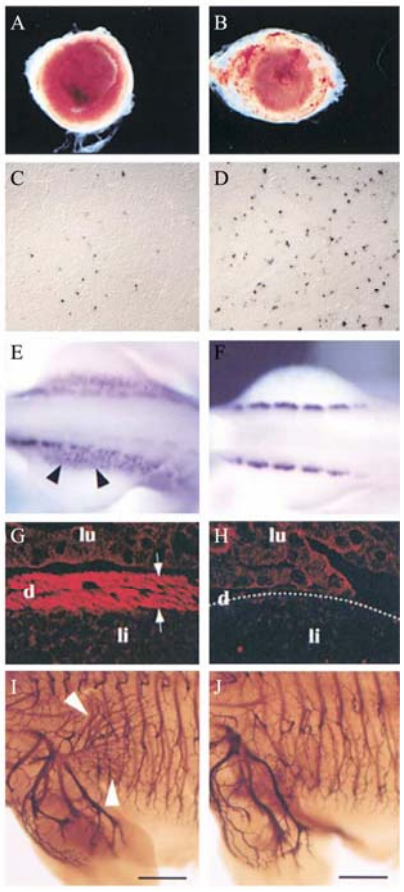


**Figure 8. Met mediates a variety of biological functions.** *Comparison of wild type (A,C,E,G,I) versus Met loss of function mutant embryos (B,D,F,H,J). The placenta morphology of E13.5 loss of function (B) and wild type (A) embryos. (C,D) Increase in apoptosis (TUNEL staining, brown dots) of the hepatocytes of Met mutant embryos (D) compared to wild type (C). (E,F) In-situ hybridization analysis using a Met specific probe. Absence of myoblasts migration in the Met loss of function (E10.5, F) compared to wild type (E). The arrowheads (E) indicate a normal pattern of migrating myoblast precursors in wild type embryos. (G,H) section of the diaphragm (d) stained with phalloidin. In the Met loss of function mutants (H) a stippled line indicates the position where the diaphragm should be. The arrows (G) indicate the thickness of the wild type diaphragm. lu: lung, li: liver. (I,J) Whole mount anti-neurofilament staining of E12.5 embryos (forelimb and thorax, dorsal up, anterior left). Arrowheads in I indicate branches of the Nervus thoracodorsalis. Scale bar is 0.6 mm. Note the absence of neurite branches in the Met loss of function embryos (J) compared to wild type (I). (Modified from Maina et al., 2001)*

## Met and HGF in pathological conditions

Deregulation of Met and HGF system has been shown to be associated with several pathological conditions and has emerged to be a crucial feature of many human malignancies. This evidence is supported by several experimental approaches: first mouse and human cell lines that are overexpressing Met and HGF become tumorigenic and metastatic when injected in mice (Rong et al., 1994). Accordingly the down-regulation of Met or HGF expression in human tumor cells decreases their tumorigenic potential (Abounader et al., 2002). Second, mice which overexpress Met or HGF as a transgene develop different types of tumors and metastatic lesions (Takayama et al., 1997b). Third, there is unequivocal evidence that Met is implicated in human cancer with the Met kinase domain having activating mutations in both sporadic and inherited human renal papillary carcinomas (Danilkovitch-Miagkova and Zbar, 2002) (Park et al., 1999).

## Met-mediated branching morphogenesis

As mentioned above among many biological activities, branching morphogenesis and invasion appear to be the most prominent and complicated cellular events induced by HGF/Met. Notably, in fact, HGF/Met is one of the very few ligand/receptor couples that can induce branching morphogenesis. These series of events are crucial steps during pattern formation in many organs and tissues including, placenta, kidney, lung, mammary glands and nervous system. Branching morphogenesis is typically mediated through changes in cell shape, asymmetric polarization of the cell in the direction of branching, branch elongation, cell-cell contact and migration. Some of these Met-mediated biological functions can be recapitulated *in-vitro* by culturing dissociated cells. Met activation induces proliferative and anti-apoptotic responses in different cell lines. Epithelial cells, and in particular the Madin-Darby Canine Kidney (MDCK) cell line or the hepatocytes precursors cell line called MLP29, respond to Met activation by "scattering", which is colony dispersal with an increase in motility. Moreover when these cells are cultured within a collagen matrix and treated with HGF, they form branched

tubules. Tubular branching is the *in-vitro* read-out for branching morphogenesis since it represents a complex phenomenon which requires tight coordination and regulation between cell growth, polarity and motility (Vande Woude G.F., 1997).

Several studies used these *in-vitro* assays as read-outs in order to dissect the complexity of HGF/Met-mediated signaling and biological function. As mentioned before one of the characteristic of Met receptor is the presence of a bidentate docking site where two crucial tyrosines are inserted in a degenerate motif. Following ligand-induced receptor stimulation these two tyrosines become phosphorylated and promiscuously recruit an array of molecules. These include phosphatidyl-inositol 3 kinase (PI3K), the non receptor tyrosine kinase Src, the adaptor protein Grb2 and Shc (and the multiadaptor protein Gab1, which in turn can bind, among others, phospholipase Cγ (PLCγ), the protein tyrosine phosphatase SHP2 and the transcription factor STAT3 (Zhang and Vande Woude, 2003) (Trusolino and Comoglio, 2002) (Furge et al., 2000). This motif can recapitulate the entire signaling requirement for execution of the invasive growth program and branching morphogenesis. When the two multifunctional tyrosines are converted into phenylalanine, cells become completely unresponsive to HGF *in-vitro* (Ponzetto et al., 1994). The formation of branched tubules has been related to the sustained GAB1 phosphorylation and to the GAB1-mediated recruitment of PLCγ and SHP2, together with activation of the STAT pathways. Furthermore the mutation of the multifunctional binding site into preferential consensus for Grb2 or PI3K has allowed the dissection of the individual transduction pathways that are responsible for the oncogenic versus migratory effect of Met. Increasing the activation of Ras signaling by mutations that duplicate the Grb2 binding site increases the ability of Met to transform the cells, but abolishes the metastatic potential. On the other hand the optimizations of PI3 kinase binding results in enhanced invasion, but even in this case the metastatic potential of Met is abrogated. The full metastatic potential is restored only when both the effectors can be recruited to the kinase (Bardelli et al., 1999). These results strongly suggest that the concomitant activation of Ras/Map kinase and PI3 kinase pathways in addition to the recruitment and phosphorylation of the multiadaptor GAB1 are all essential steps of HGF/met-mediated morphogenic activity.

**Met-mediated cytoskeleton rearrangement: Rho GTP-binding proteins**

One of the most crucial events during branching morphogenesis and epithelial-mesenchimal transition is the conversion of the cell from an immobile to a migratory phenotype. This process requires an extensive remodeling of the cell cytoskeleton (Mitchison and Cramer, 1996) (Labouesse, 2004). Members of the Rho small GTP-binding proteins, such as Rho, Cdc42 and Rac, play an important role in the process regulating actin cytoskeleton (Hall, 1998). GTPase of the Rho family critically modulate the establishment of epithelial polarity by regulating cell-cell junction assembly and cytoskeleton reorganization. It has also been shown that this family of proteins plays an important role during cell migration. In fact, upon receiving a fruitful signal to migrate, the cells orchestrate cytoskeletal remodeling and changes in the cell adhesive properties (Fig.9) (Fukata and Kaibuchi, 2001). By the use of loss and gain of function approaches, in numerous cell types, it has been established that Rho regulates the assembly of contractile actin filaments, while Rac and Cdc42 regulate the polymerization of actin to form peripheral lamellipodial and filopodial protrusions respectively (Nobes and Hall, 1995) (Ridley and Hall, 1992) (Ridley et al., 1992). It is not really surprising that the Rho-family of GTPases play a critical role during cell migration and therefore in branching morphogenesis and epithelial-mesenchimal transition (Labouesse, 2004) (Portereiko et al., 2004) (Schumacher et al., 2004) (Smallhorn et al., 2004). While Rho has been shown to regulate the contraction-retraction forces required in the cell body and at the rear, it has been shown that Rac is required at the front of the migrating cell to regulate actin polymerization and membrane protrusions. Rac activity appears to be also regulated in space so that a gradient of active Rac can be visualized with the highest concentrations at the leading edge (Kraynov et al., 2000). Also Cdc42 induces actin polymerization to generate filopodia protrusions at the leading edge (Nobes and Hall, 1995). However, recent studies on *Drosophila* suggest that Cdc42 is not required for migration per se (Sepp and Auld, 2003). Cdc42 does however play a critical role in controlling the direction of the migration and in defining cellular polarity in respect to the extracellular environment (Ridley, 2001) (Fig.9).

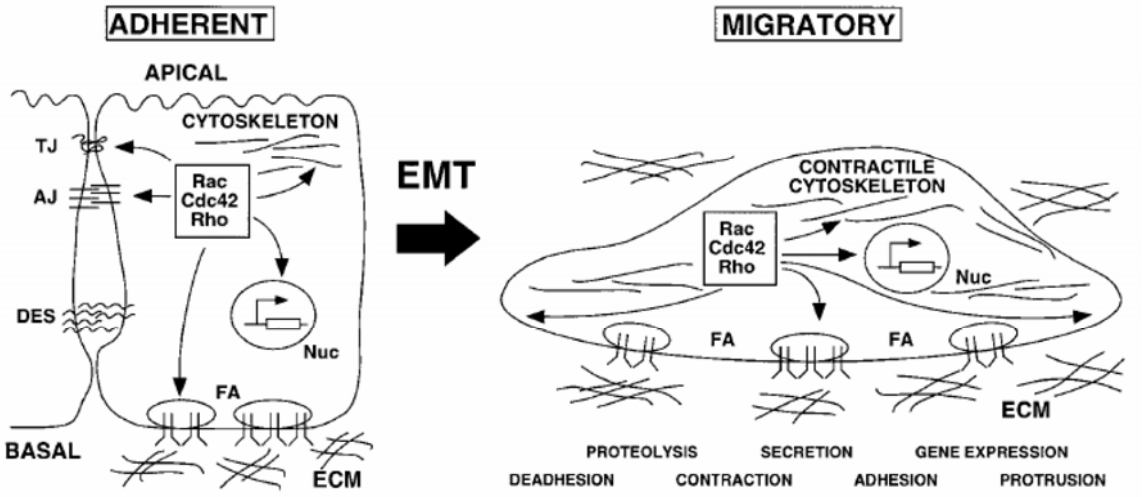


**Figure 9. Acquisition of a motile and invasive phenotype by an adherent epithelial cell**.
*Rho GTPase function is required for both the establishment of a fully polarized state (left) and a motile phenotype upon epithelial-to-mesenchymal transition (EMT; right). Movement involves a number of individual steps which include the following: loss of cell– cell adhesion, membrane protrusions in the direction of movement, de-adhesion from the extracellular matrix in the rear and re-adhesion in front, contraction of the actin cytoskeleton in order to move the body of the cell, and active remodeling of the extracellular matrix (ECM) by proteolysis and secretion. These steps also depend on alterations in the transcriptional profiling of the cell. (Nuc, nucleus; DES, desmosomes; TJ, tight junction; AJ, adherens junction) (From Schmitz et al., 2000).*

The polarized migration of many cells is reflected in the reorganization of microtubule cytoskeleton and centrosome, which usually (but not always) face the direction of migration. This facilitates the direction of the migration by directing transport pathways at the leading edge and is particularly important to achieve persistent and efficient migration over long distances (Ma et al., 2001). These studies suggest that during epithelial-mesenchimal transition, branching morphogenesis, invasion and polarized migration the driving forces for cell motility are derived from the cytoskeletal reorganization of actin which is controlled by the members of the Rho GTP-binding protein family. These proteins cycle between an inactive (GDP-bound) and an active (GTP-bound) state in which they interact with several effector proteins. The conversion

from the active to the inactive conformation is regulated by members of the guanine nucleotide exchange factors (Cerione and Zheng, 1996) whereas the conversion from the active to the inactive state is stimulated by the family of GTPase-activating protein (Lamarche et al., 1996). Rho-like GTPase interacts with numerous different downstream effector proteins that drive specific cell responses. The molecular cloning of many effectors from a variety of different organisms revealed that many of these molecules share a common Cdc42-Rho Interacting Binding domain, the CRIB domain (also known as GTPase Binding Domain, GBD or PBD). The CRIB domain-containing effectors are structurally and functionally diverse and include serine/threonine kinases, tyrosine kinases, actin binding proteins and adapter proteins (Pirone et al., 2001). Among these effectors, the p21-activated kinase (PAK) family and Rho kinase isoform have been implicated as mediators of actin reorganization (Sells et al., 1997) (Leung et al., 1996). PAK kinases bind to and are strongly activated by GTP-bound Cdc42 and Rac (Manser et al., 1994) (Martin et al., 1995), whereas Rho kinases bind to activated Rho (Leung et al., 1995) (Ishizaki et al., 1996). It is quite well established that RTK-mediated activation of Rho promotes cytoskeleton reorganization (Ridley and Hall, 1992) inducing the corresponding change on the actin cytoskeleton. PDGF, EGF and Insulin promote Rac activation (Nobes and Hall, 1995). Moreover it has been shown that HGF promotes the activation of Cdc42 and Rac (Royal et al., 2000). Furthermore, the stabilization of directional movement (chemotaxis) requires input from external cues and this is tightly controlled by Cdc42. The best studied example of this event is in macrophages cells moving along a chemotactic factor gradient. When Cdc42 is inhibited, the macrophages revert to random walk, whereas inhibition of Rac blocks cell movement completely (Allen et al., 1998). Since there is a quite broad degree of cross talk between Cdc42, Rac and Rho, it seems that Cdc42 is required to direct and/or stabilize active Rac at the front of migrating cells. Thus, the precise tuning in space and time of the Rho-like GTPases activation by external cues appears to be a key step during branching morphogenesis, epithelial-mesenchimal transitions and polarized migration.

# RESULTS

### MLP29, C2C12 and Trophoblast stem cells activate Map kinase, Akt and Gab1 upon HGF stimulation

In order to choose a suitable cell line for the identification of HGF-target genes, we first investigated, in three different cell lines (MLP29, C2C12 and Trophoblast Stem cells), the time-course and strength of activation/phosphorylation of three signal transducers known to be important for the Met receptor mediated biological functions: p44 Map kinase, PI3 kinase and the multi-adaptor protein Gab1 (Fig.10-11).

MLP29 is a liver-derived cell line which expresses physiological levels of Met receptor (Brand-Saberi et al., 1996; Medico et al., 1996), C2C12 is a myoblast cell line known to express Met receptor (Bladt et al., 1995) (Brand-Saberi et al., 1996; (Tatsumi et al., 1998), and the Trophoblast Stem cells (TS cells) are primary cell in which HGF/Met biological functions had not yet been characterized.

MLP29, C2C12 and TS cells were stimulated with 40ng/ml of HGF and harvested over a time course. The total protein lysate was subjected either to a direct western blot analysis (Fig.10) or to an immuno-precipitation using a GAB1 specific antibody followed by western blot analysis (Fig.11).

20μg of the total lysate for each experimental condition were directly analyzed by western blotting using either anti-phospho-Map kinase, anti-phospho-Akt or anti-tubulin specific antibodies. At 5' after HGF stimulation Map kinase and Akt were found to be strongly phosphorylated in all three cell lines and the activation was found to be sustained up to 4 hours after HGF stimulation in the case of MLP29 and TS cells (Fig.10 A, C).

The kinetics of Map kinase and Akt phosphorylation in the C2C12 cell line was more transient, returning to basal phosphorylation levels after 1 hour of HGF stimulation (Fig.10B).

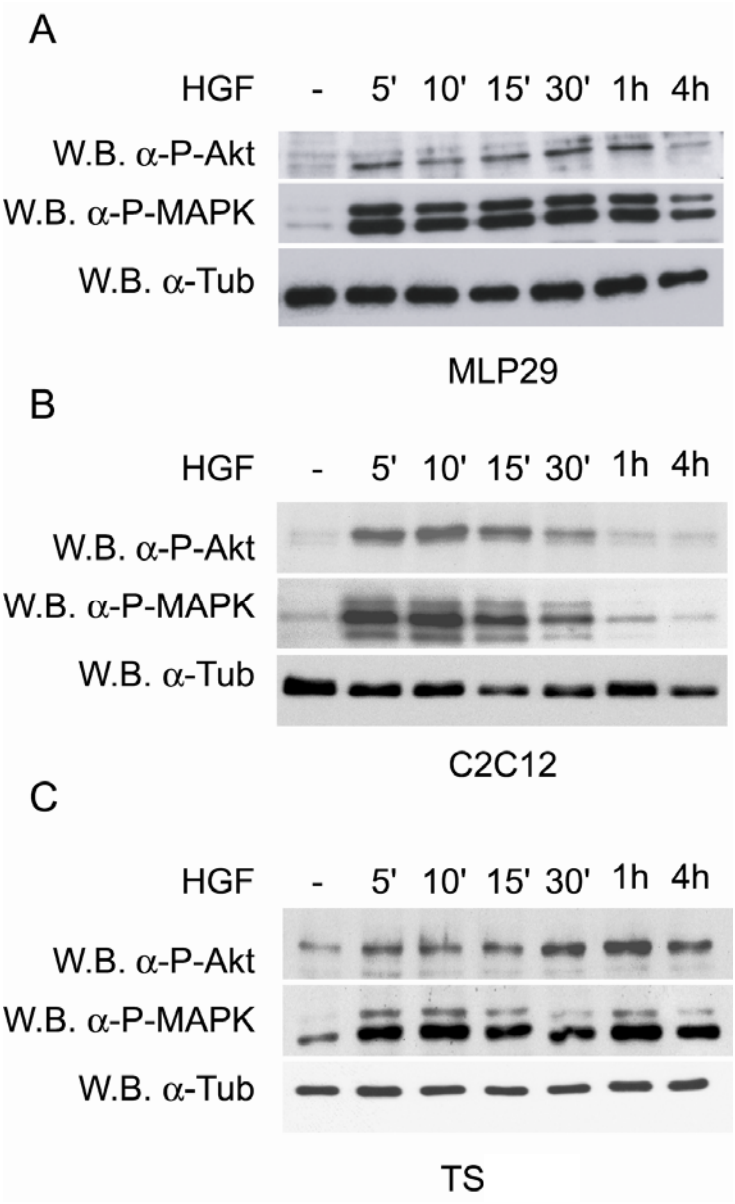


**Figure 10. MLP29, C2C12 and Trophoblast stem cells activate Map kinase and Akt upon HGF stimulation.**

*(A-C) 20μg of total lysate of MLP29 (A) C2C12 (B) and TS cells (C) stimulated over a time course with 40ng HGF and analyzed by direct western blotting using anti-phospho-Akt (α-P-Akt) anti-phospho-Map kinase (α-P-MAPK) or anti-tubulin (α-Tub) specific antibodies. The activation of Akt and Map kinase in response to HGF is comparable in all three cell lines.*

The western blot analysis with α-tubulin antibody demonstrated equal signal intensity in all samples, indicating that total proteins level loaded in each lane was comparable. In order to analyze the kinetics of phosphorylation of the multi-adaptor protein Gab1, 1mg of total protein extracted at different time points upon HGF stimulation from MLP29 and C2C12 was immuno-precipitated using the anti-GAB1 specific antibody.

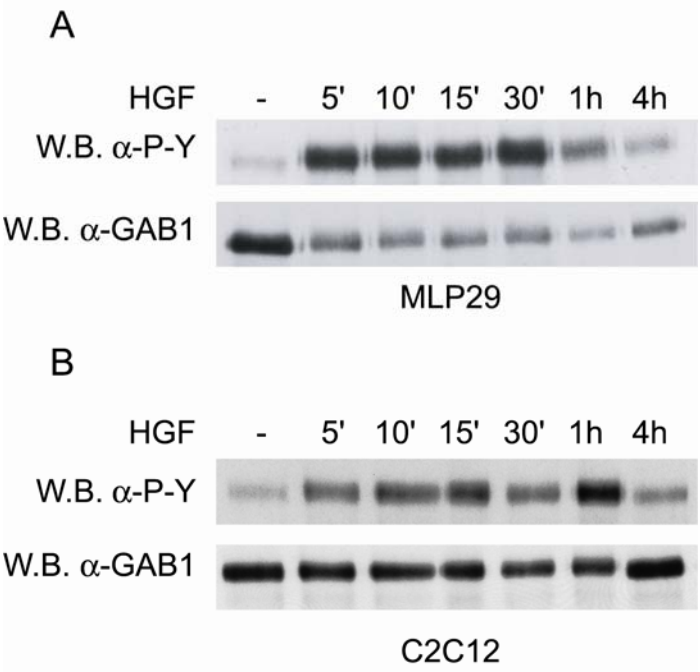


**Figure 11. Phosphorylation kinetics of the multi-adaptor protein Gab1.**

*MLP29 (A) and C2C12 (B) were stimulated with 40ng/ml of HGF for different time points. 1mg of total protein was immuno-precipitated using an α-GAB1 specific antibody. The amount of tyrosine phosphorylated GAB1 was detected by immuno-blot analysis using the α-phospho-tyrosine specific antibody (α-P-Y). The α-phospho-tyrosine specific antibody was stripped-off the membrane that was then reprobed using an α-GAB1 specific antibody (α-GAB1) showing that an equal amount of total GAB1 protein was immuno-precipitated in each sample.*

The amount of tyrosine phosphorylated GAB1 was detected by immuno-blot analysis using an anti-phospho-tyrosine specific antibody (Fig.11A-B). Upon HGF stimulation, the multi-adaptor protein GAB1 followed phosphorylation kinetics similar to that observed, in the same cell line, for the activation of Map kinase and Akt. In MLP29 and C2C12 cells, GAB1 was found tyrosine phosphorylatad upon 5 min of HGF stimulation. The phosphorylation was sustained for up to 1 hour before returning to basal phosphorylation state. In order to confirm that an equal amount of GAB1 protein was immuno-precipitated in each sample, the anti-phosphotyrosine specific antibody was stripped-off and the membrane reprobed using an α-GAB1 specific antibody.

The strong and sustained Map kinase, PI3 kinase and Gab1 phosphorylation occurring upon HGF stimulation, demonstrated that MLP29, C2C12 and TS cells responded to HGF in activating at comparable levels three of the most important signaling pathways downstream of the Met receptor.

**MLP29 proliferate and scatter upon HGF stimulation**

The ability of HGF to induce biological responses in MLP29 was verified using a BrdU incorporation assay (Fig.12). MLP29 cells were starved in 0.1% Fetal Bovine Serum (FBS) containing media for 96 hours. The cells were then stimulated with HGF for 6 hours and Bromodeoxyuridine (BrdU) was added for another 2 hours. The cells were then fixed and immuno-stained using the α-BrdU specific antibody. Figure 3 shows a significant increase in BrdU incorporation confirming that HGF induces S phase entry of MLP29 cells. Furthermore, the ability of HGF to induce scattering of MLP29 was confirmed.

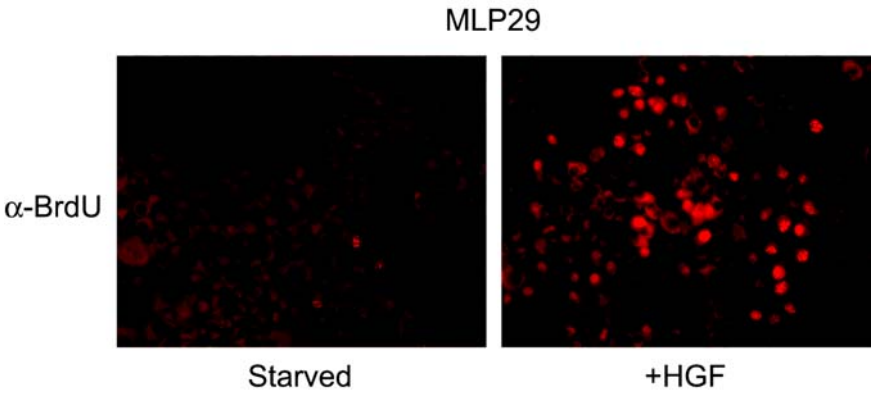


**Figure 12. MLP29 proliferate upon HGF stimulation** *MLP29 cells were starved in 0.1% FBS containing media for 96 hours. The cells were then either left in starving media (starved) or stimulated with 40ng/ml of HGF for 6 hours (+HGF). The cells were incubated for 2 hours with a Uridine homologue, BrdU, which is incorporated by the DNA polymerase into the newly synthesized DNA. Cells were then fixed and immuno-stained using the α-BrdU specific antibody thus labeling proliferating cells (Red staining).*

**Microarray analysis of HGF-stimulated MLP29 cells**

Part of the efforts to understand molecular events downstream of HGF/Met signaling has been to examine the expression of genes regulated by Met signaling.

To analyze global gene expression in HGF-stimulated MLP29 cells a high density cDNA microarray was produced in collaboration with Dr. Tomoko Iwata and Luca Dolce at the European Molecular Biology Laboratory-EMBL (Heidelberg) core facility (Wilhelm Ansorge's group) using the National Institute of Aging (NIA) 15,247 clone set (Tanaka et al., 2000). Briefly, the library was amplified by polymerase chain reaction (PCR) using two universal oligonucleotides (Cortes-Canteli et al., 2004). The size and quality of the PCR amplified products were then controlled by Agarose gel electrophoresis (Fig.13).

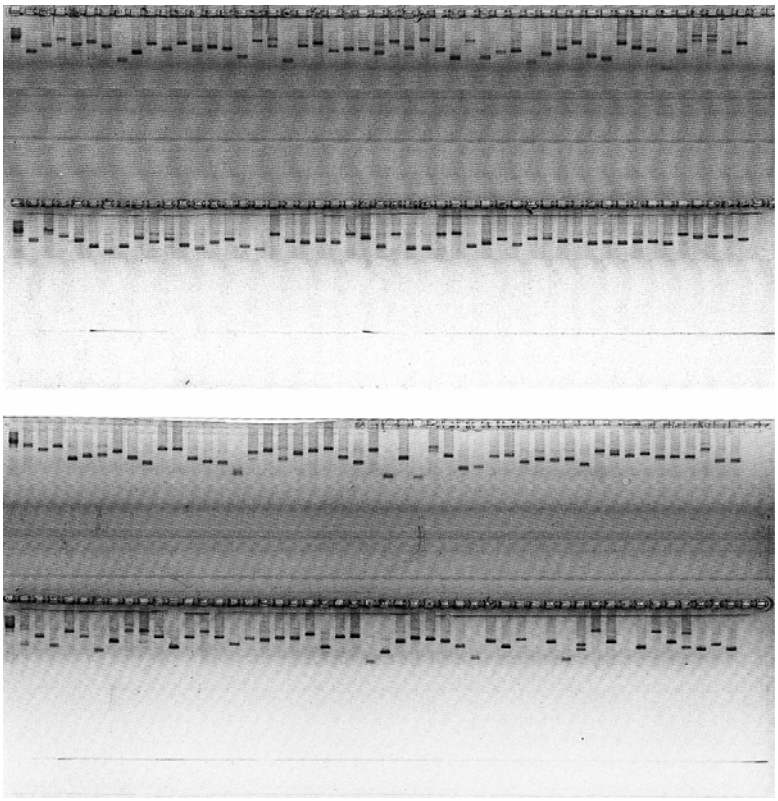

**Figure 13. Agar gel electrophoresis analysis of PCR-amplified NIA library clones.**

*The NIA 15,247 clone set (Tanaka et al., 2000) was amplified by PCR using two universal oligonucleotides (Cortes-Canteli et al., 2004). The amplified PCR products were purified and analyzed by Agarose gel electrophoresis in order to control their size and quality. The figure shows Agar gel electrophoresis analysis of 192 PCR- amplified products. The PCR-amplified clones' size (black bands) was ranging between 500 and 2000 base pairs.*

The PCR products were further purified and spotted at high density on glass coverslips. The cDNA probes derived from untreated or 4 hours HGF stimulated MLP29 cells were fluorescently labeled with Cy3-dUTP (green) or Cy5-dUTP (red), respectively. These probes were applied simultaneously onto the microarray, and the two fluorescent

images were scanned with a fluorescence laser-scanning device (Fig.14 A, C). Green and red fluorescent signals indicated genes whose expression levels were relatively higher in cells untreated or HGF-stimulated, respectively. The differential expression of each gene was calculated from the relative intensity of the Cy5 *versus* Cy3 fluorescent signal (Fig.14B,D). Two independent experiments were conducted comparing untreated and 4 hours HGF stimulated MLP29 cells and one experiment was conducted comparing two 4 hours HGF-stimulated samples (background control). Figure 14 B shows one representative plot of the differential expression of the 15,247 genes in one of the two experiments conducted comparing untreated and 4 hours HGF stimulated cells, while figure 14 D represents the plot of the control experiment carried-out comparing 4 hours HGF-stimulated samples.

As expected overall, the expression of most genes was not affected by HGF stimulation. Notably, most of the genes were differentially regulated comparing untreated versus 4 hours HGF stimulated samples (Fig.14B). Very few genes were found to be differentially regulated in the plot representing the control experiment (Fig. 14D).

Our criteria for the selection of differentially expressed genes were as follows: first, Sum of Median (SOM) value (intensity of the Cy5 and Cy3 signals) higher than 5000. Second, average of the fold of induction/repression (relative intensity of the Cy5 *versus* Cy3) higher than 1.8 fold change in two independent experiments. Third, absence from background control experiment.

Using these criteria a total of 79 genes in HGF stimulated cells had a differential expression value in all the experiments compared with untreated cells and were therefore considered to be regulated by HGF stimulation.

Among the 79 genes, we identified 59 genes that were up-regulated in cells stimulated with HGF in comparison to untreated cells, as well as 20 genes that were down-regulated. Roughly half of the identified genes (36 genes) currently do not show any homology to genes with annotation or known function upon blast searches against nucleic acid gene database. The group of HGF regulated genes was further categorized using the information provided by the NIA mouse 15k cDNA clone gene ID list initially and further modified when necessary (Table 1).

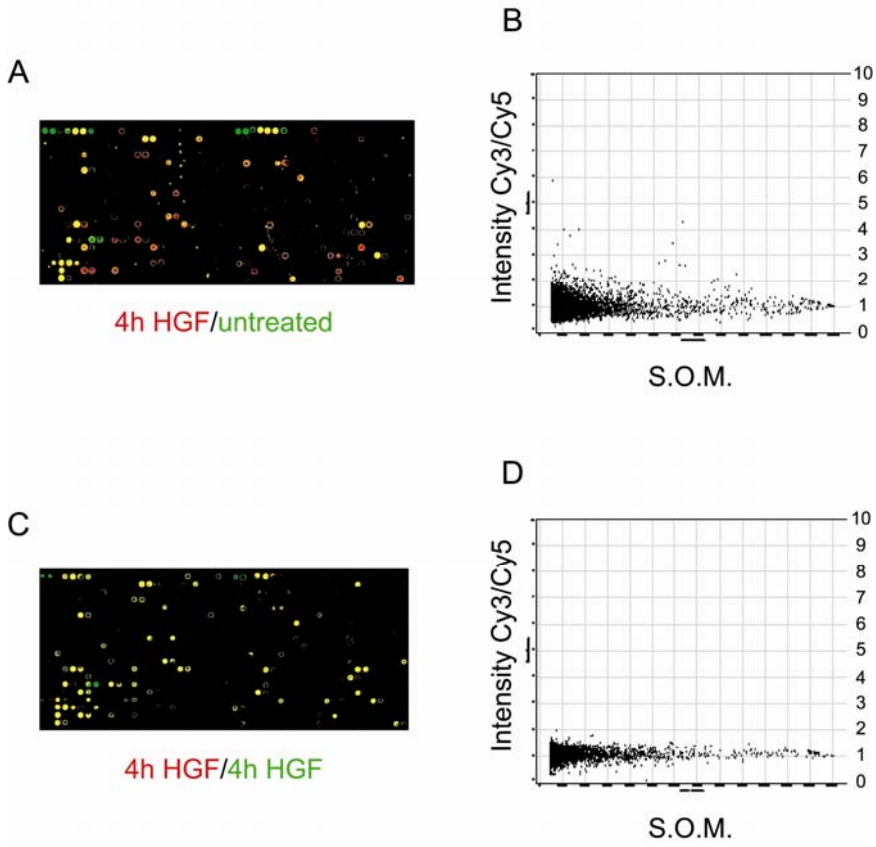


**Figure 14. Microarray analysis of HGF-stimulated MLP29 cells.**

*cDNA probes derived from untreated or 4 hours HGF stimulated MLP29 cells were fluorescently labeled with Cy3-dUTP (green) or Cy5-dUTP (red), respectively. These probes were applied simultaneously onto the microarray, and the two fluorescent images were scanned with a fluorescence laser-scanning device. (A and C) Representative area of the micro array comparing untreated and 4 hours HGF stimulated MLP29 cells (A, 4h HGF/untreated) and probes deriving only from 4 hours HGF-stimulated samples (background control, C, 4h HGF/4h HGF). The differential expression of each gene was calculated from the relative intensity of the Cy5 versus Cy3 fluorescent signal (Intensity Cy3/Cy5) Green and red fluorescent signals indicated genes whose expression levels were relatively higher in cells untreated or HGF-stimulated, respectively. (B,D) Representative plot of the differential gene expression comparing either untreated and 4 hours HGF stimulated cells (B) or two 4 hours HGF stimulated probes (D). Note that overall, the expression of most genes was not affected by HGF stimulation (Intensity Cy3/Cy5 of most of the gene =1) and that very few genes were found to be differentially regulated in the control experiment (D). Every dot in the plot corresponds to 1 gene spotted on the microarray. Only genes with more than 5,000 of the value of sum of median (S.O.M.) and with an average fold induction (Intensity Cy3/Cy5) of more than 1.8 fold were selected.*

| Functional category and gene name | GDB accession number | Unigene ID | Average fold induction |
|---|---|---|---|
| **Transcription/Chromatin** | | | |
| High mobility group AT-hook 2 | BG073094 | Mm.157190 | 3.76 |
| similar to retinoic acid inducible protein 3 | BG064659 | Mm.308014 | 2.62 |
| Nhp2 like protein 1 | BG070586 | Mm.29504 | 2.57 |
| Eukaryotic translation elongation factor 1 ψ | BG071596 | | 2.56 |
| Immediate early response 3 | BG067693 | Mm.25613 | 2.40 |
| Mannose-P-dolichol utilization defect 1 | BG069721 | Mm.89579 | 2.34 |
| H1 histone family, member 0 | BG072463 | Mm.24350 | -2.02 |
| similar to S. cerevisiae extra spindle poles like 1 | BG073068 | Mm.288324 | -1.88 |
| **Ribosomal proteins** | | | |
| Ribosomal protein S24 | BG075285 | Mm.295727 | 2.93 |
| Ribosomal protein L30 pseudogene | BG065356 | Mm.259224 | 2.59 |
| Ribosomal protein L26 | BG073775 | Mm.296462 | 2.53 |
| Ribosomal protein S29 | BG073666 | Mm.154915 | 2.23 |
| 60s ribosomal protein | BG072862 | Mm.296898 | 2.71 |
| 60s ribosomal protein L36. | BG072993 | Mm.11376 | 2.68 |
| 60s ribosomal protein L37A | BG074193 | Mm.21529 | 2.67 |
| 40s ribosomal protein S25. | BG073074 | Mm.292027 | 2.39 |
| 40s ribosomal protein | BG073071 | Mm.288212 | 2.36 |
| **Unknown function** | | | |
| Mus musculus RIKEN cDNA 2410002F23 | BG075304 | Mm.274492 | 3.63 |
| Mus musculus ES cells cDNA | AK010617 | | 3.3 |
| Unknown | BG064603 | Mm.260885 | 2.99 |
| Mus musculus RIKEN cDNA 2310004I24 | BG065268 | Mm.22511 | 2.88 |
| Unknown | BG065508 | Mm.253156 | 2.87 |
| Unknown | BG073120 | Mm.29105 | 2.78 |
| Unknown | BG074739 | | 2.67 |
| similar to Homo sapiens hypothetical 18.6 kDa protein | BG063171 | Mm.218511 | 2.53 |
| Mus musculus expressed sequence AI314311 | BG066621 | Mm.28853 | 2.50 |
| Mus musculus adult male liver tumor cDNA | AK050391 | | 2.5 |
| Mus musculus RIKEN cDNA 2610312E17 | BG069922 | Mm.171639 | 2.49 |
| Unknown | BG064729 | | 2.48 |
| Mus musculus RIKEN cDNA 1700056A21 | BG070815 | Mm.292041 | 2.42 |
| Mus musculus hypothetical protein MGC28623 | BG064830 | Mm.227260 | 2.41 |
| Unknown | BG070904 | Mm.87337 | 2.38 |
| Mus musculus RIKEN cDNA 1110007A14 | BG064536 | Mm.181880 | 2.34 |
| Unknown | BG073642 | | 2.32 |
| Unknown | BG072480 | Mm.191936 | 2.30 |
| Unknown | BG069282 | Mm.247080 | 2.28 |
| novel DNAj domain protein (isoform 2) homolog | BG064114 | Mm.21353 | 2.24 |
| Unknown | BG075010 | | 2.24 |
| Unknown | BG063611 | | 2.22 |
| Unknown | BG073747 | | 2.21 |
| Mus musculus RIKEN cDNA 3732409C05 | BG070800 | Mm.206919 | -2.52 |
| Mus musculus RIKEN cDNA 2610019A05 | BG067446 | Mm.37985 | -2.27 |
| Unknown | BG076034 | Mm.218457 | -2.14 |
| Unknown | BG068551 | | -1.97 |
| Mus musculus RIKEN cDNA 2410081M15 | BG070969 | | -1.93 |
| Unknown | BG067442 | | -1.93 |
| Unknown | BG069525 | Mm.287837 | -1.93 |
| Unknown | BG073745 | Mm.182664 | -1.9 |
| Unknown | BG070967 | | -1.9 |
| Mus musculus hypothetical protein MGC19174 | BG070747 | Mm.277713 | -1.89 |
| Unknown | BG069868 | | -1.88 |
| Unknown | BG071371 | | -1.83 |
| Unknown | BG069643 | Mm.103999 | -1.81 |
| Unknown | BG067748 | Mm.197426 | -1.8 |
| Unknown | | Mm.324850 | -1.8 |

| Functional category and gene name | GDB accession number | Unigene ID | Average fold induction |
|---|---|---|---|
| **Apoptosis** | | | |
| Tumor necrosis factor receptor superfamily member 23 | BG064436 | Mm.290780 | 2.56 |
| Tumor necrosis factor receptor superfamily, member 12a | BC025860 | | 2.08 |
| **Cell Cycle** | | | |
| Proliferation-associated 38kDa-protein, 2G4 | BG064819 | Mm.4742 | 2.92 |
| **Energy/Metabolism** | | | |
| Ornithine decarboxylase | BG069647 | Mm.34102 | 3.84 |
| S-adenosylmethionine synthetase γ -like protein | BG073682 | Mm.29815 | 2.59 |
| Basolateral Na-K-Cl transporter | BG070245 | Mm.228433 | -1.96 |
| Isopentenyl-diphosphate δ-isomerase | BG066732 | Mm.29847 | -1.87 |
| $H^+$-transporting ATPase, V1 subunit | BG068345 | Mm.217787 | -1.83 |
| Sterol-C4-methyl oxidase -like protein | BG071087 | Mm.30119 | -1.80 |
| **Heat Shock/Stress** | | | |
| Metallothionein 1 | BG064480 | Mm.192991 | 4.19 |
| Chaperonin subunit 3γ | BG064813 | Mm.256034 | 2.47 |
| Heat shock protein 1 (chaperonin) | BC016400 | | 2.4 |
| **Matrix/Structural Proteins** | | | |
| Transgelin 2 | BG064297 | Mm.271711 | 2.80 |
| Similar to γ-actin | CK334526 | Mm.298070 | 2.86 |
| Similar to β-actin | BG062949 | Mm.133292 | 2.26 |
| Karyopherin β1 | BG069743 | Mm.251013 | 2.38 |
| Keratin complex 2, gene 8 | BG064050 | Mm.289759 | 2.36 |
| **Protein Synthesis/Translational Control** | | | |
| Polypyrimidine tract binding protein 1 | CK334425 | Mm.265610 | 2.52 |
| Splicing factor 3b, subunit 4 | BG069886 | Mm.219671 | 2.39 |
| Rribonucleic acid binding protein S1 | BG073331 | Mm.1951 | 2.27 |
| Arginine/Serine-rich splicing factor 2 | BG069422 | Mm.21841 | 2.25 |
| Small nuclear ribonucleoprotein polypeptide γ | BG073131 | Mm.326751 | 2.24 |
| Eukaryotic translation initiation factor 3, subunit 4 | BG072476 | Mm.260064 | 2.23 |
| similar to HUPF3B | BG066789 | Mm.271160 | 2.25 |
| **Signal Transduction** | | | |
| Tissue-type Plasminogen activator | BG069863 | Mm.154660 | 5.60 |
| Secreted phosphoprotein 1 | BG070062 | Mm.288474 | 2.61 |
| Protein phosphatase 1, regulatory subunit 14B | BG067423 | Mm.296842 | 2.40 |
| Ras related protein Rab | BG070192 | Mm.21936 | 2.35 |
| Mus musculus RIKEN cDNA 1300002F13 (Gene33, Mig6) | BG063865 | | 2.71 |
| Mus musculus signal sequence receptor, beta (Ssr2) | NM_025448 | | 2.42 |

**Table 1. HGF Transcripts regulated by HGF in MLP29 cells**

*The tables summarize genes whose expression levels changed significantly upon HGF treatment in comparison to mock-treated cells. Average fold induction was calculated from duplicate hybridizations and genes that showed more than ±1.8 fold changes were included. Functional categorization, GDB accession number, and Unigene ID, are based on the information given in the NIA mouse 15k cDNA clone gene ID list. Gene names indicated in red ink were validated by northern blot analysis (see figure 14 and 16).*

These genes can be clustered into several groups, as genes involved in apoptosis response, cell cycle regulation and progression, energy and metabolism, stress responses, extracellular matrix protein and cellular-structural protein, translational control, signal transduction and transcriptional control. Some of these cDNA sequences also correspond to expressed sequence tags for which the full-length sequence is not available in public domain data bases and to unknown genes.

These data showed that the microarray system was able to identify known and unknown HGF/Met transcriptionally regulated genes.

**Microarray data validation by northern blot analysis**

To verify the results of the microarray experiments, northern blot analysis on RNA samples isolated from untreated and 4 hours HGF-stimulated MLP29 cells was performed. Twenty μg of total RNA was extracted either from MLP29 in the growing phase or from 4 hours HGF stimulated. The total RNA was then electroporated on Agarose gel and immobilized onto nylon membrane. As probes for the northern blot analysis, several cDNA encoding genes found to be up or down-regulated by HGF stimulation in the microarray list were isolated from the NIA mouse 15k cDNA clone set (table1, red lines), radiolabelled and hybridized on the RNA blotted membrane (Fig.15). After the removal of the quantified background signal for every sample, the ratio between the specific signal in the untreated sample (Fig.15, -) and in the 4 hours HGF stimulated sample (Fig.15, +) was calculated and normalized against glyceraldehyde-3-phosphate dehydrogenase (G3PDH) signal in order to exclude differences due to the loading of total RNA.

The majority of the selected genes were validated by northern blot analysis. However, the fold of induction calculated by northern blot analysis was in average higher compared to microarray analysis (compare table1 red lines with Fig.15 MLP29; i.e. BG073094, microarray average fold of induction: 3.76; northern blot fold of induction: 10.9).

Among the verified genes one was a known HGF/Met transcriptional target (Tissue-type plasminogen activator, tPA, BG069863) (Hecht et al., 2004) (Paciucci et al., 1998). Three

genes were signal transduction proteins (Ras related protein Rab, BG070182; Gene33/MIG6, G063865 and Signal sequence receptor beta, Ssr2, NM_025448), one structural protein (γ-actin, CK334526), one metabolic protein (Ornithine decarboxylase, BG069647) and two apoptosis related genes (Tumor necrosis factor receptor superfamily member 12a and 23, BG064436 and BG 025860).

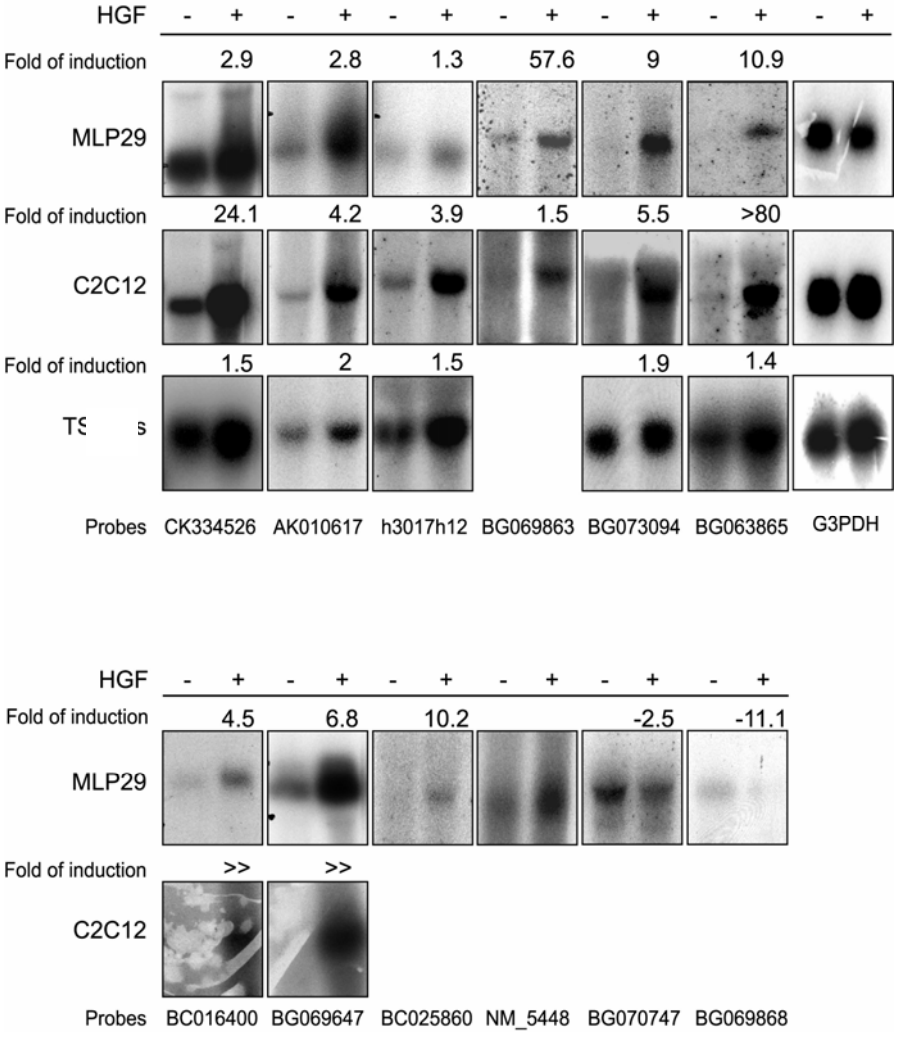


**Figure 15. Microarray data validation by northern blot analysis**

*Northern blot analysis on RNA isolated from untreated (HGF -) and 4 hours HGF-stimulated (HGF +) MLP29, C2C12 and TS cells. Several cDNA encoding genes found to be up or down-regulated by HGF stimulation in the microarray list were isolated from the NIA mouse 15k cDNA clone set and used as probes for the northern blot analysis (see also table 1 and 2, red lines). The ratio between the specific signal in the untreated sample (HGF -) and in the 4 hours HGF stimulated sample (HGF +) was calculated (Fold of induction) and normalized against the loading control G3PDH signal.*

The northern blot analysis confirmed and verified most of the genes predicted to be up or down-regulated by the micro array analysis. These results demonstrated the reliability of the microarray system as a tool for the identification of HGF/Met transcriptionally regulated genes.

**Met/HGF transcriptionally regulates the newly identified target genes in cells of different origin**

Next, we wanted to investigate whether the newly identified HGF/Met target genes were broadly regulated by HGF or if they were rather regulated in a cell line-specific manner. Using the same cDNA probes mentioned above, northern blot analysis was performed on RNA extracted from untreated and 4 hours HGF stimulated C2C12 and primary TS cells. As shown in figure 15, most of the HGF target genes were found to be regulated not only in MLP29 but in C2C12 and primary TS cells as well. Notably, even if the strength and duration of MAP kinase and Akt activation was comparable in all the three cell lines (see Fig.10), the fold of gene induction upon HGF stimulation in TS cells was, in average, lower compared to both MLP29 and C2C12.

These results suggested that most of the HGF/Met trascriptionally regulated genes were induced in three cell lines with different origin. Furthermore the data suggested that these genes may have a general function in regulating HGF/Met overall biological responses.

**Few transcripts are specifically regulated by HGF and not by other growth factors**

Since most of the genes were regulated by HGF stimulation in a cell line-independent manner, we next asked whether the transcriptional regulation of some of the newly identified genes was HGF specific. To this aim the MLP29 cells were stimulated with two other growth factors, namely Fibroblast Growth Factor-2 (FGF2) and Platelet-Derived Growth Factor (PDGF), and the regulation of target genes compared to the ones induced by HGF stimulation.

First, the ability of FGF2 and PDGF in comparison with HGF to promote Map kinase phosphorylation was assessed by western blot analysis (Fig.16). MLP29 cells were stimulated with 40ng/ml of HGF, 30ng/ml of FGF2 or with 30ng/ml of PDGF.

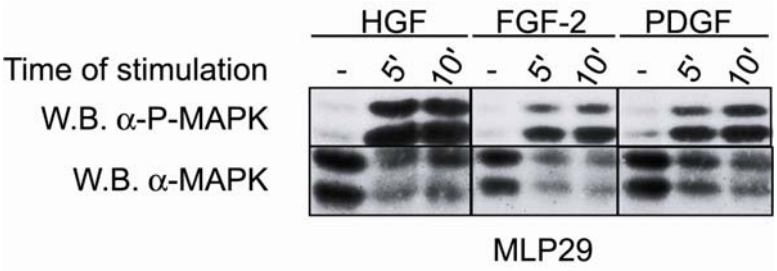


**Figure 16. HGF, FGF2 and PDGF promote Map kinase phosphorylation in MLP29**

*MLP29 cells were stimulated with 40ng/ml of HGF, 30ng/ml of FGF2 or with 30ng/ml of PDGF. The cells were then harvested at different time points and 20μg of the total lysate for each experimental condition were directly analyzed by western blotting using either an α-phospho-Map kinase (W.B. α-P-MAPK) or α-Map kinase (W.B. a-MAPK) specific antibody that was used as an internal protein loading control.*

The cells were then harvested at different time points and 20μg of the total lysate for each experimental condition were directly analyzed by western blotting using either an α-phospho-Map kinase or α-Map kinase specific antibody used as an internal protein loading control.

Even if HGF was found to be the most potent Map kinase activator in MLP29 at 5 and 10 minutes upon stimulation, FGF2 and PDGF stimulation led to a comparably strong increase in Map kinase phosphorylation.

Once verified that HGF, FGF2 and PDGF were able to activate Map kinase in a comparable manner downstream of their respective tyrosine kinase receptors, total RNA was extracted from both untreated or 4 hours HGF, FGF2 or PDGF stimulated MLP29 cells. Twenty μg of the total RNA were then subjected to northern blot analysis using as probes some of the HGF target genes (Fig.17). One gene was found to be mainly regulated by FGF2 (BC016400), three genes were found to be equally regulated by HGF, FGF2 and PDGF (CK334526; BC016400; BG064297), one gene was found to be mainly regulated by HGF and FGF2 (BG073094) and one gene was found to be mainly regulated by HGF (BG063865).

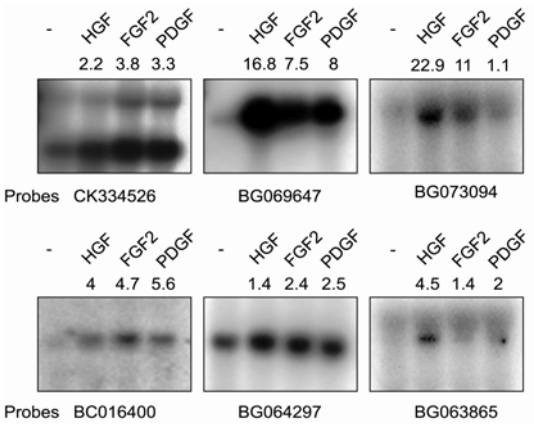


**Figure 17. Northern blot analysis of HGF, FGF2 or PDGF stimulated MLP29 cells**

*MLP29 cells were stimulated with 40ng/ml of HGF, 30ng/ml of FGF2 or with 30ng/ml of PDGF, total RNA was extracted and analyzed by northern blotting. Three genes were found to be equally regulated by HGF, FGF2 and PDGF (CK334526; BC016400; BG064297), one gene was found regulated by HGF and FGF2 (BG073094), one gene was found regulated by FGF2 (BC016400) and one gene was found regulated by HGF (BG063865). The ratio between the specific signal of the untreated sample (-) and the 4 hours stimulated sample (HGF, FGF2 and PDGF) was calculated and normalized against the loading control G3PDH signal.*

**MIG6 is specifically up-regulated by HGF stimulation**

Among the highly regulated genes, we identified and concentrated further experiments on the gene encoding Mig6 adaptor protein (GDB accession number: BG063865) as a HGF transcriptionally regulated target gene (Fig.15 and 17). As described previously, mig6 expression was induced between 1.4 – and 80-fold by 4 hours HGF stimulation depending on cell type and experiment (Fig.15). In contrast, its expression was only mildly induced by FGF-2 and PDGF (Fig.17), although both growth factors induced robust phosphorylation of Map kinase in MLP29 cells (Fig.16).

Next, mig6 induction upon HGF stimulation was examined in a more detailed northern blot analysis. MLP29 were stimulated with 40ng/ml of HGF for 1, 2, 4 and 6 hours and the northern blot analysis performed using the mig6 radiolabelled probe (Fig.18). The northern blot in figure 18 shows that mig6 mRNA was half maximally induced after 1 hour HGF stimulation and the presence of the mRNA was sustained at high level for a further 6 hours after HGF stimulation.

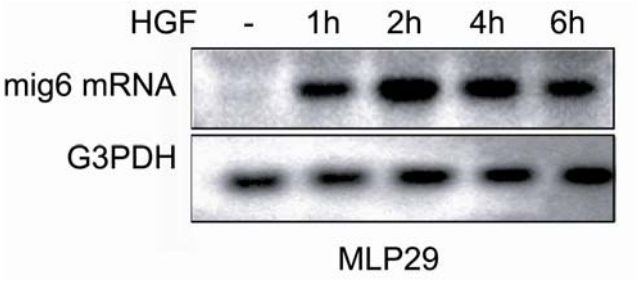


**Figure 18. Northern blot analysis of the mig6 transcript induction upon HGF stimulation**

*MLP29 were stimulated with 40ng/ml of HGF for 1, 2, 4 and 6 hours, total RNA was extracted and the northern blot analysis performed using the Mig6 radiolabelled probe. mig6 mRNA was half maximally induced after 1 hour HGF stimulation. G3PDH probe was used as an internal loading control.*

Furthermore, Mig6 protein was found to be also induced upon HGF stimulation. At different time points upon HGF stimulation, total proteins were extracted from MLP29 and western blot analysis was performed using the anti-Mig6 specific antiserum (Fig.19A). Consistent with the mig6 mRNA induction after HGF stimulation, Mig6 protein was strongly induced reaching the half maximal level at 1 hour HGF stimulation. The western blot analysis in figure 19 A shows a robust and sustained induction up to 8 hours of HGF stimulation. Moreover we asked whether Mig6 protein was up-regulated in a more physiological cell system such as the primary embryonic hepatocytes. Using the Mig6 specific antibody, western blot analysis of HGF stimulated primary hepatocytes was performed as shown in figure 19 B. Upon HGF stimulation primary hepatocytes were found to up-regulate Mig6 protein as well. The Mig6 up-regulation in primary culture followed a somehow delayed kinetics compared to MLP29 cells having the half maximal induction at around 2 hours from HGF stimulation. Consistent with these data, Met receptor tyrosine kinase was found to be co-expressed in the hepatocyte culture system.

This work provides evidence that Mig6 is a newly identified HGF-target gene, its mRNA and protein up-regulation was shown to be half maximal at 1 hour HGF stimulation. Furthermore, HGF-mediated Mig6 up-regulation was found reproducible in a more physiological system such as a primary embryonic hepatocytes culture. Furthermore Mig6 and Met receptor tyrosine kinase were demonstrated to be co-expressed in hepatocytes.

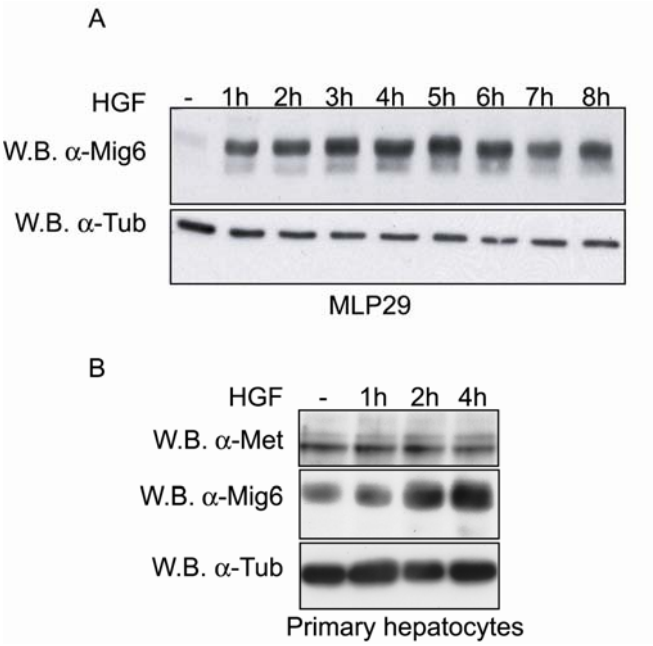


**Figure 19 Western blot analysis using Mig6 specific antibody of HGF-stimulated MLP29 and primary hepatocytes**

*(A) At different time points upon stimulation with 40ng/ml of HGF, total proteins were extracted from MLP29 and western blot analysis was performed using the anti-Mig6 specific antiserum (W.B. α-Mig6). Mig6 protein was strongly induced by HGF, reaching the half maximal level at 1 hour of stimulation. (B) Primary hepatocytes were stimulated with 40ng/ml of HGF for 1, 2 and 4 hours, total proteins were extracted and analyzed by western blotting using the anti-Mig6 (W.B. α-Mig6), anti-Met (W.B.α-Met) and anti-tubulin (W.B. α-Tub) specific antibody. The half maximal induction was found to be at around 2 hours from HGF stimulation. Consistently Met protein was found to be co-expressed in the same cell culture. The wetern blot anti-tubulin (W.B. α-tub, A and B) shows that every sample contained an equal amount of total protein.*

**mig6 and met receptor tyrosine kinase transcripts are co-expressed *in-vivo***

Next the co-expression of mig6 and met transcripts in embryonic tissues was analyzed. By in situ hybridization analysis both transcripts were found to be partially co-expressed in the embryonic somitic mesoderm at embryonic day 9.5 (E9.5) (Fig.20A, B). mig6 staining was positive in developing somites (Fig.20A) whereas only the more ventral tip of the somites was positive for met expression (Fig.20B). The artificial overlay in figure 20 C shows that mig6 and met transcripts were found to be partially co-expressed in the same somitic structure at E9.5. Coronal sections of the whole mount in-situ hybridizations (Fig.20D-G) confirmed the mig6 positive hybridization signal throughout the somitic structure. Furthermore met and mig6 transcripts were found partially co-localized at the ventral tip of the somites.

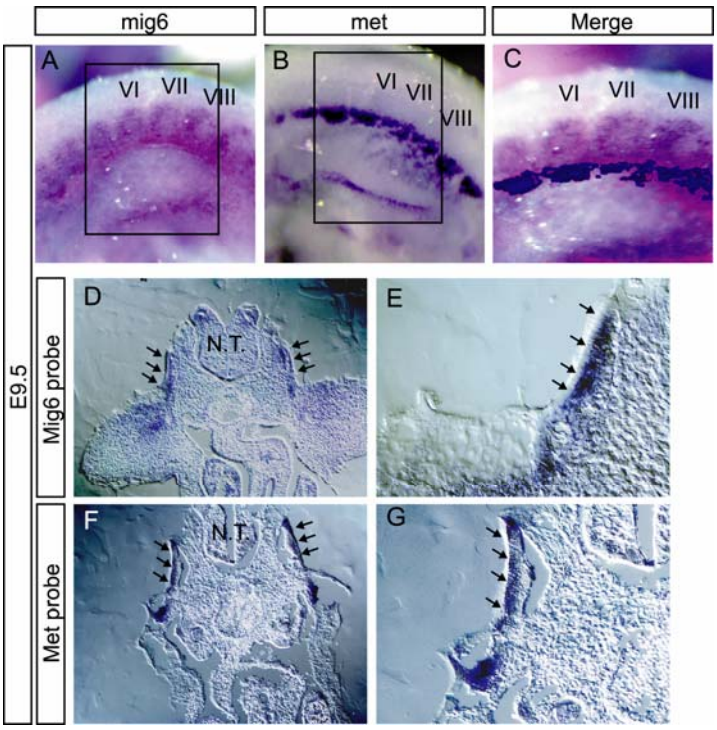


**Figure 20. mig6 and met receptor tyrosine kinase transcripts are co-*expressed* *in-vivo***

*In situ hybridization analysis using mig6 (A, D, E) and met (B, F, G) mRNA antisense-probes in the whole embryo at E9.5. Both transcripts were found to be co-expressed in the embryonic somitic mesoderm. The possible co-localization of the two transcripts was especially evident at the limb level somites (A-C, somites VI, VII and VIII). mig6 specific staining was positive in all the forming somites (A) whereas the ventral tip of the limb somites was positive for met expression (B). (C) Artificial overlay of the mig6 and met signals. mig6 and met transcripts are partially co-expressed in the same somitic structure. (D-G) Coronal sections of the whole mount in-situ hybridizations. mig6 positive hybridization signal extend throughout the somitic structure (arrow) whereas met positive signal is more evident at the ventral tip of the somites. N.T. neural tube.*

Later during development, at embryonic day 13.5, the degree of co-expression of mig6 and met transcripts was higher. Both transcripts were found in the alveoli of embryonic lung, in liver parenchyma (Fig.21B and C), and in intercostal and body wall muscles of wild-type embryos (Figure 21F and G). The mig6 mRNA sense probe was used as negative control (Fig.21A and E) confirming the specificity of mig6 *in-situ* staining.

We next asked if the Met receptor was able to regulate mig6 transcript *in vivo* by the use of embryos expressing a signaling deficient Met receptor: $met^{d/d}$ (Maina et al., 1996; Maina et al., 2001). Reduced levels of mig6 mRNA in the lung and liver of E13.5 $met^{d/d}$ embryos were found (Figure 21D).

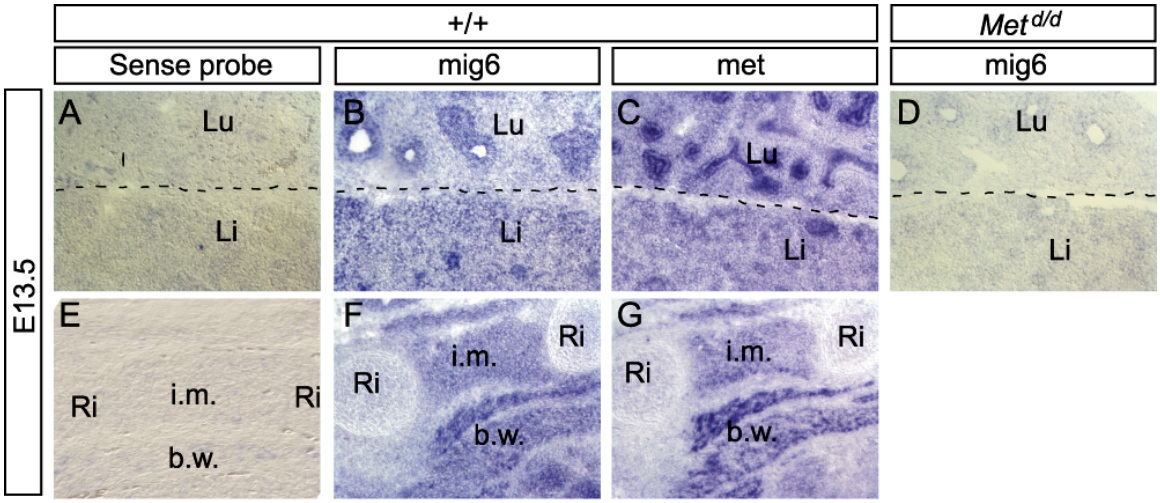


**Figure 21. mig6 and met in-situ hybridization at E13.5**

*At E13.5 mig6 and met receptor transcripts were found to be more broadly co-expressed. (B,C) Both transcripts were found in the alveoli of embryonic lung (Lu), in liver parenchyma (Li) , and in intercostal (i.m.) and body wall (b.w.) muscles of wild-type embryos (B-C; F-G). The sense probe was used as a negative control of the staining (A,E). (D) Reduced level of mig6 mRNA was found in the lung and liver parenchyma of the met$^{d/d}$ embryos. R.i. ribs. Dotted line in A-D: diaphragm.*

Furthermore using the Mig6 specific antiserum, expression of Mig6 protein was confirmed in structures positive for mig6 mRNA, including intercostal and body wall muscles (Fig.22A-B),. In order to verify further the specificity of the Mig6 immuno-staining, the antibody was pre-incubated with recombinant purified Mig6-GST fusion protein. As expected, pre-incubation of the Mig6 specific antiserum with GST alone did not have any effect on the immuno-staining signal (compare Fig.22A and B). On the other hand, pre-incubation of the Mig6 specific anti-serum with the recombinant purified Mig6 antigen strongly reduced the intensity of the immuno-staining signal (Fig.22C).

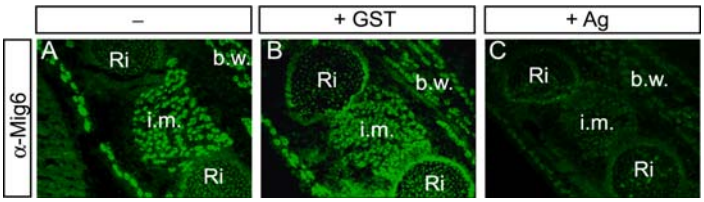


**Figure 22. Anti-Mig6 *immunostaining***

*Expression of Mig6 protein was detected in structures positive for mig6 mRNA, including intercostal (i.m.) and body wall muscles (b.w.). (B) Pre-incubation of the Mig6 specific antiserum with GST alone (GST) did not have any effect on the signal of the immuno-staining, whereas the pre-incubation of the Mig6 specific anti-serum with the recombinant purified Mig6 antigen (C, +Ag) strongly reduced the intensity of the immuno-staining signal.*

Taken together the data suggested that mig6 expression was developmentally regulated. mig6 transcripts were found in developing somites at embryonic day 9.5 where they partially co-localized with met. Moreover mig6 and met were found to co-localize at embryonic day 13.5 in the liver parenchyma, in lung alveoli, and in skeletal muscles. The results obtained using Met loss of function mice provided evidence that Met regulates mig6 transcripts *in vivo*.

**Mig6 overexpression inhibits HGF-dependent MLP29 cell migration**

The only cellular context in which Mig6 had previously been implicated was cell division (Anastasi et al., 2003; Fiorentino et al., 2000; Hackel et al., 2001; Xu et al., 2004). Since HGF/Met signaling is, however, critical for myoblast migration, the effect of Mig6 overexpression on HGF/Met-mediated cell was tested. In order to explore this function of Mig6, the full length protein was tagged using the V5 epitope ($Mig6^{FL\text{-}V5}$) and overexpressed in MLP29. We first verify by immuno-cytochemistry analysis that the fusion protein was overexpressed in MLP29 cells and that it was recognized by both the anti-Mig6 and the anti-V5 specific antibody. MLP29 cells were transfected with a control plasmid encoding the $LacZ^{V5}$ fusion protein (Fig.23A-C) or with the $Mig6^{FL\text{-}V5}$ encoding plasmid (Fig.23D-F). As shown in figure 23A, the Mig6 immuno-staining did not show any Mig6 overexpressing cells upon transfection of the control $LacZ^{V5}$ plasmid, whereas cells expressing high level of the $LacZ^{V5}$ protein were immuno-stained using a V5

specific antibody (Fig.23B, C). On the other hand the transfection of the Mig6$^{FL-V5}$ construct led to the overexpression of Mig6 protein (Fig.23D) that was recognized by immuno-fluorescence using both the V5 and the Mig6 specific antibody (Fig.23E, F).

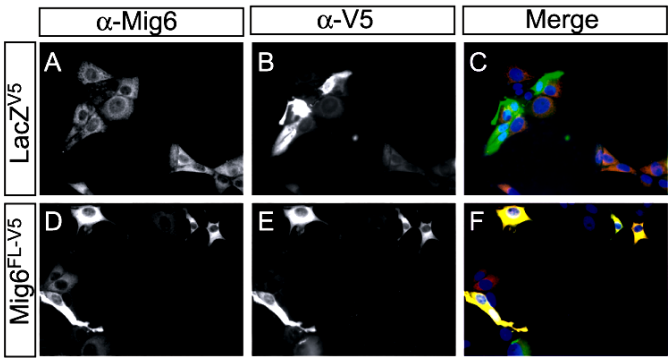


**Figure23.** Mig6$^{FL-V5}$ **fusion protein detection by immuno-fluorescence** *MLP29 cells were transfected with a control plasmid encoding the* LacZ$^{V5}$ *fusion protein (A-C) or with the* Mig6$^{FL-V5}$ *encoding plasmid (D-F). The transfected cells were immuno-stained using both the anti-Mig6 (A,D, red channel) and the anti-V5 (B,E, green channel) specific antibody. The overexpressed Mig6$^{FL-V5}$ protein is recognized by both the specific antibody (C,F, yellow signal).*

Once verified that the Mig6$^{FL-V5}$ construct was able to overexpress the tag version of the Mig6 protein we analyzed the effects of Mig6 on HGF/Met-mediated cell migration in the Boyden chamber migration assay. This assay is composed of a porous membrane that separates an upper and lower compartment. Oval cells were either transfected with a plasmid encoding yellow fluorescent protein (YFP) or co-transfected with plasmids encoding full-length Mig6$^{FL-V5}$ and YFP in a ratio of 5:1. For each experimental condition equal numbers of cells were either seeded onto coverslips for immunocytochemical analysis or onto the upper compartment of the membrane and exposed to 40ng/ml of HGF or 10% fetal bovine serum (FBS) in the lower compartment. We verified first that the YFP-positive cells were overexpressing the Mig6$^{FL-V5}$ fusion protein by immuno-cytochemistry analysis. As shown in figure 24 A-C all YFP positive cells were overexpressing Mig6 protein. It has to be noted that since the Mig6$^{FL-V5}$ encoding plasmid was transfected in a five times excess in respect to the YFP plasmid, several cells were found to express the Mig6 recombinant protein being negative for YFP expression. The transfection efficiency was calculated to be around 70%.

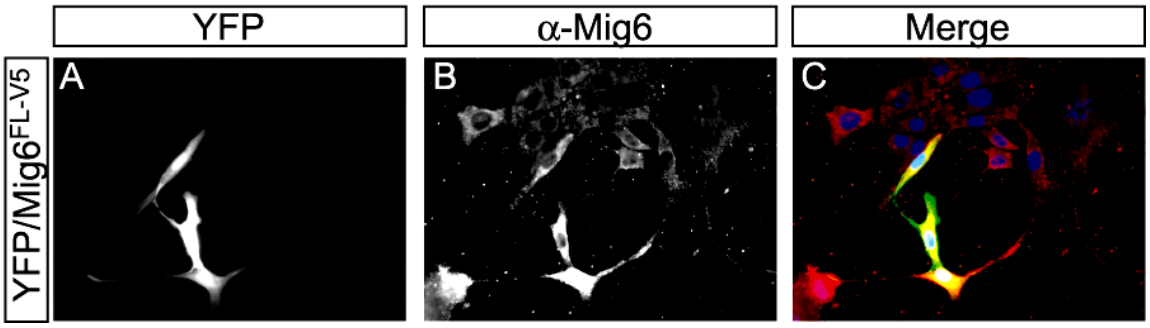


**Figure 24. YFP-positive cells overexpress the Mig6$^{FL-V5}$ fusion protein.**

*MLP29 were co-transfected with plasmids encoding full-length Mig6$^{FL-V5}$ and YFP in a ratio of 5:1. The merge (C) of the YFP signal (A) and the Mig6 specific immuno-fluorescence signal (B) shows that all the YFP-positive cells co-express Mig6$^{FL-V5}$ (B) fusion protein.*

Cell migration through the membrane into the lower compartment was stimulated by HGF in a dose-dependent manner (See Fig.28 E and 29). At 40ng/ml HGF, the migration of transfected YFP-positive cells was enhanced between 30 to 40-fold over unstimulated cells (Fig.25E). Figure 25 A-D shows representative images of YFP/Hoechst dye-labeled cells which migrated into the lower compartment of the Boyden chamber. The presence of Mig6 reduced HGF-stimulated cell migration approx. 3-fold (Fig.25E, $p<0.001$, t-test). In contrast, cell migration stimulated with 10% FBS was unaffected by Mig6 overexpression ($p=0.121$, t-test).

Since Mig6 overexpression reduced cell proliferation under a variety of conditions (Fiorentino et al., 2000; Hackel et al., 2001) we asked whether the effect on cell migration could be secondary to reduced cell proliferation. Transfected cells were therefore exposed to 1.6 µg/ml of the DNA polymerase inhibitor aphidicolin (Ikegami et al., 1978) 24h prior to plating onto the membrane and the assay was further conducted in the presence aphidicolin. In order to verify that the Aphidicolin treatment was efficiently able to block proliferation we performed a BrdU incorporation assay. The assay consists of incubating cells with a Uridine homologous, BrdU, which is incorporated by DNA polymerase into newly synthesized DNA. The BrdU is then detected by the use of an anti-BrdU specific antibody, therefore identifying the cells that are actively synthesizing DNA.

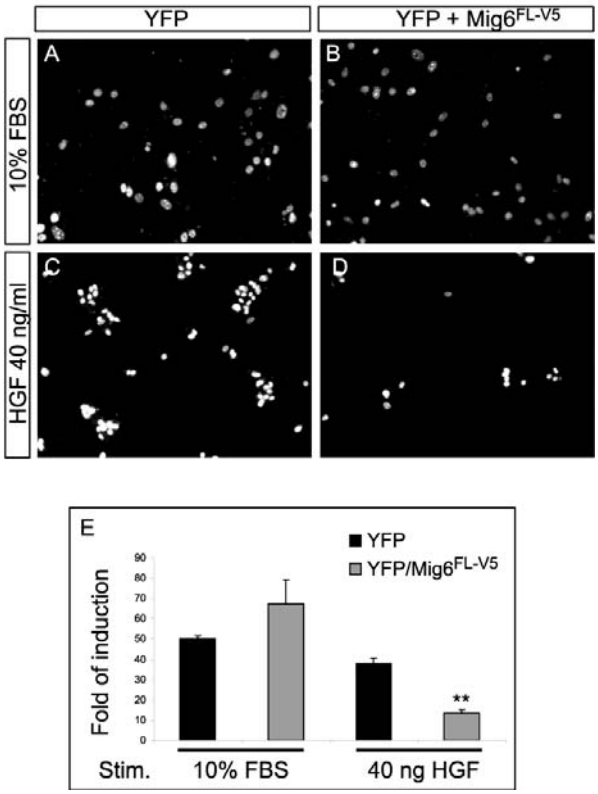


**Figure 25. Mig6 overexpression inhibits HGF-mediated migration.**

*Oval cells were either transfected with a plasmid encoding Yellow Fluorescent Protein (YFP) or co-transfected with plasmids encoding full-length Mig6-V5 and YFP in a ratio of 5:1 (YFP/Mig6$^{FL-V5}$). (A-D) Representative images of YFP positive/Hoechst dye-labeled cells which migrated into the lower compartment of the Boyden chamber in response to either serum (10% FBS) or 40ng HGF. (E) Quantification under different experimental conditions of cell migration expressed as fold of induction over unstimulated cells. Mig6 overexpression reduced HGF-stimulated cell migration approx. 4-fold ($p<0.001$, t-test). In contrast Mig6 overexpression was unaffecting serum-stimulated cell migration ($p=0.121$, t-test).*

MLP29 cells were plated onto coverslips and stimulated over-night with 40ng/ml of HGF. The cells were then incubated for 2 hours with 10µM of BrdU and immuno-stained using an anti-BrdU specific antibody. The percent of BrdU positive cells (proliferating) over negative (quiescent) was then scored. Typically, Aphidicolin treatment reduced the incorporation of BrdU into MLP29 cells 6 to 15-fold (data not shown). Under these conditions, HGF-stimulated cell migration was also significantly reduced by Mig6 overexpression indicating that Mig6 had a direct influence on Met-mediated cell migration independently of its effect on cell proliferation (Fig. 26, $p<0.01$, t-test).

Together these data indicate that Mig6 overexpression is sufficient to inhibit HGF-dependent migration in MLP29 cells. Furthermore this effect was found to be specifically downstream of HGF/Met. The overexpression of Mig6, in fact, is not sufficient to inhibit serum-dependent MLP29 cell migration, suggesting that the cells maintain the potentiality to migrate in the presence of high amount of exogenous Mig6

protein. Moreover the inhibition of HGF-dependent migration via Mig6 was not found to be a secondary effect of the known Mig6 anti-mitogenic effect, since the same result was obtained in the presence of the mitogenic inhibitor Aphidicolin.

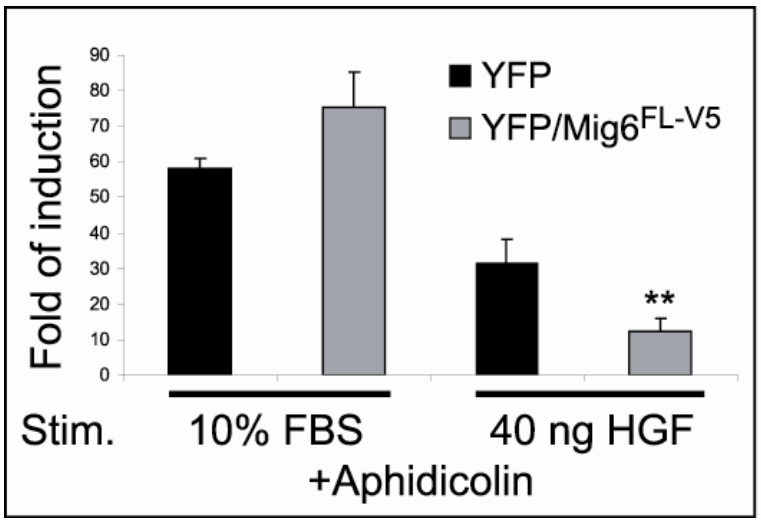


**Figure26. Mig6 inhibits cell migration independently of cell proliferation**

*Transfected cells were exposed to 1.6 µg/ml of the DNA polymerase inhibitor Aphidicolin 24h prior to plating onto the membrane. The migration assay was conducted in the presence of Aphidicolin. Mig6 overexpression (grey bars) inhibited HGF-, but not serum-, mediated migration of about 3-times compared to controls (black bars) also in the presence of the proliferation inhibitor Aphidicolin ($p<0.001$, t-test).*

**Mig6 is a physiological suppressor of Met-mediated cell migration**

We next investigated whether endogenous Mig6 suppressed HGF/Met-mediated cell migration by knocking down Mig6 protein levels using RNA interference (Elbashir et al., 2001a; Elbashir et al., 2001b). MLP29 cells were transfected with either siRNAs specific for green fluorescent protein (GFP) or mig6 and the levels of Mig6 protein analyzed by immunostaining and immunoblotting. mig6 siRNA, but not control GFP siRNA, specifically knocked down Mig6 immunoreactivity 96 hours after transfection (Fig.27A,B). mig6 siRNA suppressed HGF-stimulated induction of Mig6 (Fig.27C, compare 4h time point +/- mig6 siRNA). The knock down was specific for Mig6, since endogenous alpha-tubulin and Met levels were unaffected (Fig.27C and data not shown).

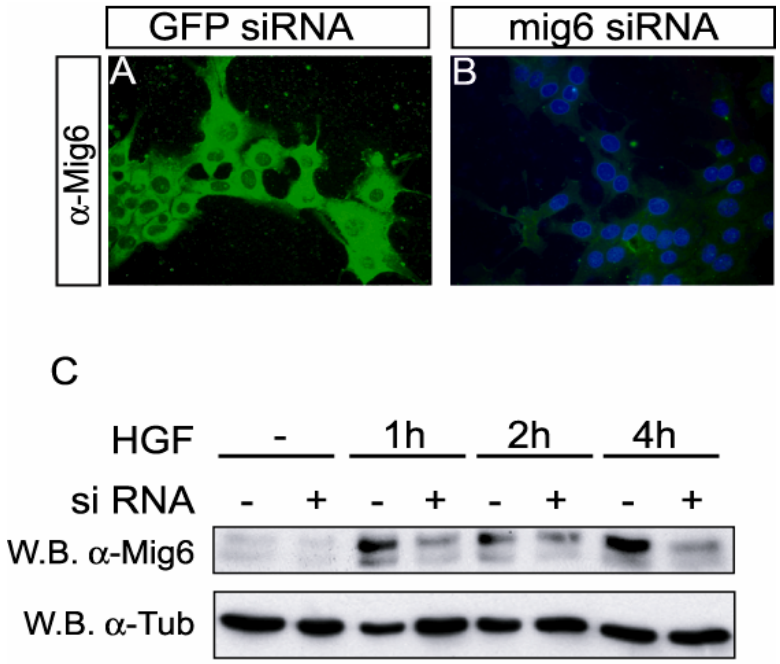


**Figure 27. mig6 siRNA efficiently knock down Mig6 protein**

*(A,B) MLP29 cells were transfected with either GFP specific siRNAs (A) or with mig6 specific siRNAs (B) for 4 days, then fixed and Mig6 protein levels detected using the Mig6 specific antibody. (B) Cells were visualized using Hoechst dye. Note the efficient knock-down of Mig6 protein level upon transfection of mig6 siRNAs. (C) Western Blot analysis of MLP29 transfected with control GFP siRNAs (-) or mig6 specific siRNAs (+) for 4 days. After transfection the cells were stimulated with 40 ng/ml of recombinant HGF for the indicated times and cell lysates analyzed using SDS-PAGE and immunoblotting using α-Mig6 or α-tubulin specific antibodies. Note the specific reduction of Mig6 levels most clearly seen at the 4h time point.*

To investigate Mig6's loss of function role in cell migration, controls and mig6 siRNA transfected cells were harvested and seeded onto the membrane (upper compartment) of the Boyden chamber. Cells were allowed to attach to the membrane and different concentrations of HGF were added to the lower chamber for 16 hours. Figure 28 A-D shows representative images of cells which migrated into the lower compartment. Quantification of the cells revealed that under optimal HGF concentrations condition, knock down of Mig6 enhanced cell migration three-fold (Fig.28E). Because the transfection efficiency was certainly less than 100% and yet all cells were counted, the effect of the Mig6 knock down may be underestimated. Similar results were obtained with a separate set of siRNA oligonucleotides (Fig.29). These findings demonstrated that Mig6 is required in order to suppress HGF/Met-mediated cell migration of MLP29.

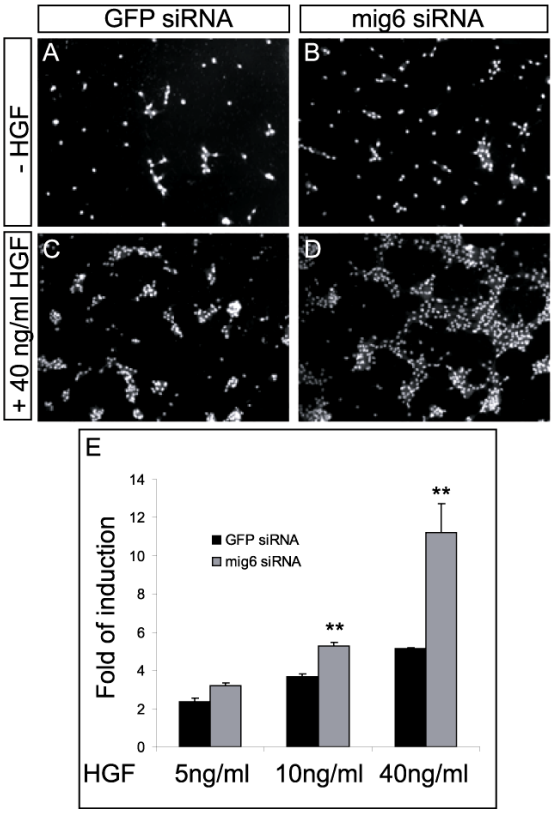


**Figure 28. Endogenous Mig6 inhibits HGF-induced cell migration in MLP29.**

*(A-D) Representative fields of Hoechst dye-labeled GFP siRNA- and mig6 siRNA-transfected MLP29 cells that have migrated into the lower compartment of the Boyden chamber in the presence (+ HGF 40ng/ml) or absence of HGF (-HGF). MLP29 cells were transfected with either GFP specific siRNAs (A,C) or with mig6 specific siRNAs (B,D) for 4 days, then transfected a second time for 24h, harvested and plated into the upper compartment of the Boyden chamber and allowed to attach on the membrane. HGF was then added to the media of the lower compartment of the Boyden chamber and the cells were allowed to migrate for 16h. (E) Quantification of MLP29 migration expressed as fold of induction over unstimulated cells. Increasing concentrations of HGF were added to the lower Boyden chamber after transfection of either control GFP siRNAs (black bars) or Mig6 siRNAs (gray bars). 5 ng/ml HGF, p=0.02; 10ng/ml HGF, p<0.0002; 40ng/ml HGF, p<0.01, t-test.*

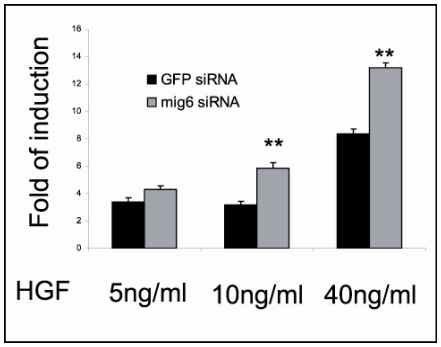


**Figure 29. A second independent set of siRNA oligos confirm that endogenous Mig6 inhibits HGF-mediated cell migration**

*MLP29 cells were transfected with either GFP specific siRNAs (A,C) or with a second set of mig6 specific siRNAs for 4 days, then transfected a second time for 24h, harvested and plated into the upper compartment of the Boyden chamber and allowed to attach on the membrane. The graph shows the quantification of MLP29 migration expressed as fold of induction over unstimulated cells. Increasing concentrations of HGF were added to the lower Boyden chamber after transfection of either control GFP siRNAs (black bars) or the second set of mig6 siRNAs (gray bars) 5 ng/ml HGF, p=0.08; 10ng/ml HGF, p<0.009; 40ng/ml HGF, p<0.01, t-test.*

**Endogenous Mig6 inhibits HGF-mediated cell migration independently of cell proliferation**

Mig6 was found to suppress proliferation upon overexpression of the recombinant protein (Fiorentino et al., 2000). Consistent with these data, Mig6 was also found to enhance cell proliferation upon endogenous protein knock-down by specific antibody microinjection (Fiorini et al., 2002). Accordingly with these observations knock-down of mig6 by siRNA also enhanced cell proliferation in MLP29 (Fig 30).

In order to separate HGF and Mig6 effects on cell migration from cell proliferation, we assayed cell migration in the presence of the cell cycle inhibitor Aphidicolin. MLP29 cells were transfected with control or mig6 siRNA specific oligos for 96 hours. The last 24 hours the cells were exposed either to a DiMethyl SulfOxide (DMSO) control media or to a media containing 1.6µg/ml Aphidicolin. Cells were then harvested, seeded either onto coverslips, for testing the proliferation rate in the different experimental condition, or onto the upper compartment of the Boyden chamber.

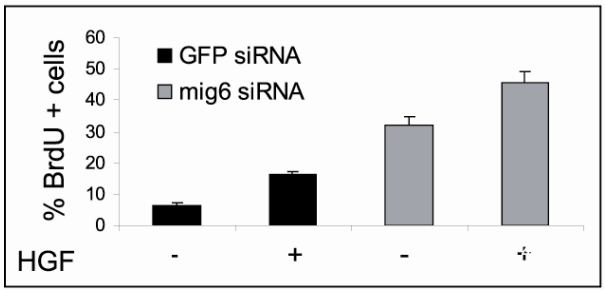


**Figure 30. The knock-down of Mig6 by siRNA enhanced cell proliferation in MLP29**

*MLP29 cells were transfected with control (black bars) or mig6 siRNA specific oligos (gray bars) for 96 hours. The last 24 hours the cells were exposed either to a DMSO control media or to 1.6µg/ml Aphidicolin. Cells were then harvested, seeded either onto coverslips and incubated with BrdU together with (HGF +) or without (HGF -) 40 ng/ml of HGF for 3 hours. The BrdU was then visualized with a α-BrdU specific antibody. The proliferation rate under different experimental conditions was calculated counting the percent of BrdU positive over the total Hoechst dye-positive cells.*

After the cells attached to the membrane, 40ng/ml of HGF was added to the lower compartment of the Boyden chamber. The experiments were conducted in the presence of either 1.6µg/ml of Aphidicolin or DMSO control media.

Consistently with previous observations, HGF stimulation and the knock-down of Mig6 protein by siRNA (Fig.30, gray bars) led to an increase in BrdU incorporating cells

compared to control conditions (Fig.30, black bars). Interestingly upon HGF stimulation, the knock down of Mig6 protein by siRNA significantly increased BrdU incorporating cells in respect to the control (Fig.30, compare black bars and grey bars). Incubating the cells for 24 hours with Aphidicolin resulted in a significant decrease in cell proliferation under different conditions (not shown).

Figure 31A-D shows representative images of Hoechst labeled cells that have migrated in response of HGF to the lower side of the filter under different experimental conditions. The knock-down of Mig6 protein by siRNA (Fig.31B,D) resulted in a significant increase of HGF-induced migration in respect to the control in the absence (Fig.31A,B) and in the presence of Aphidicolin (Fig.31C,D). Interestingly the Aphidicolin treatment resulted in an overall decrease in the number of migrating cell into the lower side of the membrane (compare Fig.31E, GFP siRNA Aphidicolin- and GFP siRNA Aphidicolin+). Since the same number of cells were plated onto the membrane, this difference is likely to represent the effect on proliferation of HGF and Mig6 during the migration assay.

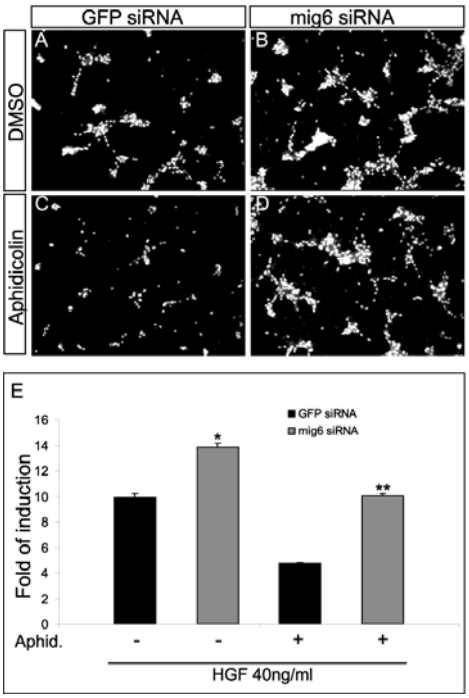


**Figure 31. Endogenous Mig6 inhibits HGF-stimulated migration independently of cell proliferation**

*Representative Hoechst dye-labeled MLP29 transfected with either GFP siRNA specific oligos (A,C) or with mig6 siRNA specific oligos (B,D) that have migrated into the lower Boyden chamber in response of HGF. The cells were transfected with siRNA for 4 days, then transfected a second time for 24h, harvested and plated into the upper compartment of the Boyden chamber and allowed to attach on the membrane. During the last 24 hours cells were exposed to either DMSO (A,B) or to 1.6 µg/ml Aphidicolin (C,D). (E) Quantification of MLP29 cell migration expressed as fold of induction over unstimulated cells. Migration was enhanced in cells transfected with Mig6 siRNA (grey bars) compared to GFP siRNA (black bars) in the absence or the presence of Aphidicolin ($p=0.019$ and $p<0.002$ respectively, t-test).*

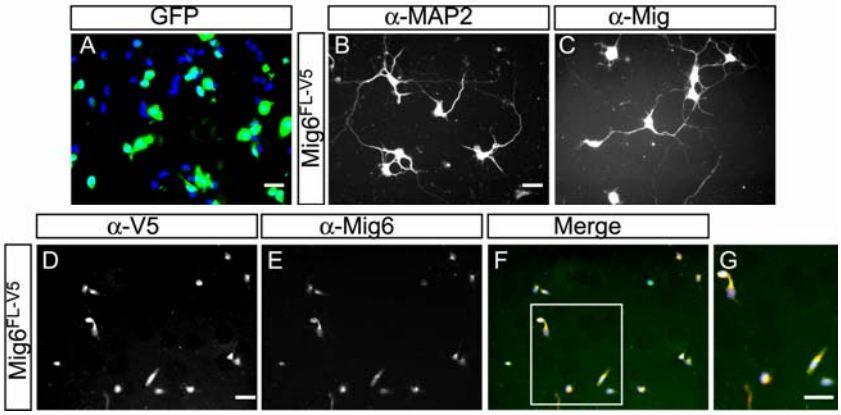


**Figure 32. E15.5 cortical neurons over-express the Mig6-V5 construct**

*Cortical neurons were dissected from E15.5 mouse embryos and electroporated with expression plasmids encoding either GFP (A) or V5-epitope tagged Mig6FL (Mig6$^{FL-V5}$; B-G). Electroporated cells were plated for either 24 hours (A) or 3 days (B,C) onto coverslips for immunocytochemical analysis. (A) GFP fluorescent cells (green) among untransfected Hoechst dye-labeled cells. Transfection efficiency was generally 40-70%. (B,C) After transfection with Mig6$^{FL-V5}$, cells were cultured for 3 days and immunostained with anti-MAP2 (B) or anti-Mig6 antibodies (C). Note that Mig6 did not affect neuronal differentiation. (D-G) Cells were fixed and doubly labeled using α-V5 (D) and α-Mig6 (E) antibodies. Note that nearly all V5-labeled cells also express Mig6. Similar results were obtained with a HIS-epitope tagged Mig6 expression plasmid (data not shown).*

**Overexpression of Mig6 suppresses HGF/Met-mediated cortical neuron migration**

Having established a critical role for Mig6 in HGF/Met-mediated migration of MLP29 cells, we next asked whether the functions of Mig6 were specific to cells of hepatic origin, or whether Mig6 had a more general role in controlling cell migration across different cell lineages. The HGF/Met system has previously been implicated in the migration of embryonic cortical interneurons from the ventral to the dorsal telencephalon (Powell et al., 2001). Consistent with a potential role as modulator of Met signaling, mig6 mRNA was found co-expressed with met in the cortical plate of E15.5 cortex, albeit at low levels (not shown).

To overexpress Mig6 in embryonic cortical neurons, we used two different tagged version of Mig6: a His-epitope-tagged (Mig6$^{FL-His}$) and a V5-epitope-tagged (Mig6$^{FL-V5}$). Cortical neurons were dissected out from E15.5 embryo cortex and electroporated with

different constructs. We first addressed the efficiency of electroporation of primary neurons by transfecting a control plasmid encoding the Yellow Fluorescent Protein (YFP). Around 40 to 70 percent of the Hoechst stained neurons were identified to be YFP positives (Fig.32A) indicating a high transfection efficiency.

Mig6 overexpression did not affect differentiation of cortical neurons as judged by microtubule-associate protein 2 (MAP2) expression, nor survival (figure 32B,C and data not shown)

Mig6$^{FL\text{-}V5}$plasmid was then electroporated and the expression of the recombinant protein verified by immuno-cytochemistry using the combination of the α-Mig6 and the α-V5 specific antibody (Fig.32D-G). Nearly all cortical neurons were found positive for both Mig6 (Fig.32E-G) and V5 expression (Fig.32D,F,G).

After having verified the overexpression of the recombinant Mig6$^{FL\text{-}V5}$ protein, HGF-induced cortical neuron migration was assayed either without any electroporation or 24 hours after electroporation of YFP, Mig6$^{FL\text{-}His}$ or Mig6$^{FL\text{-}V5}$ expression plasmids. Quantification of all (transfected and untransfected) cells on the lower face of the porous membrane revealed a 3 to 4-fold increase of migrated cells in the presence of HGF, and a 7 to 8-fold stimulation among the GFP-transfectants. In contrast, overexpression of Mig6$^{FL\text{-}His}$ completely prevented HGF from inducing cell migration (Fig.33).

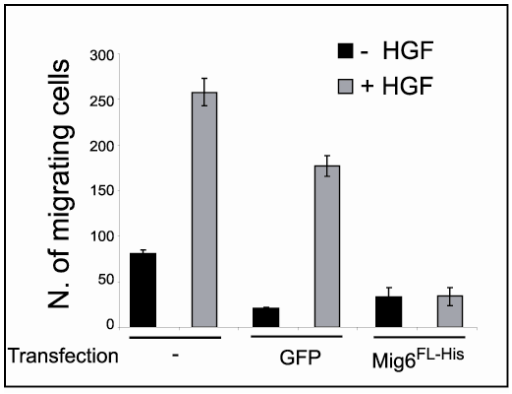


**Figure 33. Overexpression of Mig6 inhibits HGF-mediated cortical neurons migration**

*HGF-induced cortical neuron migration was assayed either without any electroporation (transfection -), with GFP (transfection GFP) or Mig6$^{FL\text{-}His}$ (transfection* Mig6$^{FL\text{-}His}$*) expression plasmids. Quantification of Hoechst positive cortical neurons on the lower face of the membrane. Non electroporated, GFP or* Mig6$^{FL\text{-}His}$ *electroporated cortical neurons were seeded onto the upper side of the Boyden chamber in the presence (black bars) or the absence (gray bars) of 50ng/ml of HGF. The cells were left to migrate for 24h, fixed and positive Hoechst nuclei counted. Mig6 was found to inhibit completely HGF-induced migration in primary cortical neurons culture (Experiment performed by Fabienne Lamballe)*

In a separate set of experiments the cells both in the upper and in the lower face of the membrane were counted. The percentage of cell in the lower face of the membrane in respect to the cell in the upper one was also calculated, having therefore a precise normalization of the migrating cells in respect to the total number of seeded one (Fig 34A,B). The cells transfected with plasmids encoding either the control $LacZ^{V5}$ or $Mig6^{FL\text{-}V5}$ in the absence or presence of HGF were compared. While $LacZ^{V5}$ control cells responded to HGF with a 6 to 7-fold higher migration rate, $Mig6^{FL\text{-}V5}$ expressing cells significantly reduced the HGF-mediated migration (figure 34A, $p<0.0001$, t-test). Furthermore, the overall ability of the cells to migrate and the specificity of Mig6 to inhibit HGF-mediated migration were assessed. Cells transfected with either $LacZ^{V5}$ control plasmid or $Mig6^{FL\text{-}V5}$ plasmid were stimulated with stromal cell-derived factor1 (SDF1) and the migration assay performed. $Mig6^{FL\text{-}V5}$ overexpression was found to be unable to inhibit the SDF1-mediated cortical neurons migration (figure 34B, $p>0.28$, t-test).

Mig6 overexpression was found therefore to inhibit HGF-mediated migration in MLP29 and in the more physiological system represented by the embryonic primary cortical neurons. Since Mig6 overexpression was not able to block SDF1-mediated migration, these data suggested that Mig6 is not affecting the overall ability of the cells to migrate but its action is rather specific for the HGF-mediated migration signals.

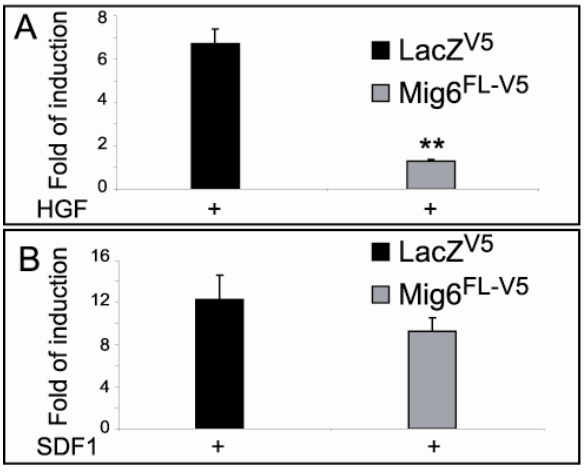


**Figure 34. Mig6 specifically inhibits HGF-mediated migration of cortical neurons**

*Quantification of migrating electroporated cortical neurons (see above and methods) with either $LacZ^{V5}$ control plasmid or $Mig6^{FL\text{-}V5}$ in the presence of either 50ng/ml of recombinant HGF ($p<0.0001$, t-test) (A) or 100 ng/ml SDF1 ($p>0.28$, t-test) (B). $Mig6^{FL\text{-}V5}$ was found to specifically inhibit HGF-mediated cortical neurons migration.*

**Mig6 suppresses HGF/Met-mediated neuronal differentiation**

Besides regulation cell migration, HGF is known as a chemo-attractant and neurite outgrowth promoting factor for subsets of central and peripheral neurons, including sympathetic neurons (Maina et al., 1998; Yang et al., 1998) (Thompson et al., 2004). To explore if Mig6 had a more general role in inhibiting HGF responses apart from cell proliferation and migration, the effects of Mig6 on neurite outgrowth of post natal primary sympathetic neurons was tested in collaboration with Jane Thompson and Alumn Davies. Postnatal sympathetic neurons of the Superior Cervical Ganglion (SCG) survive in culture without addition of neurotrophic factors. Primary culture of dissociated SCG neurons were grown for a short time in culture before being stimulated with 40ng/ml of HGF for different time. Total proteins were extracted and analyzed by western blotting using the Mig6 specific antibody. As shown in figure 35 SCGs neurons were found to up-regulate Mig6 protein in response to HGF stimulation. In this case western blot using the Map kinase specific antibody was used as an internal protein loading control.

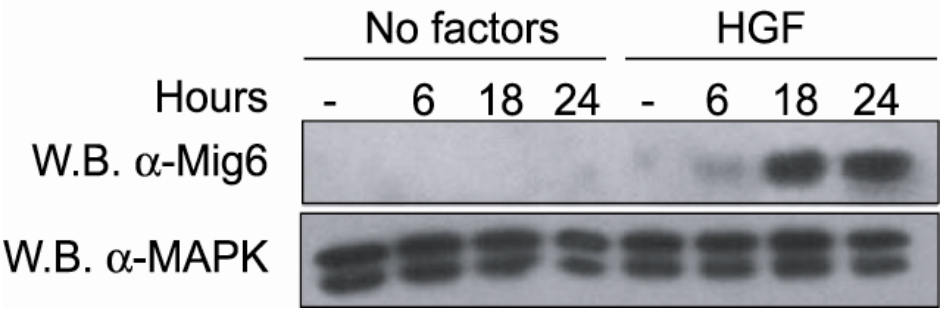


**Figure 35. P40 SCGs up-regulate Mig6 upon HGF stimulation.** *Time course of Mig6 protein induction upon HGF stimulation. Western blot analysis of post natal SCG neurons. Total lysate was extracted from SCG neurons and analyzed by western blotting using either Mig6 specific antibody (α-Mig6). Map Kinase specific antibody (α-MAPK) was used as a protein loading control (experiment performed by Jane Thompson).*

SCG neurons responded to exogenous HGF with increased outgrowth and branching of neurites (Maina et al., 1998; Thompson et al., 2004). To quantify this effect, the cells were transfected with an expression plasmid encoding YFP. The plasmid was transfected into the post natal SCG using the gene gun and Scholl analysis (see Methods) was used to determine neurite complexity. HGF (10 ng/ml) significantly increased neurite complexity and increased neurite branching as compared to non-treated control cultures (Fig.36A and 37C). The effect was most pronounced close to the soma, while there was no significant increase in complexity in the longest neurites (Fig.36A). To investigate a role of Mig6 in regulating neurite complexity, the neurite arbors of cells transfected with expression vectors encoding Mig6 plus YFP with cells expressing YFP alone was compared (Fig.36 B and 37C). Overexpression of Mig6 greatly reduced neurite outgrowth and branching of HGF-stimulated cells (Fig.36B). The effect was most pronounced close to the cell soma, where HGF had its strongest effects in comparison to control cDNAs such as YFP (Fig.36A). This effect was specific for HGF treated neurons, since in untreated neurons, expression of Mig6 did not cause a reduction of branch points (Fig.37C).

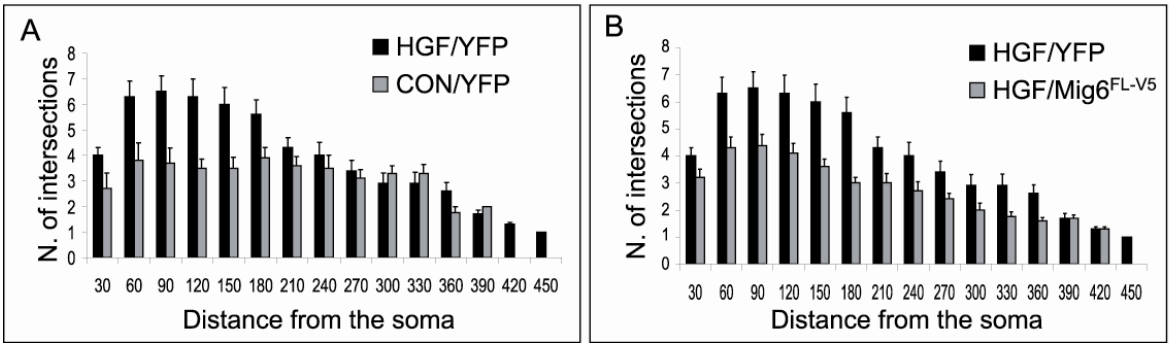


**Figure 36. Mig6 completely abolish HGF-mediated neurite outgrowth in P20 SCGs**

*(A) Scholl analysis (see methods) of P40 SCG neurons transfected with YFP alone and exposed for 48h to either control media (Con/YFP, gray bars) or 10 ng/ml HGF (HGF/YFP, black bars). (B) Scholl analysis of P40 SCG neurons stimulated with 10 ng/ml HGF after being transfected with either YFP (black bars) or YFP together with Mig6$^{FL-V5}$ (gray bars). Mig6$^{FL-V5}$ expression was able to completely block HGF-induced neurite outgrowth (compare panels D and E, gray bars) (experiment performed by Jane Thompson).*

Figure 37 A and B shows representative pictures of SCGs neurite arbors expressing either YFP alone (Fig.37A) or YFP plus Mig6 constructs (Fig.37B). Furthermore the branch points per neuron in different experimental conditions were counted (Fig. 37C). Accordingly to Mig6's role in the reduction of HGF-mediated neurite complexity, the increase in branch point number upon HGF stimulation was found to be completely abolished by the overexpression of Mig6 protein (Fig. 36C, compare HGF/YFP, HGF/MIG and CONT/YFP).

Since HGF and Met increase the survival rate of the neurons in culture we next assessed whether Mig6 overexpression was able to suppress survival. Surviving neurons in the presence of HGF were transfected with a control $LacZ^{V5}$ construct or with $Mig6^{FL-V5}$ construct and counted after 48 hours in culture. As shown in figure 38 Mig6 overexpressing neurons did not show any difference in survival rates in comparison to control transfected neurons, suggesting that Mig6 specifically inhibited Met signaling towards neurite growth.

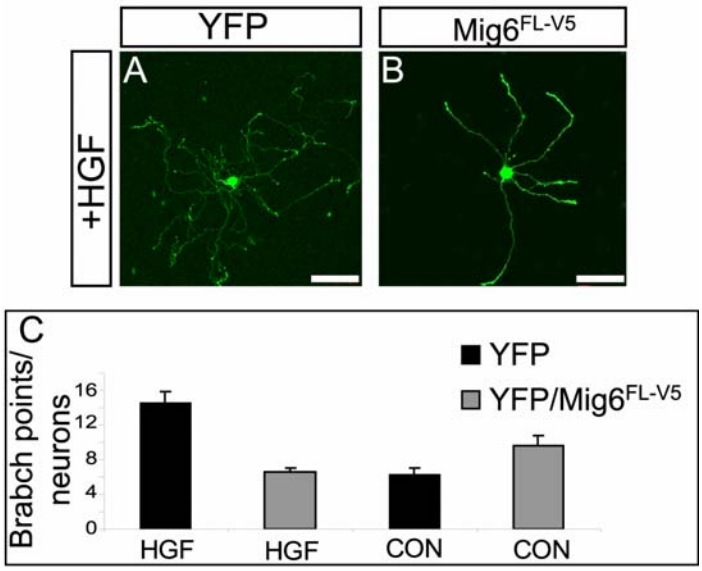


**Figure 37. Mig6 completely abolish HGF-mediated neurite outgrowth in P20 SCGs**

*(A,B) Representative postnatal SCG neurons transfected with either YFP (A) or with a mixture of YFP and $Mig6^{FL-V5}$ expression plasmids (B). Cells were grown in medium supplemented with 10ng/ml HGF for 48h. Note the significant reduction in neurite complexity of the $Mig6^{FL-V5}$-expressing cell compared to YFP control. (C) Numbers of neurite branch points per neuron in different experimental conditions. P40 SCG neurons were treated as described above and the numbers of branch points per neuron counted in the presence (HGF) or the absence (CON) of 10ng/ml HGF (experiment performed by Jane Thompson).*

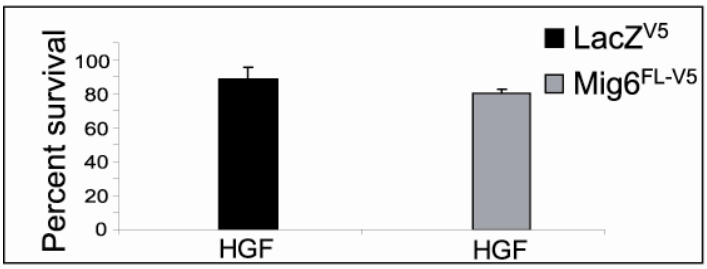


**Figure 38. Mig6 specifically inhibited Met signaling towards neurite growth**

*Percentage of surviving P40 SCG neurons in different experimental conditions. After 24h HGF exposure, the neurons were transfected with either the control $LACZ^{V5}$ (black bar) or the $Mig6^{FL-V5}$ (gray bar) expression plasmids. Upon stimulation with HGF the expression of $Mig6^{FL-V5}$ did not affect P40 SCG neuron survival (experiment performed by Jane Thompson).*

Next, Mig6 knock down experiments were performed revealing a modest increase in neurite length in mig6 siRNA-treated as compared to GFP siRNA-treated cells (Fig.39). The increase of neurite length due to Mig6 knock down was significant in processes extending furthest away from the soma. Since the induction of endogenous Mig6 protein is delayed (see Fig.35), the effect of knocking down mig6 mRNA may be visible only in the longest neurons that took the longest time to grow. These results suggested that Mig6 plays a role in suppressing neurite complexity induced by HGF/Met signaling.

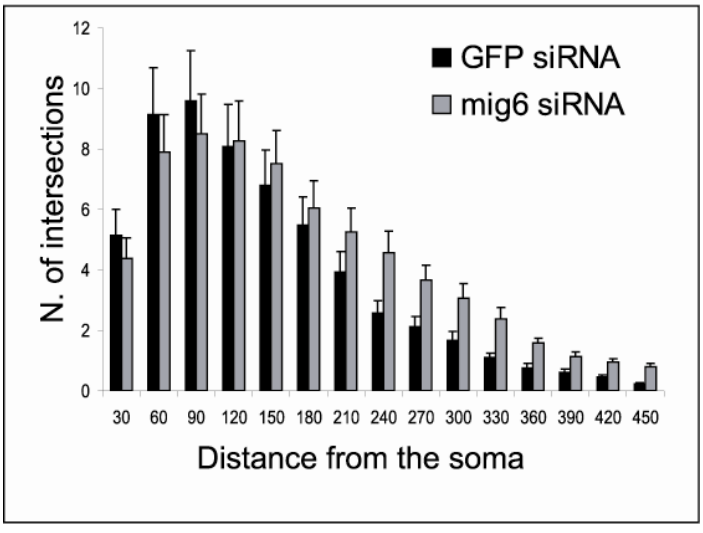


**Figure 39. Mig6 knock down in P40 SCG modestly increase in neurite length**

*Sholl analysis of SCGs neurons transfected with either mig6 specific siRNA oligos together with YFP (gray bars) or with YFP alone (black bars) in the presence of 10ng/ml HGF. Endogenous Mig6 knock-down by siRNA induced an increase of neurite branching (experiment performed by Jane Thompson).*

**The CRIB-domain of MIG6 is required and sufficient to inhibit HGF-mediated cell migration**

The mechanism of action of Mig6 downstream of EGFR/ErbB appears complex, is not well understood, and in part controversial. Mig6 was proposed to inhibit EGFR signaling by direct binding to EGFR and ErbB2, by suppressing the EGFR kinase activity, but also by a receptor distal mechanism (Anastasi et al., 2003; Fiorentino et al., 2000; Hackel et al., 2001; Xu et al., 2004). To begin dissecting the mechanism of Mig6-mediated inhibition of Met signaling, we asked whether Mig6 would directly bind Met in MLP29 cells stimulated with HGF. In pull-down experiments using bacterially-expressed, GST-tagged, purified full-length Mig6, direct association between Mig6 and Met was not found. Moreover, the minimal region that had been mapped in EGFR to be essential for the binding of Mig6 was not found in the amino acid sequence of Met (data not shown). Pull-down experiments with GST-tagged Mig6 did, however, confirm the association with Grb2 (Fig.40), which had previously been observed (Fiorentino et al., 2000). Control pull-downs with GST-tagged P21-associated serine/threonine kinase (Pak) failed to pull down Grb2 (Fig.40). This suggested the possibility that Mig6 may bind Met indirectly via Grb2 thereby inhibiting Met in a receptor-proximal fashion.

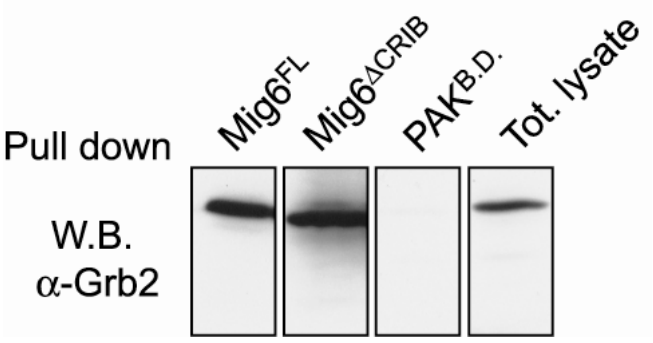


**Figure 40. Mig6 binds Grb2 *in-vitro***
*GST-Mig6$^{FL}$ and GST-Mig6$^{\Delta CRIB}$ purified fusion proteins were used to pull down endogenous Grb2 from MLP29 total cell lysate. The fusion proteins were incubated for 1 hour with total cell lysate and pulled down using glutathione-sepharose beads. Pulled down proteins were eluted from the beads and analyzed by SDS PAGE. Western blot analysis using an α-Grb2 antibody showed that Grb2 associates with Mig6 independently of its CRIB domain. A GST-PAK$^{BD}$ fusion protein was used as a negative control*

Next, the relevance of the Mig6 CRIB domain which had previously been suggested to bind the Rho family GTPase Cdc42 (Makkinje et al., 2000) was addressed. HGF had been shown to activate Rho-family GTPases in epithelial cells concomitant with a cell spreading response. Moreover, HGF-induced cell spreading was inhibited by dominant negative Cdc42 or Rac (Royal et al., 2000). Mig6 shares striking homology with the non-catalytic region of the cytoplasmic tyrosine kinase ACK which interacts with Cdc42 via its CRIB domain and inhibits Cdc42's GTPase activity ((Mott et al., 1999) and references within). We therefore asked if the CRIB domain of Mig6 was essential for Mig6's inhibition of HGF-induced cell migration. GST-tagged versions of Mig6 lacking the CRIB domain ($Mig6^{\Delta CRIB}$), a truncated N-terminal fragment of Mig6 including the CRIB domain, but lacking the ACK homology domain ($Mig6^{NT}$), and the isolated CRIB domain only ($Mig6^{CRIB}$) were generated and expressed in MLP29 cells. The mutant proteins were expressed at similar levels and in similar subcellular compartments (Fig.41A, B1-B9, C).

HGF-induced cell migration was analyzed using the Boyden chamber assay. As previously observed, HGF stimulation strongly induced cell migration above non-stimulated control cells (Fig.42). Full-length Mig6 inhibited cell migration 2-fold. In contrast, Mig6 lacking the CRIB domain had no effect on HGF-induced cell migration (Fig.42C, G). The N-terminal fragment of Mig6 including the CRIB domain ($Mig6^{NT}$) and, more importantly, the isolated CRIB domain ($Mig6^{CRIB}$), inhibited HGF-induced cell migration to an extent comparable with full-length Mig6 (Fig.42D, E, G). The effects were specific for HGF-stimulated cells, since cell migration induced by FBS was not affected by ectopic expression of $Mig6^{NT}$ or $Mig6^{CRIB}$ (Fig.42F). These results suggest that the CRIB domain of Mig6 is essential and sufficient for inhibition of HGF-induced cell migration. Moreover, the behavior of $Mig6^{\Delta CRIB}$ (lacking inhibitory activity, but retaining Grb2 binding activity; see Fig.40) suggested that Mig6 binding of Grb2 is not sufficient to mediate inhibition of cell migration.

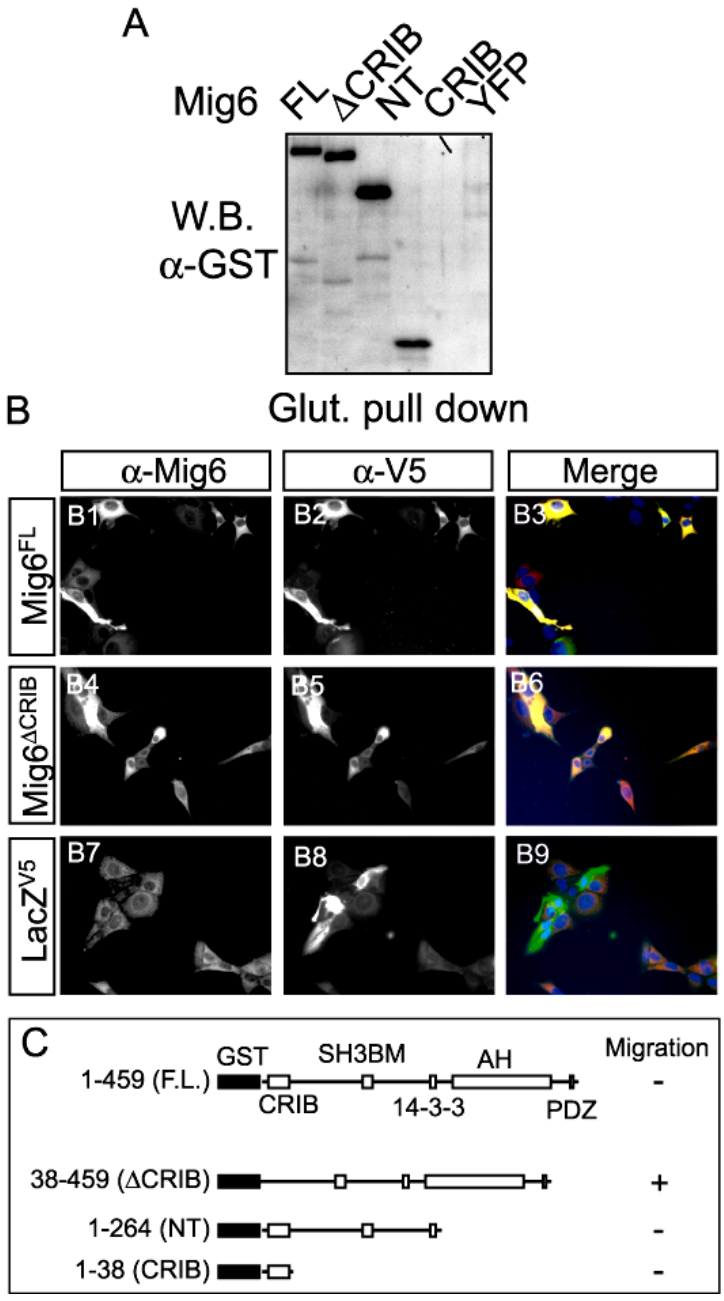


**Fig. 41 Mig6 mutant proteins are expressed at similar levels and in a similar subcellular compartment**

*(A) GST-Mig6$^{FL}$, GST-Mig6$^{\Delta CRIB}$, GST-Mig6$^{NT}$, and GST-Mig6$^{CRIB}$ were transfected in MLP29 cells and pulled down using glutathione-sepharose beads. The proteins were eluted from the beads and analyzed by SDS-PAGE. Western blot analysis using an α-GST antibody shows that the Mig6 fusion proteins were expressed at similar levels. Transfection with YFP expression plasmid was used as a negative control for the α-GST antibody.*

*(B) Immunocytochemistry analysis of MLP29 cells transfected with Mig6$^{FL\text{-}V5}$ (B1-B3), Mig6$^{\Delta CRIB\text{-}V5}$ (B4-B6) and LACZ$^{V5}$ (B7-B9) expression plasmids, using α-Mig6 (B1, B4, B7) and α-V5 antibodies (B2, B5, B8). The subcellular localization of the recombinant Mig6$^{\Delta CRIB\text{-}V5}$ protein is not affected by the absence of the CRIB domain (compare B6 and B3). The LACZ$^{V5}$ expression construct was used as a negative control for α-Mig6 antibodies.*

*(C) Schematic representation of the different GST-Mig6 deletion mutants. Their inhibitory effect on HGF-mediated cell migration is indicated as a -. Abbreviations: SH3BM: SH3 binding site; 14-3-3: 14-3-3 binding region; AH: Ack homology domain; PDZ: PDZ target site (Kay and Kehoe, 2004).*

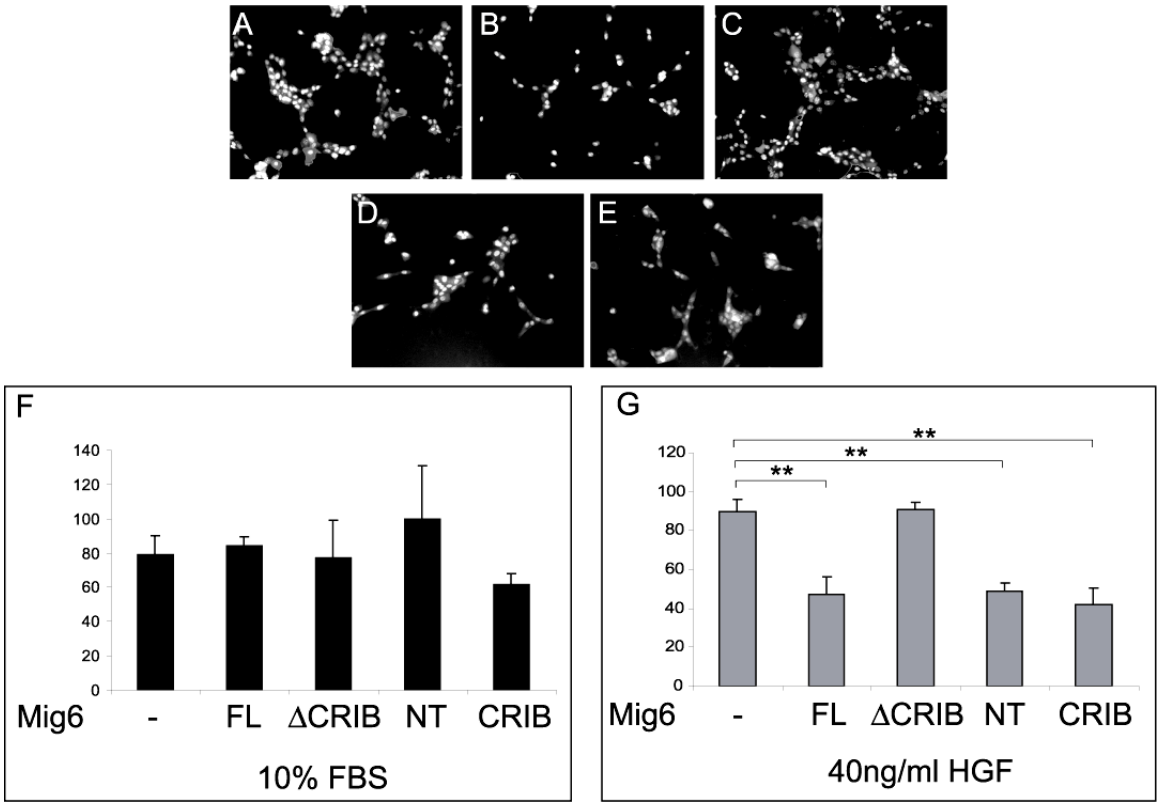


**Figure 42. The CRIB-domain of MIG6 is required and sufficient to inhibit HGF-mediated cell migration**

*(A-E) Hoechst dye-positive cells that have migrated to the lower face of the Boyden chamber upon transfection of either YFP alone (A), or a mixture of YFP and GST-Mig6$^{FL}$ (B) GST-Mig6$^{\Delta CRIB}$ (C) GST-Mig6$^{NT}$ (D) and GST-Mig6$^{CRIB}$ (E).*

*(F,G) Quantification of cell migration expressed as fold of induction over unstimulated cells in the presence of either 10% FBS (F) or HGF (G). MLP29 cells were either left untransfected or were transfected with the indicated GST-Mig6 expression plasmids and seeded onto the upper compartment of the Boyden chamber. The N-terminal half of Mig6 (Mig6$^{NT}$) and its CRIB domain (Mig6$^{CRIB}$) were able to significantly inhibit HGF-mediated migration compared to control cells (for both P=0.001, t-test). In contrast, Mig6$^{\Delta CRIB}$ was not able to significantly reduce HGF-mediated migration compared to untransfected control (P=0.88, t-test). 10%FBS-induced cell migration was not affected by any of the Mig6 expressing constructs (F).*

**Mig6 antagonizes Met signaling possibly by binding to a Rho family GTPase**

Since the CRIB domain of Mig6 was found to be required to inhibit HGF-mediated migration, we concentrated our efforts in identifying a putative molecular mechanism by which the CRIB domain could possibly mediate this function. Mig6 is known to be structurally related to the non receptor tyrosine kinase Ack1. The Ack1 homologue in *C.elegans*, Ark1, was found to inhibit EGFR functions *in vivo* (Hopper et al., 2000) (Worby and Margolis, 2000). Ack1 is known to bind with high affinity to GTP-bound Cdc42 via its CRIB domain (Gu et al., 2004) (Mott et al., 1999). Furthermore, the isolated CRIB domain of ACK1 was showed to inhibit cytoskeleton rearrangements, filopodia and lamellipodia formation (Ahmed et al., 2004). Mig6 was also showed to directly bind GTP-bound Cdc42 via its CRIB domain (Makkinje et al., 2000). Since GTP-bound state of Cdc42 was showed to be required for HGF-mediated cell scattering (Royal et al., 2000), we asked whether Mig6 binding to the active form of Cdc42 was required to inhibit HGF-mediated migration. Thus, we tested the direct interaction between several Mig6 mutant proteins and either Cdc42 or Rac small GTPases using the yeast two hybrid system. Briefly, the system consists of a bait gene (in our case the GTPase) which is expressed as a fusion to the Gal4 DNA-binding domain, and of a prey gene (in our case Mig6 constructs) which is expressed as a fusion to the Gal4-activation domain. The bait and the prey plasmids also code for two essential genes for the yeast production of leucine (Leu) and triptophane (Trp). Thus, when the plasmids are transfected into yeast, double transformants can be selected on a double drop-out media (Leu- and Trp- media). When the bait and the prey recombinant proteins interact in-vivo, the DNA-binding domain and the activation domain of GAL4 are brought into proximity thus activating the transcription of two further reporter genes, adenine (Ade) and histidine (His), allowing selection using a quadruple drop-out media (Leu-, Trp-, Ade-, His-).

$Mig6^{FL}$, $Mig6^{\Delta CRIB}$ and the CRIB domain alone ($Mig6^{CRIB}$) were transfected into Yeast together with either Cdc42 wild type, Cdc42 dominant active, Rac wild type, or Rac dominant active. Double transformants were selected on Trp-/Leu- double drop-out agar plate. Four colonies of the double transformants were then tested for direct interaction by replating onto quadruple drop-out agar plate. Furthermore Mig6 prey

plasmids were compared with the CRIB domain of Ack1 and PAK in the ability to bind specifically the GTP-bound form (dominant active form) of Cdc42 or Rac respectively.

All yeast expressing Mig6, regardless of construct, were found to weakly grow in quadruple drop-out media in the presence of either Cdc42 wild type or Rac dominant active when compared to the CRIB domain of Ack1 and PAK. The CRIB domain of Ack1 is known to bind with high specificity the GTP-bound form of Cdc42 as well as the PAK binding domain is known to bind with high specificity the GTP-bound form of Rac. However in this assay, the yeast expressing the CRIB domain of Ack1 and PAK were able to weakly grow on quadruple drop-out media when co-transfected with Rac and Cdc42 respectively. The growth rate of the yeast expressing Ack1 CRIB domain or the Pak binding domain together with the unspecific GTPase, was found to be comparable to yeast expressing Mig full length in the same conditions. Taken together these results indicated that Mig6 can weakly interact with Cdc42 and RhoA, comparable to nonspecific affinity of Ack or PAK. Thus, it is conceivable that another member of the Rho-like GTPases can more strongly and more specifically interact with the CRIB domain of Mig6

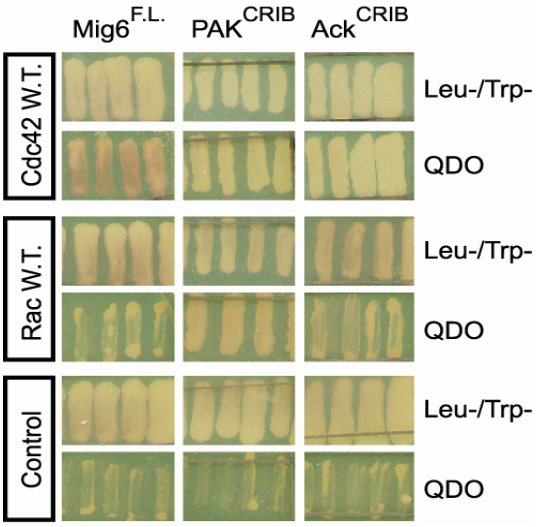


**Figure 43. Representative direct interaction between Mig6, Cdc42 and Rac analyzed by yeast two hybrid system.**

*Mig6 full length ($Mig6^{F.L.}$) (left panels) and the CRIB domain of either PAK ($PAK^{CRIB}$) (middle panels) or Ack ($Ack^{CRIB}$) (right panels) (prey genes) were co transfected into yeasts with wild type Cdc42 (Cdc42W.T.), Rac (Rac W.T.) or the empty vector (control) (bait genes). The double transformant yeasts were selected onto double dropout Agar plates (Leu-/Trp-). Direct interactors were assayed by replicating double transformants yeasts onto Quadruple DropOut (QDO) selective Agar plates. The yeasts doubly transfected with $Mig6^{F.L.}$ and Cdc42 W.T can grow on QDO selective plates comparably to the yasts doubly transfected with the $Ack^{CRIB}$ and Rac W.T. Transfection of the empty vector was used as control for the ability of the yeasts to grow on QDO plates .*

# Discussion

The complex chain of events that attenuate signal transduction of receptor tyrosine kinases is still poorly understood. Recent studies have revealed that negative receptor signaling involves intricate interactions between ubiquitin ligases, adaptor proteins, inhibitory proteins, cytoplasmic kinases and phosphatases (Dikic and Giordano, 2003). Some of these negative regulators can act on rather specific targets. For example, the protein tyrosine phosphatase PTP1B has been shown to inhibit insulin and insulin-like growth factor-I- stimulated signaling; SHP1 and Lnk have been reported to specifically inhibit Kit-mediated biological functions; and SLAP has been shown to inhibit PDGFR signaling. In contrast, other negative regulators, such as c-Cbl ubiquitin ligase and Sprouty, appear to inhibit multiple RTKs and generic signaling pathways (Ostman and Bohmer, 2001). Negative regulation of Met signaling is particularly critical, since deregulation of Met activity is believed to be causative in the development of many human malignancies (Birchmeier et al., 2003; Comoglio and Boccaccio, 2001). The same is true for the ErbB family of RTKs, which are already targets for anti-tumor therapy (Rowinsky, 2004).

Work presented in this thesis has demonstrated that Mig6 is induced by HGF in multiple cell lineages. Mig6 negatively regulates HGF/Met-mediated cellular responses, including cell migration and neurite outgrowth, suggesting that Mig6 negatively controls Met signaling, thereby fine tuning signaling output. Although further experiments are needed to clarify the exact mechanism of Mig6 action, the data suggest an important role for Mig6 interaction with Rho family GTPases.

### Transcriptional profile of HGF-stimulated MLP29

MLP29, C2C12 and TS cells responded to HGF stimulation in a similar manner. HGF induced MAPK, Akt and Gab1 phosphorylation was comparable in time-course and strength of activation (Fig.10). Because MLP29 cells were found to enter S-phase

(Fig.12) and to scatter upon HGF stimulation they were chosen as a model to characterize genes transcriptionally regulated by HGF/Met signaling.

The microarray data and their validation by northern blot analysis in different cell lines (MLP29, C2C12 and TS cells) provided evidence that the majority of the transcriptionally regulated genes were targets of HGF signaling (Fig.14) in multiple cell types. These data raised the interesting possibility that the newly identified genes had an essential role in regulating HGF/Met functions.

Next, the specificity of transcriptional regulation of target genes was addressed by comparing induction via HGF to induction via FGF2 and PDGF. Consistent with the observation that the growth factors we tested can activate a similar array of signal transduction pathways, they were also found to transcriptionally regulate common genes. Mig6 was unusual in that and HGF was found to be the main inducer, compared to FGF2 and PDGF, of mig6 transcript (Fig.17). This observation supports a model in which each receptor emits, above a generic signaling threshold, qualitatively different signals resulting in differences in transcriptional response and these specific targets contribute to specific functions. Indeed, Mig6 was found to specifically inhibit HGF-mediated cell motility, which is the most characteristic function mediated by this growth factor.

Taken together, these results suggest that different tyrosine kinase receptors share activation of common downstream signaling pathways and part of their transcriptional response as well. Nevertheless the RTKs we tested retained portion of regulated transcripts unique to them. It is reasonable to think that the specificity of transcriptional regulation for each receptor may be responsible for the differences in the functions that each receptor can mediate.

**Mig6 induction by external signals**

Mig6 was identified in MLP29 cells as a transcript highly induced by HGF, and rather weakly by FGF2 and PDGF. Other investigators founded Mig6 induced by serum, EGF and related ligands, and cellular stress factors (Chu et al., 1988; Wick et al., 1995) (Makkinje et al., 2000) and references within). The time course of Mig6 induction

appeared to depend mainly on the external signal (PDGF causing a transient and EGF causing sustained induction of Mig6 (Xu et al., 2004). The strength of induction appeared to depend more on the cellular context than on the type of external signal. MLP29 and C2C12 cells showed very robust (on average >10-fold) transcriptional activation of Mig6 by HGF, whereas primary hepatocytes induced Mig6 protein approx. 2 to 4-fold (Fig.15 and 19). Primary sympathetic neurons were found to upregulate Mig6 in response to HGF as well (Fig.35), whereas cortical neurons did not show any induction of mig6 transcripts (data not shown). This work provided evidence that Met signaling is a major pathway for Mig6 expression in lungs and liver of E13.5 embryos by showing a reduction of mig6 transcript levels in mouse mutants expressing a severe signaling hypomorph of Met (Fig.21).

Mig6 was frequently found expressed at low levels, and its expression induced by HGF/Met signaling with some delay after the initiation of Met signaling. In presence of low Mig6 levels the cell will respond robustly to Met signaling until Mig6 levels are high enough to attenuate the receptor response. Alternatively, other external signals might have already induced the expression of Mig6 before the cells were exposed to HGF, thereby reducing the cell's ability to respond to Met signaling. Loss of the ability to induce the expression of Mig6 might be part of the multiple step process towards malignancy. Consistent with this model, a recent large-scale expression profiling study identified Mig6 expression to be downregulated in breast cancer patients with short survival time (Amatschek et al., 2004). It appears that loss of Mig6 provides a growth advantage and perhaps metastatic potential for breast cancer cells.

**Mig6 modulates a variety of cellular responses**

Previous work had shown that Mig6 inhibits cell proliferation downstream of ErbB family receptors (Anastasi et al., 2003; Fiorentino et al., 2000; Hackel et al., 2001). This includes a recent study in which Mig6 was silenced by RNA interference providing first evidence for a role as an endogenous inhibitor of EGFR-mediated proliferation (Xu et al., 2004).

The work presented in this thesis has concentrated on the role of Mig6 in Met-mediated cell migration, although the data presented also provides evidence that Mig6 inhibited the mitogenic activity of Met (Fig.30). However these data suggested that the mig6 knock-down by siRNA in MLP29 cells is sufficient to increase the number of cells entering S-phase independently of HGF stimulation. Thus, Mig6 may be also part of a HGF-independent pathway that regulates the cell cycle of MLP29 cells via a mechanism that is still unknown.

The inhibition of HGF-dependent migration via Mig6 was found to be independent of the previously known Mig6 anti-mitogenic effect. HGF-mediated cell migration has been studied in a number of different cellular contexts, including myoblast migration during development, scattering and branching morphogenesis of epithelial cells, neuronal migration in the developing forebrain (Powell et al., 2001) (Birchmeier et al., 2003; Rosario and Birchmeier, 2003). Mig6 overexpression was found to effectively and specifically reduce HGF-induced migration of a hepatic cell line and of primary cortical neurons. In converse experiments, mig6 knock down effectively enhanced cell migration of hepatic progenitor cells. Furthermore, the data presented here suggested that Mig6 overexpression does not influence the overall cell migration capability. In fact, the migration of MLP29 and cortical neurons stimulated with 10% serum and SDF1 respectively was not affected by Mig6 overexpression. These results suggested that the inhibitory function of Mig6 did not affect general cell motility mechanisms but rather specific signaling pathways responsible for HGF-mediated cell migration. This data provided first evidence that Mig6 plays a specific role in regulating HGF-mediated migration independently of its anti-mitogenic function.

The role of Mig6 in ErbB-mediated cell migration has still not been addressed. This is will have to be addressed in the future, since numerous studies have demonstrated that EGF and related ligands for EGFR/ErbB receptors stimulate chemotactic responses in vertebrate and invertebrate systems (Caric et al., 2001; Gambarotta et al., 2004; Marone et al., 2004; Wells and Lillien, 2004).

**Mig6 negatively regulates HGF-mediated neurite extensions and branching but not survival of sympathetic neurons**

Central nervous system development is also characterized by invasive growth. The precise anatomical connections that are required for the central nervous system's functions rely on the directional movement of axons that sprout and branch following extracellular signals that determine their motile activity (Yu and Bargmann, 2001). Indeed, Met signaling is critical for neurite extension and branching of different neuronal subpopulations (reviewed in (Maina and Klein, 1999); see also (Thompson et al., 2004), a process that has similarities with invasive growth of malignant cells (Trusolino and Comoglio, 2002). This study provided evidence that Mig6 overexpression effectively blocked HGF-induced neurite outgrowth of primary sympathetic neurons without affecting HGF-mediated survival of the neurons. Conversely, mig6 knockdown moderately enhanced HGF-mediated neurite outgrowth of sympathetic neurons. It has to be noted that since Mig6 protein, in the SCG, is induced after 16 hours from HGF stimulation (Fig.35), the reduction of neurite length due to the knock-down of the endogenous Mig6 is relevant when quantified at higher distances from the cell soma (from 210μm to 380μm) (Fig.39). Conversely, the decrease in neurite branching due to Mig6 overexpression was found to be signicant at distances closer to the cell soma (from 60μm to 240μm) (Fig.36B). Therefore, exogenously supplied Mig6 immediately blocked HGF-dependent neurite extension, resulting in a general decrease of neurite complexity. On the other hand, the endogenous Mig6 protein exerted its inhibitory effect only after 16 hours upon HGF stimulation. Most probably HGF induced the outgrowth of primary branches close to the cell soma prior to substantial Mig6 expression and then promoted the outgrowth of neurites further from the cell soma. In this model, the increasing level of Mig6 protein would limit limit later HGF-mediated neurite growth. These data suggested that endogenous Mig6-effect inhibits the HGF-mediated growth of specific neurites that extend far from the cell soma.

Mig6 was found to inhibit HGF-mediated neurite outgrowth but not survival consistent with a role in the inhibition of specific Met-mediated functions. These data, together with the observation that Mig6 overexpression affected only migration in

cortical neurons (while neurite growth and survival were found unaffected), suggested that Mig6-mediated inhibition is limited to specific Met-mediated effects in a cell specific manner. It is likely that Mig6 inhibits a Met-activated signaling pathway, which results in cell motility, in the context of MLP29 and cortical neurons, and in neurite outgrowth, in the context of SCG neurons.

These data support the idea that Mig6 inhibits specific pathways downstream of Met without affecting its overall functions, therefore fine tuning the receptor output. Furthermore, these data represent the first evidence that Mig6 plays a crucial role in the inhibition of specific HGF-mediated effects on sympathetic neurons.

**Mig6 and Met are partially coexpressed in the somites and in the developing muscles**

Work presented here demonstrates that at E9.5 mig6 mRNA is expressed in developing somites (Fig.20). Interestingly mig6 was found to be expressed in the medial region of the forming somites, which later give rise to epaxial muscles (deep back muscles). Mig6 was also found in the more medio-lateral region that is known to give rise to hypaxial muscles (most body and limb muscles). Conversely, met mRNA expression was confirmed to be restricted to the most lateral domain of the somites. Whithin this somitic domain, met transcripts only partially co localized with mig6 mRNA. Intriguingly, a recent study (Chung et al., 2004) has reported an essential role for the *Xenopus* homologue of Mig6 (XMig6) during muscles differentiation. In particular, Xmig6 was found to be a potential downstream transcriptional target of eFGF with specific roles in muscle differentiation. *Xenopus* embryos in which mig6 was knocked down by siRNA were reported to have a significant down-regulation of the early myogenic marker *Mif5* and to lack well-differentiated muscles. Low level of Mig6 may therefore act during early myogenesis to allow the migratory Met-positive muscle precursors to properly migrate toward their final targets. Subsequently, once the cells reached their target tissues and migration ceases, prolonged HGF signaling together with other extracellular signals (such as FGF) may induce Mig6 expression. Mig6 may therefore participate to attenuate Met signals. Consistent with this model, the termination

of Met signals is required for the muscle precursors to express myogenic genes (such as *Myf5* and *MyoD*) (Scaal et al., 1999). Because the loss of Met functions in embryos does not affect the expression of early myogenic genes (*Mif5* and *MyoD*) (Prunotto et al., 2004) (Maina et al., 1996) and since Mig6 can drive the expression of *Mif5* (Chung et al., 2004), Mig6 may also contribute to muscle differentiation in a HGF-independent manner. Consistent with this model, HGF is expressed along the entire route followed by the migratory myoblasts, that in turn express Met until they reach their final target tissue (Dietrich et al., 1999). The prolonged requirement for an active Met signaling during long range migration may also address the need of the muscle precursors to maintain the undifferentiated state (Scaal et al., 1999) and to sustain their proliferation and survival (Ponzetto et al., 2000). However, Met signals needs to be tightly regulated in space and time during muscle development. Mice expressing HGF ectopically showed an aberrant development of muscles around the spinal cord (Takayama et al., 1996) implying that an excess of Met signaling in muscle precursors results in the misrouting of migratory myoblasts and in the development of an aberrant phenotype. Furthermore, accordingly to the essential role played by Met during the formation of secondary muscle fibers (Maina et al., 1996) (Maina et al., 2001) mature hypaxial muscles fibers (intercostal, body wall and limb muscles) were confirmed positive for met expression (Fig.21 and not shown). Interestingly, the hypaxial muscle fibers were found positive for mig6 expression as well (Fig.21 and 22 and not shown). Therefore, whether Mig6 plays a role during myoblast migration and muscle differentiation in a HGF dependent and/or independent manner, is an important question that will have to be addressed in the future.

**Mig6 acts distally from Met via interaction with Rho family GTPases**

The cDNA for Mig6 is predicted to encode a cytosolic polypeptide of 459 amino acids with the attributes of an adaptor protein. The first 38 amino acid residues in the amino terminus of Mig6 show significant homologies with the conserved Cdc42/Rho Interacting Binding domain (CRIB domain) which is present in several other proteins. Mig6 also contains other conserved domains, among them a putative binding site for SH3-containing molecules (a.a. 146-160) which has been shown to bind Grb2, PI3K and

PLCγ (Fiorentino et al., 2000); a 14-3-3 binding region (a.a. 246-253); and a putative binding motif for PDZ domain containing proteins. Notably, Mig6 also includes a C-terminal motif highly homologous to the non-catalytic portion of ACK1. A region within this ACK1 Homology domain (AH domain) was previously identified as an EGFR binding motif (Fiorentino et al., 2000) (Anastasi et al., 2003), and more recently the AH domain of Mig6 has been shown to be necessary and sufficient for the inhibition of EGFR (Xu et al., 2005). Although Mig6 was found unable to directly bind Met, the observation of molecular association between Mig6 and Grb2 (Fig.40) suggested the possibility that Mig6 may bind Met indirectly, thereby inhibiting Met in a receptor-proximal fashion.

The CRIB domain of Mig6 has been reported to bind Cdc42 in a GTP-dependant manner (Makkinje et al., 2000). The activation of Cdc42 downstream of HGF stimulation is required for lamellipodia formation and cell movement (Royal et al., 2000). This raised the possibility that Mig6, via its CRIB domain, inhibits Cdc42-mediated cell movement. Results in this thesis are consistent with this model. This study provides evidence that the CRIB domain of Mig6 is sufficient and required for the inhibition of HGF-mediated migration. Overexpression of a Mig6 construct lacking the CRIB domain, but retaining Grb2 binding capabilities, did not suppress HGF-induced migration. Conversely, overexpression of the Mig6 CRIB domain alone is sufficient to inhibit HGF-mediated migration. These data also indicate that the association between Mig6 and Grb2 is not sufficient to inhibit cell migration. The mechanism of Mig6 inhibition of Met therefore resembles the mechanism of Ack1 inhibition of EGFR. The *C. elegans* orthologue of Ack1, Ark, associates with EGFR via binding to Sem5, the *C. elegans* orthologue of Grb2 (reviewed in ((Worby and Margolis, 2000). Similar to Mig6, overexpression of the CRIB domain of Ack was found to be sufficient to inhibit growth factor induced activation of Cdc42 (Nur et al., 1999). The possible involvement of the Mig6 CRIB domain in the negative regulation of HGF-mediated cell movement is also supported by the observation that the overexpression of the CRIB domain of Ack is sufficient to inhibit Cdc42-mediated cell growth and movement (Ahmed et al., 2004). Furthermore the overexpression of the CRIB domain of another small GTPase-binding protein (PAK, an effector of Rac1) via its interaction with Rac1 was found to inhibit the Sema3A- (a

repulsive factor for specific neuro population) growth cone collapse (Vastrik et al., 1999). Together these results suggested that CRIB domains inhibit specific GTPases, possibly by competing with alternate downstream effectors.

The involvement of a Rho-like GTPase and the CRIB domain of Mig6 in the regulation of HGF-mediated biological functions is furthermore supported by experiments conducted in SCG neurons. Activated mutants of Cdc42 and Rho are known to induce SCG neuronal death, whereas expression of the dominant negative counterparts can protect them from apoptosis, even in the case of trophic factor withdrawal (Bazenet et al., 1998). Combining these data with our model by which Mig6 can inhibit/modulate Rho-like GTPases, the HGF-mediated survival of SCG neuron was not affected by Mig6 overexpression. In this case Mig6 overexpression might inhibit or modulate HGF-mediated GTPase activation, allowing increased neuronal survival. Conversely, overexpression of the Mig6 construct lacking the CRIB domain resulted in a significant decrease in neuronal survival (not shown). Because the Mig6$^{\Delta CRIB}$ protein is unable to downregulate HGF-dependent activation of the GTPase, this may result in the increase of neuronal death.

From these data it is possible to picture Mig6 as a molecular switch that inhibits/modulates the Rho-like GTPase activity. Further experiments are needed in order to establish whether or not the Rho-like GTPase modulation/inhibition via Mig6 is required for a correct HGF-mediated migration of MLP29 cells and cortical neurons, and to promote a correct survival rate and neurite outgrowth of SCG neurons.

These are important possibilities that will have to be addressed in the future in order to properly characterize the role and mechanism of Mig6 action in the context of Met receptor negative regulation.

## Concluding remarks

This work inserts Mig6 as a member of a network of negative signaling molecules that fine tune and attenuate Met and possibly ErbB signaling in development and disease. Mig6 was found to negatively regulate HGF-mediated migration and neuronal differentiation. Additional work is required in order to exclude other possible

mechanisms of Mig6 action (for example via Grb2, PI3K or 14-3-3) and in order to clarify the Mig6's molecular partners. Nevetheless there is strong evidence that the CRIB domain of Mig6, via the interaction with a Rho-like small GTPase, is essential in mediating Mig6's function. The analysis of mig6 null mutant mice is in progress (I. Ferby, R. Klein, unpublished) and will help to elucidate the function of Mig6 in the context of development and of an intact tissue.

Finally, the finding that Met biological effects can be limited by modulation of its signaling pathways raises the possibility that control of Met-specific effects might be obtained by inducing the expression of Met antagonists such as Mig6. The advantage of a physiological and specific inhibitor of Met signaling is evident: the metastogenic and tumorigenic properties of scatter factors must be separated from their beneficial trophic properties. If and how Mig6 contributes to the complex chain of events that drive cancer progression and metastasis and whether Mig6 is able to suppress HGF-mediated metastogenic effects without perturbing its trophic properties are all fascinating questions that deserve further investigations.

# Materials and Methods

## Materials

Met$^{d/d}$ mutants were generated by Flavio Maina (Maina et al., 1996). Mutant mice were maintained in a C57/Black6/CD1 mix genetic background. For experiments, only offspring of heterozygous intercrosses was used.

### Plasmids

| Plasmid | Insert | Comments | Reference |
|---|---|---|---|
| **GP6** | Mig6 FL | C-term V5 | Pante et al., 2005 |
| **pDEST26** | Mig6 FL | C-term His | Pante et al., 2005 |
| **GP15** | Mig6 FL | N-term GST | Pante et al., 2005 |
| **GP16** | Mig6 DCRIB | N-term GST | Pante et al., 2005 |
| **GP17** | Mig6 N-terminal | N-term GST | Pante et al., 2005 |
| **GP34** | Mig6 CRIB domain | N-term GST | Pante et al., 2005 |
| **pDONOR201** | | | Invitrogen |
| **pMet-5'** | Met5' | In-situ probe | Helmbacher et al., 2001 |
| **pMet-3'** | Met3' | In-situ probe | Helmbacher et al., 2001 |
| **h3011f08** | Mig6 partial codons | In-situ/northern probe | NIA clone set |
| **h3046a05** | CK334526 | Northern probe | NIA clone set |
| **h3142b10** | AK010617 | Northern probe | NIA clone set |
| **h3017h12** | h3017h12 | Northern probe | NIA clone set |
| **h3080h11** | BG069863 | Northern probe | NIA clone set |
| **h3118f05** | BG073094 | Northern probe | NIA clone set |
| **h3011f08** | BG063865 | Northern probe | NIA clone set |
| **h3016f11** | BC016400 | Northern probe | NIA clone set |
| **h3028f05** | BG069647 | Northern probe | NIA clone set |
| **h3057e07** | BC025860 | Northern probe | NIA clone set |
| **h3019f06** | NM_025448 | Northern probe | NIA clone set |
| **h3090g02** | BG070747 | Northern probe | NIA clone set |
| **h3081a04** | BG069868 | Northern probe | NIA clone set |

## Chemicals, enzymes and commercial kits

Chemicals were purchased from the companies Merk, Sigma, Fluka, and Roth. Only in the cases where the suppliers were different it is indicated together with the method. All water used to generate solutions was filtered with the "Milli-Q-Water-System" from Millipore. Restriction enzymes were purchased from New England Biolabs (NEB). Special suppliers and kits are mentioned in the methods.

## Media and standard solutions

| | |
|---|---|
| LB (Luria-Bertani) media | 10g bacto-trypton<br>5g Yeast extract<br>5g NaCl<br>Add H2O to 1l, pH7.5 |
| LB plates | supplemented with 15g/l agar |
| | |
| Antibiotics 1000X | |
| Ampicillin | Stock 100mg/ml in H2O |
| Kanamycinsulfate | Stock 50mg/ml |

## Media and supplements for primary culture

| | |
|---|---|
| Neurobasal media/B27 | Gibco, 500ml were supplemented with 10ml of B27 supplement |
| | |
| HBSS | Gibco |
| | |
| Supplements | Trypsin/EDTA (GibcoBRL)<br>Poly-D-Ornithin (Sigma)<br>Fibronectin (Sigma) |

| | |
|---|---|
| Stimulating factors | HGF (R&D)<br>FGF2 (Sigma)<br>PDGF (Sigma)<br>FGF4 (Sigma) |

**Buffers and solutions**

| | |
|---|---|
| 10X PBS | 1.3M NaCl<br>70mM Na2HPO4<br>30mM NaH2PO4, pH7.2 |
| TE buffer | 10mM Tris/HCl<br>1mM EDTA, pH8 |
| 50X TAE | 2M Tris-Acetate<br>50mM EDTA |
| 20X SSC | 3M NaCl<br>0.3M NaCitrate, pH7.5/4.5 |

**Northern blot**

| | |
|---|---|
| RNA loading buffer | 13.4% formamide,<br>4.4% of 37% formaldehyde,<br>80µg bromophenolblu<br>dissolve in 1X MOPS |
| 1X MOPS pH 7 | 0.418 % MOPS<br>2mM Na-Acetate<br>1mM EDTA pH 8 |

| | |
|---|---|
| 5X Denhardt solution | 1% Ficoll 400<br>1% polyvinylpirrolidone<br>1% BSA<br>Dissolve in $H_2O$ |

**Microarray**

| | |
|---|---|
| Hybridization buffer | 50% formaldehyde<br>6X SSC<br>0.5% SDS<br>5X Denhardt |

**Genotyping PCR**

| | |
|---|---|
| Tail lysis buffer | 100mM Tris pH7.5<br>1mM EDTA<br>250mM NaCl<br>0.2% SDS |

**SiRNA**

| | |
|---|---|
| SiRNA annealing buffer | 100mM K-Acetate<br>30mM Hepes-KOH<br>2mM Mg-Acetate |

***In-situ* hybridization**

| | |
|---|---|
| Hybridization buffer | 0.19M NaCl |

| | |
|---|---|
| | 10mM Tris pH7.2 |
| | 5mM $NaH_2PO_4 \cdot 2H_2O$ |
| | 50mM EDTA |
| | 50% formamide |
| | 10% dextrane sulfate |
| | 1mg/ml Yeast rRNA |
| | 1X Denhardt solution |
| Washing buffer | 50% formammide |
| | 2X SSC |
| | 0.1% tween20 |

**Whole mount *in-situ* hybridization**

| | |
|---|---|
| Prehybridization solution | 50% formamide |
| | 5X SSC pH4.5 |
| | 0.1% tween20 |
| | 0.5% chaps |
| | 2% blocking reagent |
| | 50µg/ml of tRNA |
| | 50µg/ml heparin |
| | 5mM EDTA pH8.1 |

**Embryo powder**

Several litters of CD1 E12.5 to E14.5 embryos were dissected in PBS and fast freezed in liquid nitrogen. The embryos were mechanically destroyed.

## Antibodies

### Primary antibodies

| | |
|---|---|
| Anti-phospho-MAPK | New England biolabs, mouse monoclonal<br>WB 1:5000 |
| Anti-MAPK | New England biolabs, rabbit polyclonal<br>WB 1:1000 |
| Anti-phospho-AKT | New England biolabs, rabbit polyclonal<br>W.B. 1:1000 |
| Anti-tubulin | Sigma, mouse monoclonal<br>W.B. 1:2000 |
| Anti-phospho-tyrosine (4G10) | Upstate Biotechnology, mouse monoclonal<br>W.B. 1:5000 |
| Anti-Mig6 | Pante et al., in preparation, rabbit polyclonal<br>W.B. 1:500, IF 1:250 |
| Anti V5 | Invitrogen, mouse monoclonal<br>IF 1:250 |
| Anti-BrdU | Boehringer, mouse monoclonal<br>IF 1:250 |
| Anti GAB1 | Gift from Liliana Minichiello, rabbit polyclonal<br>WB 1:2000 |
| Anti Met | Biomol, rabbit polyclonal<br>WB 1:500 |
| Anti-GST | Santa Cruz, rabbit polyclonal<br>WB 1:500 |

### Secondary antibodies

| | |
|---|---|
| Anti-mouse HRP | Amersham, goat polyclonal<br>WB 1:2000 |
| Anti-rabbit HRP | Amersham, goat polyclonal<br>WB 1:2000 |
| Anti-mouse texas red | Sigma, goat polyclonal<br>IF 1:200 |
| Anti-rabbit CY3 | Jackson, donkey polyclonal<br>IF 1:200 |
| Anti-mouse alexa488 | Molecular Probes, donkey polyclonal<br>IF 1:200 |
| Anti-Digoxigenin | Roche, sheep polyclonal<br>*In-situ* 1:2000 |
| Nuclear staining | Hoechst nuclear stain, Hoechst, IF 1:1500 |
| Glutathyon-sepharose beads | Amersham |

## Methods

### Molecular biology

All the molecular techniques, unless otherwise specified, were carried out according to Sambrook (Sambrook et al., 1989).

**Cloning and generation of *in-situ* and northern blot probes**

The V5 C-terminal, GST N-terminal or His C-terminal tagged Mig6 full length and mutants proteins were generated using the Gateway Cloning technology according to the manufacturer instructions (Invitrogen). Briefly, Mig6 full length and deletion mutants were amplified by Polymerase Chain Reaction (PCR) from IRAK clone IRAKp961F0910 using oligonucleotides containing the minimal recombination sequences (5'-ATTB1 and 3'-ATTB2). 300ng of the PCR amplified products were recombined into 300ng of the pDONOR201 vector (Invitrogen) by the use of a mixture of recombination proteins provided by manufacturer. 300ng of the pDONOR201 vector containing Mig6 full length and deletion mutants were then shuttled into pCDNA 6.2 C-terminal V5 (Invitrogen), pDEST 27 N-terminal GST (Invitrogen) and pDEST26 N-terminal His (Invitrogen) plasmids. These plasmids were used for all the Mig6 full length and deletion mutants overexpression experiments in mammalian cells.

For the generation of the in-situ probes 10µg of the plasmid containing either Met5', Met3' (Helmbacher et al., 2003) or Mig6 (N.I.A. clone H3011F08) were digested with enzymes cutting either downstream (for the sense probe) or upstream (for the antisense probe) to linearize the plasmid. Following 4h digestion at 37°C the linearized plasmid DNA was extracted with phenol/chloroform. Phenol was added to the restriction mix (1:1), mixed, and centrifuged for 10 min. at 4°C. The supernatant was extracted with 1 volume phenol and 1 volume chloroform/isoamylic alcohol (24:1) using the same procedure. The supernatant was then incubated with 0.7 volume of isopropanol 20 min at -20°C. The purified DNA was then precipitated by centrifugation at 13.000 rpm for 20 min, washed twice with 70% ethanol and resuspended in 50µl of Tris buffer (10 mM, pH8). To generate digoxigenin-labelled RNA probe 1µg of linearized plasmid was incubated with transcription buffer (Roche, in-situ probe labeling kit), digoxigenin-conjugated dNTPs, RNAse inhibitors, and the specific RNA polymerase which would recognize a site upstream or downstream of the cDNA insert, for 3h at 37°C. In order to precipitate short RNAs, LiCl and 100% Ethanol were added. The mixture was left at -20°C for 30 min. Subsequently, the mix was centrifuged for 20 min. at 4°C. The

precipitated RNA was washed twice with 70% Ethanol and left 30 min. to dry at room temperature. The dried pellet was resuspended in 150ul of TE buffer and stored at -80°C.

For the generation of the northern blot probes the clones selected from the NIA library were amplified and the plasmids isolated using the miniprep kit (Qiagen). 5µg of the isolated plasmids were digested using NotI and SalI restriction enzymes which were universal enzymes for excising the NIA library inserts (Tanaka et al., 2000). The restriction digest was then subjected to Agarose gel electrophoresis and the excised insert recovered and purified from the gel using the Gel Extraction Kit (Qiagen).

**Northern blot**

Total RNA was extracted from different cell lines in various experimental conditions using the RNAClean Solution (Hybaid) according to the manufacturer instructions. The media of cells growing in 10cm dishes was removed and 2ml of RNAClean solution was added. After resuspending the cells several times by passing through a pipette tip the solution was transferred on ice and 200µl of chloroform added. The solution was incubated for 5 min. on ice and centrifuged at 12.000 rpm for 15 min. The aqueous phase was transferred into a fresh tube and the total RNA precipitated by adding an equal volume of isopropanol. The samples were then incubated at -20°C for 20 min. The total RNA was harvested by centrifugation at 12000 rpm for 20 min. The RNA pellet was washed twice with 70% ethanol and dried completely. Total RNA was then resuspended in 100µl of RNAse-free water. The quality and concentration of the total RNA were checked by Agarose gel electrophoresis and further confirmed reading the absorbance of the sample at 260 and 280 nm.

30µl of loading buffer was added to 20µg of RNA and each sample was brought to a total volume of 40µl. The RNA was denatured by heating at 60°C for 10 min. The samples were then chilled on ice for 5 min. and loaded on a gel containing 1% Agarose, 1.8% formaldehyde dissolved in 1X MOPS. The total RNA was then blotted by capillarity on the Genescreen nylon membrane (NEN life science) according to standard procedures. The membrane was saturated at 65°C for 3 hours in a blocking solution containing 6X SSC, 5X Denhardt solution and 100µg salmon sperm.

The purified probes were radio-labeled using the random prime labeling system (Rediprime$^{TM}$II, amersham pharmacia biotech). 100ng of the probes were denaturated at 95°C for 5 min. and then incubated for 1 hour at 37°C with a solution containing DNA polymerase, random primers and a dNTPs mix with [$^{32}$P ] dCTP (amersham pharmacia biotech). The radio-labeled probe was then separated from the unincorporated labeled dCTP by the use of Probequant$^{TM}$ G-50 Micro columns (amersham pharmacia biotech) according to the manufacturer instructions.

The radiolabelled probe was then diluted in 10ml of hybridization solution (6X SSC, 5X Denhardt solution and 100µg salmon sperm) for 18 hours at 65°C. The membrane were subjected to several washes of 15 min. at 65°C progressively increasing the stringency of the solution (1$^{st}$ wash: 2X SSC, 0.1% SDS; 2$^{nd}$ wash: 0.5X SSC, 0.1% SDS; 3$^{rd}$ wash: 0.2X SSC). The membranes were then exposed either to X-ray film (Kodak) for 18 hours at -80°C or to the phosphoimmager detection screen for 3 hours in order to quantify the signal.

**Microarray production and probe labeling**

Global gene expression was analyzed using a cDNA microarray. The high-density glass microarray chips were prepared at the EMBL core facility by the use of the NIA 15K cDNA mouse clone set (Tanaka et al., 2000). The NIA 15,247 mouse library was first replicated inoculating 2µl of the original bacterial suspension into 50µl of LB broth. The replica plates were incubated 18 hours at 37°C. 1ul of the bacteria replica culture was then amplified by PCR using two universal oligonucleotides. The 15,247 PCR products were further purified from unincorporated dNTPs and oligonucleotides using the PCR purification kit (Macherey-Nagel). The purified PCR products were eluted in 100µl TE buffer. The size and quality of the PCR amplified products were then controlled by Agarose gel electrophoresis. The PCR amplified products were spotted at high density on glass coverslips by the use of a spotting device. The spotted slides were further incubated at 50°C for 3 hours and the DNA was denatured at 100°C for 10 min. The microarray slides were then stored at room temperature in a dark place.

Total RNA was extracted from different cell lines under different experimental conditions using the RNAClean Solution (Hybaid) as described above. 40µg of total RNA was then retro-transcribed and fluorescently labeled using a mixture of 3µg poly-dT oligonucleotide (GIBCO), 6µl of retro-transcriptase superscript II (GIBCO), 0.1M DTT, 3µl of either Cy3-dUTP (Amersham) (for the RNA derived from the unstimulated cells) or Cy5-dUTP (Amersham) (for the RNA derived from the stimulated cells) and 25µM of dNTPs. The retro-transcription reaction was incubated for 4 hours at 42°C and stopped with 1.5µl of 1M NaOH/20 mM EDTA. The labeled cDNA was then purified using the PCR purification kit (Qiagen). Thus, the cDNA probes derived from untreated or from variously stimulated cells were fluorescently labeled with Cy3-dUTP (green) or Cy5-dUTP (red), respectively.

**Microarray hybridization**

The microarray cDNAs were denatured for 2 min. in boiling water before the hybridization with the cDNA probes. The Cy5 and Cy3-labelled cDNA probes were mixed, dried and resuspended in 30µl water. 2.4µg salmon sperm DNA, 10µg Poly-dA oligonucleotide (Invitrogen) and 24µl hybridization buffer was added to the cDNA probes and the mixture denaturated by incubation for 2 min. at 95°C. The cDNA probes were then hybridized on the microarray slide and incubated for 16 hours at 42°C in a water bath. After the hybridization, the Microarray slide was washed twice with 0.1X SSC, 0.1% SDS for 10 min. at room temperature and twice with 0.5 X SSC for 10 min. Finally, the two fluorescent images were scanned with a fluorescence laser-scanning device (Gene pix 400B, Axon instruments).

**Microarray analysis**

The hybridizations were performed in duplicate using total RNA samples extracted from two independent batches of cultured cells**.**

Green and red fluorescent signals indicated genes whose expression levels were relatively higher in cells untreated or HGF-stimulated, respectively. The differential expression of each gene was calculated from the relative intensity of the Cy5 *versus* Cy3 fluorescent signals. Two independent experiments were conducted comparing untreated cells and cells stimulated with HGF for 4 hours and one experiment was conducted comparing two 4 hours HGF-stimulated samples (background control).

The data acquisition and initial data analysis was performed with GenePix Pro 3.0 and the data tables were analyzed further in Microsoft Excel in order to obtain the gene list. Quality control was performed, firstly by eye, to confirm scanner alignment and absence of significant bubbles and scratches. Scatter plots were further used to eliminate unacceptable hybridization data. The multiple spike-in controls RNA template were added to the sample upon direct labeling, and the successful labeling and hybridization was confirmed in each hybridizations (Richter et al., 2002).

GenePix Pro program calculates the normalization factor of each hybridization, based on the premise that the arithmetic mean of the ratios from every feature on the given array should be equal to 1. Normalization was therefore performed by multiplying the factor to Ratio of Medians (ROM) in each gene. The genes that passed all these criteria were first sorted by Sum of Median (SOM), which indicates the intensity of hybridization. In order to obtain the list of genes that are relatively abundant, the genes that showed more than 5,000 of SOM were selected. Finally, the genes were sorted by ROM. The genes that showed more than ±1.8 fold changes were selected in the data table from each hybridization. Finally, the data tables were compared between the two hybridizations and average ROM was calculated. Gene functions were categorized based on the information given in the NIA mouse 15k cDNA clone gene ID list at the first instance and modified when necessary.

**Tail DNA preparation and genotyping PCR**

Genetic determination of mice was done using PCR analysis. Tail biopsies were taken from the mice at weaning age of about 3 weeks. For genotyping embryos, the amniotic tissue was collected and washed several times with PBS to avoid possible

contamination with maternal tissue. 2-5mm of tail were cut and incubated overnight at 56°C with tail lysis buffer plus 100µg/ml of Proteinase K (Quiagen). The proteinase K was inactivated by heating the solution at 95°C for 10 min. The solution was then diluted 2.25 times with water and 1µl of this DNA solution was used for PCR analysis. 17.5pM specific primers to amplify a sequence of the genomic DNA specific for an allele were added together with PCR buffer (Perkin Elmer), dNTPs, and Taq polymerase (Perkin Elmer). 15µl of the PCR mix after PCR amplification were loaded on an Agarose gel.

**Yeast methods**

**Strains, growth and media**

The S. cerevisiae strain PJ69-4A (James et al., 1996) was used for all two hybrid experiments, the genotype of which is:

*MATα, trp1-901, leu2-3, 112, ura3-52, his3-200, gal4Δ, gal80 Δ, LYS2::GAL1*$_{UAS}$*-GAL1*$_{TATA}$*-HIS3, GAL2*$_{UAS}$*-GAL2*$_{TATA}$*-ADE2, MEL1 met2=GAL7-LacZ.*

Yeasts were grown in either YPDA or SC dropout media selecting for appropriate plasmids at 30°C. Short term storage was on plates at 4°C.

YPDA media consisted of 20g/l peptone (Difco/Becton-Dickinson), 10g/l yeast extract (Difco), and 20g/l glucose (plus 20g/l Bacto-agar for YPDA-agar). The media was then sterilized in an autoclave and, after cooling to approximately 55°C, 6ml 0.2% filtered adenine hemi sulfate was added.

Synthetic complete (SC) dropout media was prepared as follows:

Amino acid base (-His/-Trp/-Leu/-Ura) was prepared by mixing 20g alanine, arginine, asparagine, aspartic acid, cysteine, glutammine, glutammic acid, glycine, inositol, isoleucine, lysine, methionine, phenylalanine, proline, serine, threonine, tyrosine, and valine with 5g adenine and 2g para-aminobenzoic acid. To prepare dropout mixes, 36.7g of amino acid base was mixed with either 2g histidine, 4g leucine, 2g triptophane, or 2g uracile, as appropriate to form the appropriate dropout mix. SC dropout mix consisted of 6.7g/l nitrogen base (without amino acid, Difco), 2g/l appropriate dropout mix, 20g/l

glucose and pH adjusted to between 5.5 and 6.5 (plus 20g/l Bacto-agar for SC dropout agar). After autoclaving and cooling to approximatively 55°C, 6ml 0.2% sterile filtered adenine hemisulfate was added, unless dropout media was also to be –adenine.

**Yeast transformation (frozen cell method)**

To prepare frozen competent yeast cells, several colonies were picked from a freshly grown plate and grown overnight in YPDA at 30°C with shaking. The following morning the overnight culture was diluted to an $OD_{600}$ of 0.15 in fresh medium and grown at 30°C to an $OD_{600}$ of 0.5-0.6 ($1.2\text{-}1.5X10^7$ cells). The cells were then harvested at 3000 rpm for 2 min at room temperature. The cells were then washed in one half culture volume sterile water and spun as before. An additional spin was made to remove residual supernatant. The cells were then resuspended in 1/8 culture volume of LiSorb (100mM LiOAc, 10mM Tris-HCl, pH 8.0, 1M sorbitol (molecular biology quality, filter sterilized). The resuspended pellet was incubated for 5 min at room temperature before being spun as before. An additional spin was made to remove residual supernatant. The cell pellet was again resuspended in LiSorb (600µl per 100ml original culture). Carrier DNA was then added (10µl per 100µl yeast of 10mg/ml salmon sperm DNA (Gibco), heat-treated at 95°C for 5 min.) Cells were then aliquoted and frozen directly in a -80°C freezer where they were stored until use.

To transform frozen yeast cells, the cells were thawed at room temperature. 25µl cells were used per transformation. 0.5µl plasmid DNA for transformation was added to the cells, followed by 150µl LiPEG (100mM LiOAC, 10mM Tris-HCl, pH 8.0, 1mM EDTA, pH 8.0, 40% PEG3350, filter sterilize) The cells were then vortexed and incubated for 20 min. at room temperature. 17.5µl DMSO was then added and the cells were heat shocked for 15 min. in a 42°C water bath. The cells were then pelleted at low speed in a centrifuge, the supernatant removed, and the cells resuspended in 200µl sterile PBS. 100µl were plated onto appropriate selective plates and grown at 30°C.

.

## Biochemistry

### Western blotting

Cell lysates were obtained by lysing the cells in cell lysis buffer plus a cocktail of proteases inhibitors. The lysates were then clarified by centrifugation at 13000 rpm at 4°C. Cell lysates derived from different cell lines under different experimental conditions were resolved by SDS PAGE according to standard procedures. Gels were transferred to nitrocellulose membranes by semi-dry blotting for 1 hour at 1mA per membrane $cm^2$. The membranes were then washed twice in PBS and incubated with blocking solution (PBS, 0.1% tween20, 4% milk powder) for1 hour at room temperature.

Following the saturation with the blocking solution, membranes were incubated either for 2 hours at room temperature or for overnight at 4°C with primary antibody diluted in blocking solution. Subsequently, membranes were washed for 3 times 20 min. in PBS plus 0.1% tween20 at room temperature to remove the excess of the primary antibody. The secondary antibody linked to Horse Radish Peroxidase (HRP) was used to specifically recognize the primary antibody. After incubation with the secondary antibody for 1 hour at room temperature, membranes were washed again for 3 times 10 min. in PBS plus 0.1% tween20. To visualize the HRP enzymatic activity, ECL solution (Amersham) was incubated on the membrane for 1 min. at room temperature and the membranes were then exposed to X-ray-film.

### Recombinant protein purification

The purification of the recombinant protein used for the anti-Mig6 antibody production and the immunization of the rabbits were conducted in collaboration with Rodrigo Sanchez.

For the purification of the Mig6 recombinant protein the expression plasmids pGEX-GST-Mig6 (kindly provided by Dr Axel Ullrich), containing the Mig6 C-terminal half cDNA (from a.a. 273 to 459), the pDest15-Mig6 full length, N-terminal and ΔCRIB

were transformed by the heat shock method into the BL21 E.Coli strain. A single BL21 colony transformed with the expression plasmids were selected using the ampicillin resistance and inoculated into 500ml of LB broth media in the presence of ampicillin. The bacterial culture was grown at 37°C in constant agitation until the absorbance at 750 nm reached the value of 0.4 ($O.D._{750}$: 0.4). The recombinant proteins were then induced adding 1mM isopropyl-D-1-thiogalactopyranoside (IPTG) for 2 hours at 37°C in constant agitation. The bacteria were pelleted at 4000 rpm in a 4°C centrifuge. The bacterial pellet was washed twice in cold PBS and resuspended in 50 ml of PBS containing a cocktail of protease inhibitors purchased by Roche diagnostics and 1mM of 1,4-DiThioThreitol (DTT). The bacteria were mechanically lysed by passing the bacterial suspention 4 times through a French press. The lysate was first clarified at 4°C by centrifugation at 10.000 rpm for 10 min. and then by filtration using 0.24µm pore filter. The recombinant protein used for antibody production was then purified by Fast Protein Liquid Chromatography (FPLC) using the ÄKTA EXPLORER FPLC device. In brief a ready to use 1ml affinity chromatography column (Pharmacia GSTRAP$^{TM}$ FF 1ml) containing immobilized glutathione was equilibrated with 10 volume of PBS. The recombinant protein was purified by applying 1ml per minute of the clarified bacterial lysate to the affinity chromatography column that was then washed with 15ml of PBS. The recombinant protein was eluted with 10ml of TRIS buffer (50mM pH. 8) containing 10mM glutathione. The eluate was collected into 10 separate fractions of 1ml. The fractions containing the highest concentration of recombinant Mig6 protein were then dialyzed in PBS and concentrated to approximately 1mg/ml using CENTRIPLUS YM10 centrifugal filter device (Millipore Corporation) with an exclusion molecular weight of 30.000 Dalton.

**Pull down**

The bacteria transformed with the different expression plasmid were lysed and clarified as described above. 10% glycerol was added and the lysate further centrifuged at 13000 rpm for 15 min. at 4°C. The supernatant was recovered, aliquoted and stored at -80°C. 25µl for each recombinant protein were incubated 1 hour at 4°C with 20µl of

glutathione-sepharose beads in a final volume of 500µl. The beads were washed several times with cell lysis buffer and incubated for 1 hour at 4°C with protein derived from cell in different experimental conditions. The supernatant was removed and the beads washed several times with the cell lysis buffer. SDS-PAGE loading buffer was added and the samples denatured by incubation at 95°C for 4 min. The samples were then loaded on a SDS-PAGE gel as described above.

**Immunization of the rabbit**

In order to raise the basal immunogenic response of the White New Zeeland Rabbits 1 ml of the Freunds adjuvant completed with mycobacterium tuberculosis was subcutaneously injected in the animals. After 14 days from this first injection, the rabbits were immunized subcutaneously injecting 150µg of recombinant Mig6 protein resuspended into an equal volume of Freunds Adjuvant (without mycobacterium tuberculosis). All the following immunizations were performed in 14 days intervals. After the $6^{th}$ immunization the rabbits were sacrificed and the blood harvested. The blood was incubated at 37°C for 1 hour and the cloth removed. The blood was then incubated overnight at 4°C and clarified by centrifugation at 12.000 rpm. Finally, the crude anti-Mig6 anti-serum was harvested.

**Antigen purification of the antibody**

The anti-Mig6 antibody was antigen purified using Affigel beads (BIORAD). 2ml of Affigel beads were covalently coupled with 2mg of Mig6-GST antigen according to the manufacturer instruction. 12ml of the crude anti-Mig6 anti-serum was incubated 2h at 4°C with the antigen pre-coupled Affigel beads. The Mig6 antibody was then eluted from the beads with 10 ml of Glycin (0.2M, pH 2.8). The eluate was collected in 10 separated fractions of 1 ml. In order to neutralize the acidic pH of the Glycin, 200µl of TRIS (1M, pH8) was then added to each of the fractions. The quality and the concentration of the purified antibody were controlled by loading 10µl of each fraction onto a SDS-PAGE gel

and a Comassie blue staining was performed. 3 fractions containing the highest concentration of the purified Mig6 antibody were mixed and stored at -80°C.

## Cell cultures

### MLP29 and C2C12 cell lines

MLP29 and C2C12 cell line were grown in DMEM medium containing 10% Fetal Bovine Serum (FBS, GIBCO), 1% glutammine and 1% Penicilline/Streptomycine (P/S) at 37°C in the presence of 5% $CO_2$. The cells were starved in DMEM + 0.1% FBS for different amounts of time depending on the experiment and stimulated for different length of time with 40ng/ml human recombinant HGF (R&D), 30ng/ml human recombinant PDGF (Sigma) or 25ng/ml of human recombinant FGF2 (Sigma).

### Cortical neuron culture and electroporation

All the experiments with cortical neurons were performed in collaboration with Fabienne Lamballe and Flavio Maina.

The day before the cortical neuron culture, Boyden chamber and coverslips were coated with poly-Ornithin (Poly-O) for 3 hours at room temperature. The poly-O solution was removed and the membrane or the coverslips dried at room temperature for 30 min. Boyden chamber and coverslips were then incubated with DMEM plus 10% horse serum (Gibco) in the cell incubator.

The cortical neurons were taken from E15.5 embryos. Embryos were taken out from the uterus and kept on ice in HBSS buffer (Gibco). Brain cortices were cut off from the midbrain and brainstem and meninges were pulled off. The striatum was cut out. The cortices were incubated with Trypsin-EDTA (Gibco) at 37°C for 15 min. The Trypsin-EDTA was removed and the cortices washed 3 times with DMEM plus 10% HS in order to neutralize the trypsin. Cells were then dissociated with a Pasteur glass pipette in 1.5ml of DMEM plus 10% Horse Serum (HS, Gibco).

For the electroporation $6X10^5$ cells were mixed with 12µg of expression plasmid and cold PBS up to a final volume of 100µl. The mixture was transferred into electroporation cuvettes (MBP molecular bioproducts) and electroporated (5 pulses of 3 msec separated by 1 sec interval at 270 V) with an electroporator device (Electrosqare porator ECM830, BTX). The cells were then incubated on ice for 10 min., resuspended and plated either onto the upper compartment of the Boyden chamber or onto coverslips. After 3 hours the media was changed into DMEM-F12 (Gibco) plus P/S plus 10% HS. The cells were then stimulated with the appropriate growth factors as described above and fixed after 18 hours.

**SCGs cultures**

All the experiments using SCGs were performed in collaboration with Jane Thompson and Alun Davies.

Superior cervical ganglia were dissected from P40 CD1 mice. The ganglia were treated with 2mg/ml collagenase in HBSS for 30 min. at 4°C before trypsinization for 20 min. at 37°C and trituration. Most of the non neuronal cells were removed by differential sedimentation and the neurons (>90% pure) were plated in defined, serum-free medium in 35-mm culture dishes coated with poly-O and Laminin. The neurons were then stimulated with HGF.

To study survival under different experimental conditions, neurons were plated at low density (100 to 300 neurons per 35-mm dish), and the number of neurons attached within a 12X12 mm grid in the center of each dish was counted 6 hours after plating. The number of neurons surviving in this grid was then counted at 24 hourly intervals, and the number of surviving neurons in the grid at these time points was expressed as a percentage of the initial count taken at 6 hours. In each experiment, triplicate cultures were set up for all conditions.

To study neurite out-growth, cultures were set up following the same experimental procedures as before, except that the neurons were plated at higher density (400 to 800 neurons per 35-mm dish). Total neurite length was measured for each experimental condition using digital stereology (Kinetic imaging Ltd.), and the average

neurite length per neuron was calculated dividing this figure by neuron number per unit area.

For protein extraction, primary culture of dissociated P20 SCGs neurons were grown for 3 to 6 hours in culture before being stimulated for different time with HGF. Cells were harvested and homogenized as described above.

**Trophoblast Stem (TS) cells culture**

TS cells were generously provided by Janet Rossant laboratory (Tanaka et al., 1998, science). The Feeder Conditioned Medium (Feeder-CM) was used to culture the TS cells in the absence of fibroblasts. In order to prepare the Feeder-CM medium, primary Embryonic Fibrolasts (EMFIs) were prepared from E13.5 CD1 embryos. $2X10^6$ cells were plated into 10cm dish in RPMI medium (Gibco). The EMFIs were treated with MitomycinC for 2 hours and washed extensively with RPMI medium. 10ml of RPMI medium were added to the cells and after 72 hours the media was collected and clarified by centrifugation at 1000 rpm 15 min. TS cells were grown on 10cm dishes in RPMI (Gibco) plus P/S plus 70% of Feeder-CM plus 25ng/ml of FGF4 (Sigma) and 1µg/ml of heparin (Sigma).

**Plasmid transfection and Boyden chamber assay**

All the migration assays were repeated with independent sets of cells at least twice and each experimental condition was carried out at least in duplicate. The numbers of Hoechst positive nuclei were counted in six visual fields for each experimental condition.

MLP29 cells were grown in DMEM media supplemented with 10% FBS (Gibco), glutammine (Q, Gibco) and 1% of a mixture of penicilline/streptomycine at 37°C in the presence of 5% $CO_2$. One day before transfection the cells were trypsinized and $10^6$ cells were seeded on a 10cm dish (Falkon). The day of transfection the media was changed and 5ml of DMEM supplemented with Q and P/S (without FBS) were added to the media. 10µg expression plasmids were mixed with 1µg of Yellow Fluorescent Protein (YFP)

plasmid, Optimem serum-free medium (Invitrogen) and 24µl of Lipofectamine2000 reagent (Invitrogen) following the manufacturer instructions. The mixture was incubated for 20 min. at room temperature and then gently dropped onto the cells. The cells were then returned to the incubator for 4 hours. 5ml of DMEM supplemented with 20% FBS, Q and P/S were added to the cells for another 18 hours.

For the migration assay experiments, the membranes of the Boyden chamber (8µm pore size, Costar) were coated for 18 hours at 4°C with 0.15µg per $cm^2$ of fibronectin (Sigma). The filters were then washed twice with PBS and incubated for 1-2 hours with DMEM plus 0.1% FBS in the cell incubator. After transfection, the cells were starved in DMEM plus 0.1% FBS plus Q and P/S for 24 hours, harvested and $10^5$ cells were seeded either in the upper compartment of the Boyden chamber or on coverslips for immunofluorescense analysis. The Boyden chamber was then transferred to the cell incubator for an additional 3 hours and either DMEM plus 10% FBS or 40ng/ml of human recombinant HGF was added for 18 hours to the lower compartment. The membranes were washed once with PBS and the cell fixed at room temperature for 15 min. with 4% paraformaldheyde (PFA). The filters were then washed twice with PBS, the upper compartment cells were scraped off the membrane and the nuclei stained with Hoechst fluorescent dye. The filters were directly analyzed under a Zeiss fluorescent microscope.

**SiRNA transfection and Boyden chamber assay**

5µl stock solution (400µM) of the sense and anti-sense siRNA oligonucleotides (DARMAKOM) were mixed with 90µl of annealing buffer. The siRNAs were denatured for 1 min at 90°C and annealed by 1 hour incubation at 37°C. The annealed solution of siRNA duplex was aliquoted and stored at -20°C.

MLP29 cells ($4X10^5$) were plated on 10cm dishes (Falkon) the day before transfection. After few hours the media was changed into DMEM plus 0.1% FBS. For every 10 cm dish, 5µl of either Mig6 or GFP siRNA duplex were mixed with Optimem and with 9µl of Oligofectamine (Invitrogen) according to the manufacturer instructions. The solution was then incubated at room temperature for 20 min. and gently pipetted onto

the cells. After 96 hours the cells were transfected a second time as above and Aphidicolin was eventually added at this step. After another 24 hours the cell were either lysed for western blotting analysis or harvested, and seeded either onto coverslips for BrdU incorporation assay and immunofluorescence analysis or onto the upper compartment of the Boyden chamber in the presence or the absence of Aphidicolin and the migration assay was performed as described above.

**BrdU assay**

After the transfection with either siRNA or with overexpression plasmids, the cells were stimulated as described above. 100μM of Bromodeoxyuridine (BrdU) was added to the culture media for the last 2 hours of stimulation. MLP29 cells were then fixed in Methanol and the BrdU was visualized by immunofluorescence analysis. The percent of BrdU positive versus Hoechst positive nuclei was calculated.

**Immunofluorescence**

After transfection of either siRNA oligos or overexpressing constructs as described before the cells were fixed 15 min. at room temperature with 4% PFA and 4% sucrose. In order to deactivate the PFA, the cells were incubated for 10 min. at room temperature with 50mM $NH_4Cl$. The cells were then permeabilized by incubation for 5 min. at room temperature with PBS plus 0.1% tritonX100, washed 3 times in PBS and incubated for 1 hour at room temperature with blocking solution (PBS, 5% sheep serum, 5% goat serum). The cells were incubated for 2 hours at room temperature with the primary antibody diluted in blocking solution. The excess of the primary antibody was removed by washing at room temperature 3 times with PBS and the cells were incubated for 30 min. at room temperature with the fluorophore-conjugated secondary antibody. Finally the cells were washed 3 times at room temperature with PBS and the coverslips mounted with an aqueous solution mounting medium (MOWIOL).

**Mouse work**

Mutant and control mice were maintained in a mixed genetic background (C57/Black6/CD1). For experiments with adult mice, mice were separated from their parents at the age of around 3 weeks and males and females were housed separately. Tail biopsies were taken and mice were ear tagged using six-digit ear tags from Natialband & tag company. For the experiments with embryos, breedings were set up with one male and two females. Vaginal plug-checks were done starting the following morning. A plug was counted as pregnancy for 0.5 days. Embryos were taken according to experimental procedures. For genotyping of embryos younger than E13.5 yolk sacs were separated from the placenta and used for subsequent DNA extraction.

**Histology**

**Cryostat sections and *in-situ* hybridization**

Cryostat sections of E13.5 embryos were used for *in-situ* hybridization. Embryos were dissected in PBS and fixed overnight in 4% PFA at 4°C. They were washed 3 times in cold PBS and placed in a 30% sucrose solution for overnight at 4°C. OCT embedding medium was placed in embedding molds and embryos were dried and placed into the embedding medium. Subsequently, the embedding molds were placed in isopentane that was in turn submerged in liquid nitrogen for several minutes in order to harden the embedding medium. For sections on the slides, 18µm serial sections were cut at -20°C and directly transferred to gelatin coated slides (Menzel-gläser). The sections were either processed directly or stored at -20°C for later processing. The sections were incubated overnight at 70°C with 200µl of hybridization buffer plus 80µl of labeled probe. The excess of probe was washed away at 65°C 3 times with washing buffer. The tissue was then blocked for 1 hour at room temperature with 1ml of blocking solution containing 2% blocking agent (Roche), 20% sheep serum and 0.1% tween20. The labeled probe was then recognized by an anti-digoxigenin specific antibody (Roche) conjugated with the alkaline phosphatase (ROCHE). Thus the tissue was incubated for overnight with the

anti-digoxigenin specific antibody diluted 1:2000 in blocking solution. Excess antibody was removed by washing the slides several times in MABT at room temperature. The alkaline phosphatase enzymatic activity was then visualized incubating the slides for several hours with a mixture of substrate colorants (NBT and BCIP). Subsequently, the slides were washed in PBS plus 0.1% tween20 and fixed overnight with 4% PFA.

**Whole mount *in-situ* hybridization**

E9.5 wild type and mutant embryos were dissected in PBS and dehydrated by solutions containing increasing concentrations of methanol. The embryos were stored at -20°C in 100% methanol for several weeks. In order to inhibit endogenous alkaline phosphatases the embryos were washed in a solution containing 80% methanol plus 6% $H_2O_2$ for 1 hour at room temperature. The embryos were then rehydrated by incubation in a reverse methanol series, washed 3 times for 5 min. with PBS plus 0.1% tween20 and digested in a 20mg/ml of proteinaseK solution for 30 min. at room temperature. The embryos were then post-fixed in a solution containing 4% PFA and 0.2% glutaraldheyde at 4°C. The embryos were then blocked for 1h at 70°C in prehybridization solution. 40µl of labeled probe was added to 1ml of prehybridization solution and the embryos incubated at 70°C for 18 hours. Excess probe was removed by 3 washes of 30 min. each in 3 different washing solutions with increasing stringency properties: wash I at 70°C (50% formamide, 5X SSC pH4.5, 0.1% tween20, 0.5% chaps), wash II at 65°C (50% formamide, 2X SSC pH4.5, 0.1% tween20, 0.5% chaps), wash III at 65°C (2X SSC pH4.5, 0.1% tween20, 0.5% chaps). Meanwhile 2µl/ml of the anti-digoxigenin specific antibody was preabsorbed in a solution containing 8mg of embryo powder for 2 hours at 4°C. The embryo powder was removed by centrifugation and the supernatant mixed with a solution containing 2% blocking reagent and 20% sheep serum. The embryos were then incubated with the antibody solution for 18 hours at 4°C. Excess of the antibody was removed by several washes in PBS plus 0.1% tween20 and the antibody detected as described before.

**Cryosections of gelatin embedded whole mount *in-situ* hybridization**

The whole mount in-situ hybridizations were fixed in 4% PFA for overnight at 4°C, washed 3 times for 5 min in PBS and incubated in a solution of PBS plus 20% sucrose for 3 hours. The embryos were then transferred into embedding molds containing the embedding gelatin solution (7.5% gelatin, 50% sucrose) and left on ice for several minutes. When the gelatin solution was hardened and the embedding molds were frozen in dry ice and 25µm sections were then cut at -20°C using the cryostat.

**Antibody staining on cryostat sections**

18µm cryostat sagittal sections of E15.5 embryos were cut as described above. The sections were dried at 37°C for 30 min. and washed in PBS for 5 min. The sections were fixed with 4% PFA for 5 min. at room temperature and washed once with PBS. The tissue was permeabilized washing the sections 3 times with PBS plus 0.5% tritonX100 for 15 min. The sections were then washed 2 times in PBS and incubated for 1 hour at room temperature with blocking solution (0.5% tritonX100, 5% sheep serum, 5% goat serum). In order to verify the antibody specificity, the primary anti-Mig6 specific antibody was then diluted 1:100 in blocking solution and incubated with either 5µg/ml of GST or 5µg /ml of GST-Mig6 antigen fusion protein for 3 hours at 4°C. The primary antibody was then incubated on the sections for 2 hours at room temperature. Excess antibody was removed by washing 3 times in PBS plus 0.5% tritonX100. The sections were blocked again for 1 hour at room temperature with blocking solution and incubated with the fluorophore-conjugated secondary antibody. Excess secondary antibody was removed by washing 3 times with PBS plus 0.5% tritonX100 and the slides were mounted with an aqueous mounting media (MOWIOL). The sections were directly analyzed with a fluorescent microscope and representative pictures taken.

# Acknowledgements

Four years ago I thought I would have never managed to reach the end of this work because I didn't know most of the people mentioned on this page. Every one of them gave me an essential contribution to reach the end of this work.

My thesis supervisor Dr. Rüdiger Klein gave me the chance to work independently. He drove me, step by step, through this work. The environment he created in the lab and the discussions, suggestions, encouragements, pressure, responsibility and critics I received from him were all essential to grow up as a scientist and more importantly as a person. I felt honored sharing with him the 'idea' of Science. Thank you Rüdiger!

If in the lab, my hands and my brain were doing their job (not often, though) was because of my Teacher: Dr. Flavio "il Maestro" Maina. During all these years Flavio has always been generously present for suggestions, critics, and encouragements. His presence has been of an invaluable importance to me. Grazie Flavio.

I learnt from Dr Tomoko Iwata the power of organization. I will be eternally thankful to her. I really had a good time during our short, but intense collaboration. Thank you Tomoko.

I also thank Prof. Alun Davies, Dr Jane Thompson and Dr Fabienne Lamballe for the fruitful collaboration and discussions. I am grateful to Rodrigo "Sancho" Sanchez for helping me with the antibody production.

I thank Dr Francis Barr for the precious time he offered me during sunny Sundays, for all the suggestions and all the precious help I received from him. Thanks a lot, Francis.

This experience was made possible also because Prof. Carola Ponzetto offered me the enthusiasm and passion for Science that motivated me during all these years. Grazie Carola.

I thank Dr Amparo Palmer for answering to all kinds of "stupid" scientific questions I had….and I had a lot!

The whole universe of Biochemistry was discovered thankfully to Dr Joaquim Egea. Gracias por el tiempo que me has dedicado, pelon!

If I discussed with somebody, this person was undoubtedly Dr Francoise Helmbacher. From science to life we discussed about everything. Thank you Framboise.

Despite the results that are difficult to obtain, I shared with Katrin Deininger some faith in science. Thanks a lot for all the helpful critics and suggestions on this thesis. Never give up Deininger!

But also the whole Klein, Palmer and Tavosanis' lab made of my PhD a unique experience and I should thank them all. In particular I thank Manuel "-ito" Zimmer for dinners and discussions, Ilona Grunwald for fruitful critics and lot of fun, George Wilkinson for nice conversations, suggestions and nervous lips, Archana Mishra for Indian mythology reports, Luca Dolce for sharing with me part of the microarray project, John Bailey for the proof reading of this thesis and for the help with job applications, Ingvar Ferby for the "loose your dream and face reality" sentence, Taija Makkinen for all the Finnish I learnt.

The soundtracks of these four years were mainly provided by Ben Short. Without him it would have been much, much longer and boring. Thank you Ben. Thank you also for all the Yeast two hybrid methods you tought me. I should also thank Bjorn Schumacker for the fun we had during these years. I am really thankful to Catherine, Pitt and Mia because I felt somehow at home most probably because of the excellent wine and food we shared….. even if French.

La maggioranza di voi non capirà molto di questa tesi, tuttavia non sentitevi estranei a questo lavoro in quanto siete stati tutti, a vostro modo, indispensabili per scriverlo nel corso di questi anni. Grazie!

I registi delle mie scelte durante tutti questi anni sono sempre stati i miei genitori Angelo ed Ester. A loro va il mio ringraziamento e la mia stima per avermi regalato il bene piú prezioso: la liberta' di scelta. La colonna sonora è stata regalata da mio fratello Pippo e da Paola. La voglia di continuare a restare piccolo, crescendo, è stata fornita da Mariasole ed Ottavia. "Un altro punto di vista", l'alloggio e l'alta cucina sono stati offerti da mio fratello Miky e da Danie. La sensazione di non perdersi la gente per strada e la gestione delle emergenze è stata fornita da Giulio "Prodigal friend". Il valore e la sicurezza dell'amicizia sono stati offerti da Manú. Ogni tipo di supporto compreso quello logistico è stato fornito da Enzo Monja e ?. I materiali per dare un taglio giusto alla storia sono stati offerti da Andrea "il Basket". I costumi sono stati gentilmente offerti da "FOЯVM"-Roma. L'Hornet e' stata spesso gentilmente fornita da Paolo Acco. Markus Müller, Alessandro Ieraci e Paolino Forni hanno fortemente contribuito all'idea originale ed ancora continuano a farlo. Gioie e dolori, donne e motori, e molto altro ancora della vita quotidiana sono stati condivisi con Giulia Guarguaglini. Grazie Giulia

Il motivo di questo lavoro, di quattro anni passati lontano da casa ed il senso di ricominciare nuovamente sono stati regalati da Martina. Grazie Martina! per questo e per tanto altro ancora.

I paradossi della vita giornaliera sono stati tratti da "il discobolo" di Paolo Filardo, edizioni "il primitivo". Fletto i muscoli e sono nel vuoto.

# References

Abounader, R., B. Lal, C. Luddy, G. Koe, B. Davidson, E.M. Rosen, and J. Laterra. 2002. In vivo targeting of SF/HGF and c-met expression via U1snRNA/ribozymes inhibits glioma growth and angiogenesis and promotes apoptosis. *Faseb J*. 16:108-10.

Ahmed, I., Y. Calle, M.A. Sayed, J.M. Kamal, P. Rengaswamy, E. Manser, S. Meiners, and E.K.A. Nur. 2004. Cdc42-dependent nuclear translocation of non-receptor tyrosine kinase, ACK. *Biochem Biophys Res Commun*. 314:571-9.

Ahmed, Z., B.J. Smith, K. Kotani, P. Wilden, and T.S. Pillay. 1999. APS, an adapter protein with a PH and SH2 domain, is a substrate for the insulin receptor kinase. *Biochem J*. 341 ( Pt 3):665-8.

Ahmed, Z., B.J. Smith, and T.S. Pillay. 2000. The APS adapter protein couples the insulin receptor to the phosphorylation of c-Cbl and facilitates ligand-stimulated ubiquitination of the insulin receptor. *FEBS Lett*. 475:31-4.

Allen, W.E., D. Zicha, A.J. Ridley, and G.E. Jones. 1998. A role for Cdc42 in macrophage chemotaxis. *J Cell Biol*. 141:1147-57.

Alonso, A., S. Rahmouni, S. Williams, M. van Stipdonk, L. Jaroszewski, A. Godzik, R.T. Abraham, S.P. Schoenberger, and T. Mustelin. 2003. Tyrosine phosphorylation of VHR phosphatase by ZAP-70. *Nat Immunol*. 4:44-8.

Alonso, A., J. Sasin, N. Bottini, I. Friedberg, A. Osterman, A. Godzik, T. Hunter, J. Dixon, and T. Mustelin. 2004. Protein tyrosine phosphatases in the human genome. *Cell*. 117:699-711.

Amatschek, S., U. Koenig, H. Auer, P. Steinlein, M. Pacher, A. Gruenfelder, G. Dekan, S. Vogl, E. Kubista, K.H. Heider, C. Stratowa, M. Schreiber, and W. Sommergruber. 2004. Tissue-wide expression profiling using cDNA subtraction and microarrays to identify tumor-specific genes. *Cancer Res*. 64:844-56.

Anastasi, S., L. Fiorentino, M. Fiorini, R. Fraioli, G. Sala, L. Castellani, S. Alema, M. Alimandi, and O. Segatto. 2003. Feedback inhibition by RALT controls signal output by the ErbB network. *Oncogene*. 22:4221-34.

Bardelli, A., M.L. Basile, E. Audero, S. Giordano, S. Wennstrom, S. Menard, P.M. Comoglio, and C. Ponzetto. 1999. Concomitant activation of pathways downstream of Grb2 and PI 3-kinase is required for MET-mediated metastasis. *Oncogene*. 18:1139-46.

Bazenet, C.E., M.A. Mota, and L.L. Rubin. 1998. The small GTP-binding protein Cdc42 is required for nerve growth factor withdrawal-induced neuronal death. *Proc Natl Acad Sci U S A*. 95:3984-9.

Billiau, A. 1996. Interferon-gamma: biology and role in pathogenesis. *Adv Immunol*. 62:61-130.

Birchmeier, C., W. Birchmeier, E. Gherardi, and G.F. Vande Woude. 2003. Met, metastasis, motility and more. *Nat Rev Mol Cell Biol*. 4:915-25.

Bladt, F., D. Riethmacher, S. Isenmann, A. Aguzzi, and C. Birchmeier. 1995. Essential role for the c-met receptor in the migration of myogenic precursor cells into the limb bud. *Nature*. 376:768-71.

Boehm, U., T. Klamp, M. Groot, and J.C. Howard. 1997. Cellular responses to interferon-gamma. *Annu Rev Immunol*. 15:749-95.

Bordo, D., and P. Bork. 2002. The rhodanese/Cdc25 phosphatase superfamily. Sequence-structure-function relations. *EMBO Rep*. 3:741-6.

Bottaro, D.P., J.S. Rubin, D.L. Faletto, A.M. Chan, T.E. Kmiecik, G.F. Vande Woude, and S.A. Aaronson. 1991. Identification of the hepatocyte growth factor receptor as the c-met proto-oncogene product. *Science*. 251:802-4.

Brand-Saberi, B., T.S. Muller, J. Wilting, B. Christ, and C. Birchmeier. 1996. Scatter factor/hepatocyte growth factor (SF/HGF) induces emigration of myogenic cells at interlimb level in vivo. *Dev Biol*. 179:303-8.

Bruce Alberts, A.J., Julian Lewis, Martin Raff, Keith Roberts, Peter Walter. 2002. Molecular Biology of the Cell. Taylor & Francis group.

Brysha, M., J.G. Zhang, P. Bertolino, J.E. Corbin, W.S. Alexander, N.A. Nicola, D.J. Hilton, and R. Starr. 2001. Suppressor of cytokine signaling-1 attenuates the duration of interferon gamma signal transduction in vitro and in vivo. *J Biol Chem*. 276:22086-9.

Caric, D., H. Raphael, J. Viti, A. Feathers, D. Wancio, and L. Lillien. 2001. EGFRs mediate chemotactic migration in the developing telencephalon. *Development*. 128:4203-16.

Casci, T., J. Vinos, and M. Freeman. 1999. Sprouty, an intracellular inhibitor of Ras signaling. *Cell*. 96:655-65.

Cerione, R.A., and Y. Zheng. 1996. The Dbl family of oncogenes. *Curr Opin Cell Biol*. 8:216-22.

Chu, D.T., C.M. Davis, N.B. Chrapkiewicz, and D.K. Granner. 1988. Reciprocal regulation of gene transcription by insulin. Inhibition of the phosphoenolpyruvate carboxykinase gene and stimulation of gene 33 in a single cell type. *J Biol Chem*. 263:13007-11.

Chung, H.A., J. Hyodo-Miura, A. Kitayama, C. Terasaka, T. Nagamune, and N. Ueno. 2004. Screening of FGF target genes in Xenopus by microarray: temporal dissection of the signalling pathway using a chemical inhibitor. *Genes Cells*. 9:749-61.

Comoglio, P.M., and C. Boccaccio. 2001. Scatter factors and invasive growth. *Semin Cancer Biol*. 11:153-65.

Cooper, C.S., M. Park, D.G. Blair, M.A. Tainsky, K. Huebner, C.M. Croce, and G.F. Vande Woude. 1984. Molecular cloning of a new transforming gene from a chemically transformed human cell line. *Nature*. 311:29-33.

Cortes-Canteli, M., M. Wagner, W. Ansorge, and A. Perez-Castillo. 2004. Microarray analysis supports a role for ccaat/enhancer-binding protein-beta in brain injury. *J Biol Chem*. 279:14409-17.

Danilkovitch-Miagkova, A., and B. Zbar. 2002. Dysregulation of Met receptor tyrosine kinase activity in invasive tumors. *J Clin Invest*. 109:863-7.

De Maeyer-Guignard, J., E. Lauret, L. Eusebe, and E. De Maeyer. 1993. Accelerated tumor development in interferon-treated B6.C-Hyal-1 a mice. *Proc Natl Acad Sci U S A*. 90:5708-12.

De Sepulveda, P., K. Okkenhaug, J.L. Rose, R.G. Hawley, P. Dubreuil, and R. Rottapel. 1999. Socs1 binds to multiple signalling proteins and suppresses steel factor-dependent proliferation. *Embo J*. 18:904-15.

Dietrich, S., F. Abou-Rebyeh, H. Brohmann, F. Bladt, E. Sonnenberg-Riethmacher, T. Yamaai, A. Lumsden, B. Brand-Saberi, and C. Birchmeier. 1999. The role of SF/HGF and c-Met in the development of skeletal muscle. *Development*. 126:1621-9.

Dikic, I. 2002. CIN85/CMS family of adaptor molecules. *FEBS Lett*. 529:110-5.

Dikic, I., and S. Giordano. 2003. Negative receptor signalling. *Curr Opin Cell Biol*. 15:128-35.

Elbashir, S.M., J. Harborth, W. Lendeckel, A. Yalcin, K. Weber, and T. Tuschl. 2001a. Duplexes of 21-nucleotide RNAs mediate RNA interference in cultured mammalian cells. *Nature*. 411:494-8.

Elbashir, S.M., W. Lendeckel, and T. Tuschl. 2001b. RNA interference is mediated by 21- and 22-nucleotide RNAs. *Genes Dev*. 15:188-200.

Elchebly, M., P. Payette, E. Michaliszyn, W. Cromlish, S. Collins, A.L. Loy, D. Normandin, A. Cheng, J. Himms-Hagen, C.C. Chan, C. Ramachandran, M.J. Gresser, M.L. Tremblay, and B.P. Kennedy. 1999. Increased insulin sensitivity and obesity resistance in mice lacking the protein tyrosine phosphatase-1B gene. *Science*. 283:1544-8.

Endo, T.A., M. Masuhara, M. Yokouchi, R. Suzuki, H. Sakamoto, K. Mitsui, A. Matsumoto, S. Tanimura, M. Ohtsubo, H. Misawa, T. Miyazaki, N. Leonor, T. Taniguchi, T. Fujita, Y. Kanakura, S. Komiya, and A. Yoshimura. 1997. A new protein containing an SH2 domain that inhibits JAK kinases. *Nature*. 387:921-4.

Fambrough, D., K. McClure, A. Kazlauskas, and E.S. Lander. 1999. Diverse signaling pathways activated by growth factor receptors induce broadly overlapping, rather than independent, sets of genes. *Cell*. 97:727-41.

Fiorentino, L., C. Pertica, M. Fiorini, C. Talora, M. Crescenzi, L. Castellani, S. Alema, P. Benedetti, and O. Segatto. 2000. Inhibition of ErbB-2 mitogenic and transforming activity by RALT, a mitogen-induced signal transducer which binds to the ErbB-2 kinase domain. *Mol Cell Biol*. 20:7735-50.

Fiorini, M., C. Ballaro, G. Sala, G. Falcone, S. Alema, and O. Segatto. 2002. Expression of RALT, a feedback inhibitor of ErbB receptors, is subjected to an integrated transcriptional and post-translational control. *Oncogene*. 21:6530-9.

Freeman, M. 1997. Cell determination strategies in the Drosophila eye. *Development*. 124:261-70.

Freeman, M. 1998. Complexity of EGF receptor signalling revealed in Drosophila. *Curr Opin Genet Dev*. 8:407-11.

Freeman, M., C. Klambt, C.S. Goodman, and G.M. Rubin. 1992. The argos gene encodes a diffusible factor that regulates cell fate decisions in the Drosophila eye. *Cell*. 69:963-75.

Fukata, M., and K. Kaibuchi. 2001. Rho-family GTPases in cadherin-mediated cell-cell adhesion. *Nat Rev Mol Cell Biol*. 2:887-97.

Furge, K.A., Y.W. Zhang, and G.F. Vande Woude. 2000. Met receptor tyrosine kinase: enhanced signaling through adapter proteins. *Oncogene*. 19:5582-9.

Gambarotta, G., D. Garzotto, E. Destro, B. Mautino, C. Giampietro, S. Cutrupi, C. Dati, E. Cattaneo, A. Fasolo, and I. Perroteau. 2004. ErbB4 expression in neural progenitor cells (ST14A) is necessary to mediate neuregulin-1beta1-induced migration. *J Biol Chem*. 279:48808-16.

Gherardi, E., and M. Stoker. 1990. Hepatocytes and scatter factor. *Nature*. 346:228.

Ghiglione, C., K.L. Carraway, 3rd, L.T. Amundadottir, R.E. Boswell, N. Perrimon, and J.B. Duffy. 1999. The transmembrane molecule kekkon 1 acts in a feedback loop to negatively regulate the activity of the Drosophila EGF receptor during oogenesis. *Cell*. 96:847-56.

Gresser, I. 1982. Can interferon induce disease? *Interferon*. 4:95-127.

Gu, Y., Q. Lin, C. Childress, and W. Yang. 2004. Identification of the region in Cdc42 that confers the binding specificity to activated Cdc42-associated kinase. *J Biol Chem*. 279:30507-13.

Hackel, P.O., M. Gishizky, and A. Ullrich. 2001. Mig-6 is a negative regulator of the epidermal growth factor receptor signal. *Biol Chem*. 382:1649-62.

Haglund, K., N. Shimokawa, I. Szymkiewicz, and I. Dikic. 2002. Cbl-directed monoubiquitination of CIN85 is involved in regulation of ligand-induced degradation of EGF receptors. *Proc Natl Acad Sci U S A*. 99:12191-6.

Haj, F.G., P.J. Verveer, A. Squire, B.G. Neel, and P.I. Bastiaens. 2002. Imaging sites of receptor dephosphorylation by PTP1B on the surface of the endoplasmic reticulum. *Science*. 295:1708-11.

Hall, A. 1998. Rho GTPases and the actin cytoskeleton. *Science*. 279:509-14.

Hartmann, G., T. Prospero, V. Brinkmann, C. Ozcelik, G. Winter, J. Hepple, S. Batley, F. Bladt, M. Sachs, C. Birchmeier, W. Birchmeier, and E. Gherardi. 1998. Engineered mutants of HGF/SF with reduced binding to heparan sulphate proteoglycans, decreased clearance and enhanced activity in vivo. *Curr Biol*. 8:125-34.

Hecht, M., M. Papoutsi, H.D. Tran, J. Wilting, and L. Schweigerer. 2004. Hepatocyte growth factor/c-Met signaling promotes the progression of experimental human neuroblastomas. *Cancer Res*. 64:6109-18.

Helmbacher, F., E. Dessaud, S. Arber, O. deLapeyriere, C.E. Henderson, R. Klein, and F. Maina. 2003. Met signaling is required for recruitment of motor neurons to PEA3-positive motor pools. *Neuron*. 39:767-77.

Hemmi, S., R. Bohni, G. Stark, F. Di Marco, and M. Aguet. 1994. A novel member of the interferon receptor family complements functionality of the murine interferon gamma receptor in human cells. *Cell*. 76:803-10.

Hicke, L. 2001. Protein regulation by monoubiquitin. *Nat Rev Mol Cell Biol*. 2:195-201.

Hopper, N.A., J. Lee, and P.W. Sternberg. 2000. ARK-1 inhibits EGFR signaling in C. elegans. *Mol Cell*. 6:65-75.

Hunter, T. 1995. Protein kinases and phosphatases: the yin and yang of protein phosphorylation and signaling. *Cell*. 80:225-36.

Ikegami, S., T. Taguchi, M. Ohashi, M. Oguro, H. Nagano, and Y. Mano. 1978. Aphidicolin prevents mitotic cell division by interfering with the activity of DNA polymerase-alpha. *Nature*. 275:458-60.

Ishizaki, T., M. Maekawa, K. Fujisawa, K. Okawa, A. Iwamatsu, A. Fujita, N. Watanabe, Y. Saito, A. Kakizuka, N. Morii, and S. Narumiya. 1996. The small GTP-binding protein Rho binds to and activates a 160 kDa Ser/Thr protein kinase homologous to myotonic dystrophy kinase. *Embo J*. 15:1885-93.

Jallal, B., J. Schlessinger, and A. Ullrich. 1992. Tyrosine phosphatase inhibition permits analysis of signal transduction complexes in p185HER2/neu-overexpressing human tumor cells. *J Biol Chem*. 267:4357-63.

James, P., J. Halladay, and E.A. Craig. 1996. Genomic libraries and a host strain designed for highly efficient two-hybrid selection in yeast. *Genetics*. 144:1425-36.

Jeffers, M., M. Fiscella, C.P. Webb, M. Anver, S. Koochekpour, and G.F. Vande Woude. 1998. The mutationally activated Met receptor mediates motility and metastasis. *Proc Natl Acad Sci U S A*. 95:14417-22.

Joazeiro, C.A., and A.M. Weissman. 2000. RING finger proteins: mediators of ubiquitin ligase activity. *Cell*. 102:549-52.

Kay, B.K., and J.W. Kehoe. 2004. PDZ domains and their ligands. *Chem Biol*. 11:423-5.

Keyse, S.M. 1998. Protein phosphatases and the regulation of MAP kinase activity. *Semin Cell Dev Biol*. 9:143-52.

Klaman, L.D., O. Boss, O.D. Peroni, J.K. Kim, J.L. Martino, J.M. Zabolotny, N. Moghal, M. Lubkin, Y.B. Kim, A.H. Sharpe, A. Stricker-Krongrad, G.I. Shulman, B.G. Neel, and B.B. Kahn. 2000. Increased energy expenditure, decreased adiposity, and tissue-specific insulin sensitivity in protein-tyrosine phosphatase 1B-deficient mice. *Mol Cell Biol*. 20:5479-89.

Klingmuller, U., U. Lorenz, L.C. Cantley, B.G. Neel, and H.F. Lodish. 1995. Specific recruitment of SH-PTP1 to the erythropoietin receptor causes inactivation of JAK2 and termination of proliferative signals. *Cell*. 80:729-38.

Koch, C.A., D. Anderson, M.F. Moran, C. Ellis, and T. Pawson. 1991. SH2 and SH3 domains: elements that control interactions of cytoplasmic signaling proteins. *Science*. 252:668-74.

Kotani, K., P. Wilden, and T.S. Pillay. 1998. SH2-Balpha is an insulin-receptor adapter protein and substrate that interacts with the activation loop of the insulin-receptor kinase. *Biochem J*. 335 ( Pt 1):103-9.

Kraynov, V.S., C. Chamberlain, G.M. Bokoch, M.A. Schwartz, S. Slabaugh, and K.M. Hahn. 2000. Localized Rac activation dynamics visualized in living cells. *Science*. 290:333-7.

Labouesse, M. 2004. Epithelium-mesenchyme: a balancing act of RhoGAP and RhoGEF. *Curr Biol*. 14:R508-10.

Lamarche, N., N. Tapon, L. Stowers, P.D. Burbelo, P. Aspenstrom, T. Bridges, J. Chant, and A. Hall. 1996. Rac and Cdc42 induce actin polymerization and G1 cell cycle progression independently of p65PAK and the JNK/SAPK MAP kinase cascade. *Cell*. 87:519-29.

Leung, T., X.Q. Chen, E. Manser, and L. Lim. 1996. The p160 RhoA-binding kinase ROK alpha is a member of a kinase family and is involved in the reorganization of the cytoskeleton. *Mol Cell Biol*. 16:5313-27.

Leung, T., E. Manser, L. Tan, and L. Lim. 1995. A novel serine/threonine kinase binding the Ras-related RhoA GTPase which translocates the kinase to peripheral membranes. *J Biol Chem*. 270:29051-4.

Liang, T.J., A.E. Reid, R. Xavier, R.D. Cardiff, and T.C. Wang. 1996. Transgenic expression of tpr-met oncogene leads to development of mammary hyperplasia and tumors. *J Clin Invest*. 97:2872-7.

Ma, S., P. Fey, and R.L. Chisholm. 2001. Molecular motors and membrane traffic in Dictyostelium. *Biochim Biophys Acta*. 1525:234-44.

Maina, F., F. Casagranda, E. Audero, A. Simeone, P.M. Comoglio, R. Klein, and C. Ponzetto. 1996. Uncoupling of Grb2 from the Met receptor in vivo reveals complex roles in muscle development. *Cell*. 87:531-42.

Maina, F., M.C. Hilton, R. Andres, S. Wyatt, R. Klein, and A.M. Davies. 1998. Multiple roles for hepatocyte growth factor in sympathetic neuron development. *Neuron*. 20:835-46.

Maina, F., and R. Klein. 1999. Hepatocyte growth factor, a versatile signal for developing neurons. *Nat Neurosci*. 2:213-7.

Maina, F., G. Pante, F. Helmbacher, R. Andres, A. Porthin, A.M. Davies, C. Ponzetto, and R. Klein. 2001. Coupling Met to specific pathways results in distinct developmental outcomes. *Mol Cell*. 7:1293-306.

Makkinje, A., D.A. Quinn, A. Chen, C.L. Cadilla, T. Force, J.V. Bonventre, and J.M. Kyriakis. 2000. Gene 33/Mig-6, a transcriptionally inducible adapter protein that binds GTP-Cdc42 and activates SAPK/JNK. A potential marker transcript for chronic pathologic conditions, such as diabetic nephropathy. Possible role in the response to persistent stress. *J Biol Chem*. 275:17838-47.

Manes, G., P. Bello, and S. Roche. 2000. Slap negatively regulates Src mitogenic function but does not revert Src-induced cell morphology changes. *Mol Cell Biol*. 20:3396-406.

Manser, E., T. Leung, H. Salihuddin, Z.S. Zhao, and L. Lim. 1994. A brain serine/threonine protein kinase activated by Cdc42 and Rac1. *Nature*. 367:40-6.

Marone, R., D. Hess, D. Dankort, W.J. Muller, N.E. Hynes, and A. Badache. 2004. Memo mediates ErbB2-driven cell motility. *Nat Cell Biol*. 6:515-22.

Martin, G.A., G. Bollag, F. McCormick, and A. Abo. 1995. A novel serine kinase activated by rac1/CDC42Hs-dependent autophosphorylation is related to PAK65 and STE20. *Embo J*. 14:1970-8.

Medico, E., A.M. Mongiovi, J. Huff, M.A. Jelinek, A. Follenzi, G. Gaudino, J.T. Parsons, and P.M. Comoglio. 1996. The tyrosine kinase receptors Ron and Sea control "scattering" and morphogenesis of liver progenitor cells in vitro. *Mol Biol Cell*. 7:495-504.

Mitchison, T.J., and L.P. Cramer. 1996. Actin-based cell motility and cell locomotion. *Cell*. 84:371-9.

Mohammadi, M., I. Dikic, A. Sorokin, W.H. Burgess, M. Jaye, and J. Schlessinger. 1996a. Identification of six novel autophosphorylation sites on fibroblast growth factor receptor 1 and elucidation of their importance in receptor activation and signal transduction. *Mol Cell Biol*. 16:977-89.

Mohammadi, M., J. Schlessinger, and S.R. Hubbard. 1996b. Structure of the FGF receptor tyrosine kinase domain reveals a novel autoinhibitory mechanism. *Cell*. 86:577-87.

Moodie, S.A., J. Alleman-Sposeto, and T.A. Gustafson. 1999. Identification of the APS protein as a novel insulin receptor substrate. *J Biol Chem*. 274:11186-93.

Mott, H.R., D. Owen, D. Nietlispach, P.N. Lowe, E. Manser, L. Lim, and E.D. Laue. 1999. Structure of the small G protein Cdc42 bound to the GTPase-binding domain of ACK. *Nature*. 399:384-8.

Mustelin, T. 2002. Keeping the T-cell immune response in balance: role of protein tyrosine phosphatases in autoimmunity. *Curr Dir Autoimmun*. 5:176-90.

Nakamura, T., T. Nishizawa, M. Hagiya, T. Seki, M. Shimonishi, A. Sugimura, K. Tashiro, and S. Shimizu. 1989. Molecular cloning and expression of human hepatocyte growth factor. *Nature*. 342:440-3.

Nobes, C.D., and A. Hall. 1995. Rho, rac, and cdc42 GTPases regulate the assembly of multimolecular focal complexes associated with actin stress fibers, lamellipodia, and filopodia. *Cell*. 81:53-62.

Novick, D., B. Cohen, and M. Rubinstein. 1994. The human interferon alpha/beta receptor: characterization and molecular cloning. *Cell*. 77:391-400.

Nur, E.K.M.S., J.M. Kamal, M.M. Qureshi, and H. Maruta. 1999. The CDC42-specific inhibitor derived from ACK-1 blocks v-Ha-Ras-induced transformation. *Oncogene*. 18:7787-93.

Ohtsuka, S., S. Takaki, M. Iseki, K. Miyoshi, N. Nakagata, Y. Kataoka, N. Yoshida, K. Takatsu, and A. Yoshimura. 2002. SH2-B is required for both male and female reproduction. *Mol Cell Biol*. 22:3066-77.

Ostman, A., and F.D. Bohmer. 2001. Regulation of receptor tyrosine kinase signaling by protein tyrosine phosphatases. *Trends Cell Biol*. 11:258-66.

Otsuka, T., H. Takayama, R. Sharp, G. Celli, W.J. LaRochelle, D.P. Bottaro, N. Ellmore, W. Vieira, J.W. Owens, M. Anver, and G. Merlino. 1998. c-Met autocrine activation induces development of malignant melanoma and acquisition of the metastatic phenotype. *Cancer Res*. 58:5157-67.

Paciucci, R., M.R. Vila, T. Adell, V.M. Diaz, M. Tora, T. Nakamura, and F.X. Real. 1998. Activation of the urokinase plasminogen activator/urokinase plasminogen activator receptor system and redistribution of E-cadherin are associated with hepatocyte growth factor-induced motility of pancreas tumor cells overexpressing Met. *Am J Pathol*. 153:201-12.

Park, M., M. Dean, C.S. Cooper, M. Schmidt, S.J. O'Brien, D.G. Blair, and G.F. Vande Woude. 1986. Mechanism of met oncogene activation. *Cell*. 45:895-904.

Park, W.S., S.M. Dong, S.Y. Kim, E.Y. Na, M.S. Shin, J.H. Pi, B.J. Kim, J.H. Bae, Y.K. Hong, K.S. Lee, S.H. Lee, N.J. Yoo, J.J. Jang, S. Pack, Z. Zhuang, L. Schmidt, B. Zbar, and J.Y. Lee. 1999. Somatic mutations in the kinase domain of the Met/hepatocyte growth factor receptor gene in childhood hepatocellular carcinomas. *Cancer Res*. 59:307-10.

Paulson, R.F., S. Vesely, K.A. Siminovitch, and A. Bernstein. 1996. Signalling by the W/Kit receptor tyrosine kinase is negatively regulated in vivo by the protein tyrosine phosphatase Shp1. *Nat Genet*. 13:309-15.

Perkins, L.A., I. Larsen, and N. Perrimon. 1992. corkscrew encodes a putative protein tyrosine phosphatase that functions to transduce the terminal signal from the receptor tyrosine kinase torso. *Cell*. 70:225-36.

Peschard, P., T.M. Fournier, L. Lamorte, M.A. Naujokas, H. Band, W.Y. Langdon, and M. Park. 2001. Mutation of the c-Cbl TKB domain binding site on the Met receptor tyrosine kinase converts it into a transforming protein. *Mol Cell*. 8:995-1004.

Peschard, P., N. Ishiyama, T. Lin, S. Lipkowitz, and M. Park. 2004. A conserved DpYR motif in the juxtamembrane domain of the Met receptor family forms an atypical c-Cbl/Cbl-b tyrosine kinase binding domain binding site required for suppression of oncogenic activation. *J Biol Chem*. 279:29565-71.

Petrelli, A., G.F. Gilestro, S. Lanzardo, P.M. Comoglio, N. Migone, and S. Giordano. 2002. The endophilin-CIN85-Cbl complex mediates ligand-dependent downregulation of c-Met. *Nature*. 416:187-90.

Pickart, C.M. 2001. Ubiquitin enters the new millennium. *Mol Cell*. 8:499-504.

Pirone, D.M., D.E. Carter, and P.D. Burbelo. 2001. Evolutionary expansion of CRIB-containing Cdc42 effector proteins. *Trends Genet*. 17:370-3.

Ponzetto, C., A. Bardelli, Z. Zhen, F. Maina, P. dalla Zonca, S. Giordano, A. Graziani, G. Panayotou, and P.M. Comoglio. 1994. A multifunctional docking site mediates signaling and transformation by the hepatocyte growth factor/scatter factor receptor family. *Cell*. 77:261-71.

Ponzetto, C., G. Pante, C. Prunotto, A. Ieraci, and F. Maina. 2000. Met signaling mutants as tools for developmental studies. *Int J Dev Biol*. 44:645-53.

Portereiko, M.F., J. Saam, and S.E. Mango. 2004. ZEN-4/MKLP1 is required to polarize the foregut epithelium. *Curr Biol*. 14:932-41.

Powell, E.M., W.M. Mars, and P. Levitt. 2001. Hepatocyte growth factor/scatter factor is a motogen for interneurons migrating from the ventral to dorsal telencephalon. *Neuron*. 30:79-89.

Prunotto, C., T. Crepaldi, P.E. Forni, A. Ieraci, R.G. Kelly, S. Tajbakhsh, M. Buckingham, and C. Ponzetto. 2004. Analysis of Mlc-lacZ Met mutants highlights the essential function of Met for migratory precursors of hypaxial muscles and reveals a role for Met in the development of hyoid arch-derived facial muscles. *Dev Dyn*. 231:582-91.

Qian, X., A. Riccio, Y. Zhang, and D.D. Ginty. 1998. Identification and characterization of novel substrates of Trk receptors in developing neurons. *Neuron*. 21:1017-29.

Richter, A., C. Schwager, S. Hentze, W. Ansorge, M.W. Hentze, and M. Muckenthaler. 2002. Comparison of fluorescent tag DNA labeling methods used for expression analysis by DNA microarrays. *Biotechniques*. 33:620-8, 630.

Ridley, A.J. 2001. Rho GTPases and cell migration. *J Cell Sci*. 114:2713-22.

Ridley, A.J., and A. Hall. 1992. The small GTP-binding protein rho regulates the assembly of focal adhesions and actin stress fibers in response to growth factors. *Cell*. 70:389-99.

Ridley, A.J., H.F. Paterson, C.L. Johnston, D. Diekmann, and A. Hall. 1992. The small GTP-binding protein rac regulates growth factor-induced membrane ruffling. *Cell*. 70:401-10.

Riedel, H., J. Wang, H. Hansen, and N. Yousaf. 1997. PSM, an insulin-dependent, pro-rich, PH, SH2 domain containing partner of the insulin receptor. *J Biochem (Tokyo)*. 122:1105-13.

Roche, S., G. Alonso, A. Kazlauskas, V.M. Dixit, S.A. Courtneidge, and A. Pandey. 1998. Src-like adaptor protein (Slap) is a negative regulator of mitogenesis. *Curr Biol*. 8:975-8.

Rong, S., S. Segal, M. Anver, J.H. Resau, and G.F. Vande Woude. 1994. Invasiveness and metastasis of NIH 3T3 cells induced by Met-hepatocyte growth factor/scatter factor autocrine stimulation. *Proc Natl Acad Sci U S A*. 91:4731-5.

Rosario, M., and W. Birchmeier. 2003. How to make tubes: signaling by the Met receptor tyrosine kinase. *Trends Cell Biol*. 13:328-35.

Rowinsky, E.K. 2004. The erbB family: targets for therapeutic development against cancer and therapeutic strategies using monoclonal antibodies and tyrosine kinase inhibitors. *Annu Rev Med*. 55:433-57.

Royal, I., N. Lamarche-Vane, L. Lamorte, K. Kaibuchi, and M. Park. 2000. Activation of cdc42, rac, PAK, and rho-kinase in response to hepatocyte growth factor differentially regulates epithelial cell colony spreading and dissociation. *Mol Biol Cell*. 11:1709-25.

Saxena, M., and T. Mustelin. 2000. Extracellular signals and scores of phosphatases: all roads lead to MAP kinase. *Semin Immunol*. 12:387-96.

Scaal, M., A. Bonafede, V. Dathe, M. Sachs, G. Cann, B. Christ, and B. Brand-Saberi. 1999. SF/HGF is a mediator between limb patterning and muscle development. *Development*. 126:4885-93.

Schmidt, C., F. Bladt, S. Goedecke, V. Brinkmann, W. Zschiesche, M. Sharpe, E. Gherardi, and C. Birchmeier. 1995. Scatter factor/hepatocyte growth factor is essential for liver development. *Nature*. 373:699-702.

Schumacher, S., T. Gryzik, S. Tannebaum, and H.A. Muller. 2004. The RhoGEF Pebble is required for cell shape changes during cell migration triggered by the Drosophila FGF receptor Heartless. *Development*. 131:2631-40.

Schwall, R.H., L.Y. Chang, P.J. Godowski, D.W. Kahn, K.J. Hillan, K.D. Bauer, and T.F. Zioncheck. 1996. Heparin induces dimerization and confers proliferative activity onto the hepatocyte growth factor antagonists NK1 and NK2. *J Cell Biol*. 133:709-18.

Schweitzer, R., R. Howes, R. Smith, B.Z. Shilo, and M. Freeman. 1995. Inhibition of Drosophila EGF receptor activation by the secreted protein Argos. *Nature*. 376:699-702.

Sells, M.A., U.G. Knaus, S. Bagrodia, D.M. Ambrose, G.M. Bokoch, and J. Chernoff. 1997. Human p21-activated kinase (Pak1) regulates actin organization in mammalian cells. *Curr Biol*. 7:202-10.

Sepp, K.J., and V.J. Auld. 2003. RhoA and Rac1 GTPases mediate the dynamic rearrangement of actin in peripheral glia. *Development*. 130:1825-35.

Simon, M.A. 2000. Receptor tyrosine kinases: specific outcomes from general signals. *Cell*. 103:13-5.

Smallhorn, M., M.J. Murray, and R. Saint. 2004. The epithelial-mesenchymal transition of the Drosophila mesoderm requires the Rho GTP exchange factor Pebble. *Development*. 131:2641-51.

Smolen, P., D.A. Baxter, and J.H. Byrne. 2000. Mathematical modeling of gene networks. *Neuron*. 26:567-80.

Snyder, M.A., and J.M. Bishop. 1984. A mutation at the major phosphotyrosine in pp60v-src alters oncogenic potential. *Virology*. 136:375-86.

Soubeyran, P., K. Kowanetz, I. Szymkiewicz, W.Y. Langdon, and I. Dikic. 2002. Cbl-CIN85-endophilin complex mediates ligand-induced downregulation of EGF receptors. *Nature*. 416:183-7.

Starr, R., T.A. Willson, E.M. Viney, L.J. Murray, J.R. Rayner, B.J. Jenkins, T.J. Gonda, W.S. Alexander, D. Metcalf, N.A. Nicola, and D.J. Hilton. 1997. A family of cytokine-inducible inhibitors of signalling. *Nature*. 387:917-21.

Stoker, M., E. Gherardi, M. Perryman, and J. Gray. 1987. Scatter factor is a fibroblast-derived modulator of epithelial cell mobility. *Nature*. 327:239-42.

Suzuki, A., J.L. de la Pompa, V. Stambolic, A.J. Elia, T. Sasaki, I. del Barco Barrantes, A. Ho, A. Wakeham, A. Itie, W. Khoo, M. Fukumoto, and T.W. Mak. 1998. High cancer susceptibility and embryonic lethality associated with mutation of the PTEN tumor suppressor gene in mice. *Curr Biol*. 8:1169-78.

Takaki, S., Y. Tezuka, K. Sauer, C. Kubo, S.M. Kwon, E. Armstead, K. Nakao, M. Katsuki, R.M. Perlmutter, and K. Takatsu. 2003. Impaired lymphopoiesis and altered B cell subpopulations in mice overexpressing Lnk adaptor protein. *J Immunol*. 170:703-10.

Takayama, H., W.J. La Rochelle, M. Anver, D.E. Bockman, and G. Merlino. 1996. Scatter factor/hepatocyte growth factor as a regulator of skeletal muscle and neural crest development. *Proc Natl Acad Sci U S A*. 93:5866-71.

Takayama, H., W.J. LaRochelle, S.G. Sabnis, T. Otsuka, and G. Merlino. 1997a. Renal tubular hyperplasia, polycystic disease, and glomerulosclerosis in transgenic mice overexpressing hepatocyte growth factor/scatter factor. *Lab Invest*. 77:131-8.

Takayama, H., W.J. LaRochelle, R. Sharp, T. Otsuka, P. Kriebel, M. Anver, S.A. Aaronson, and G. Merlino. 1997b. Diverse tumorigenesis associated with aberrant development in mice overexpressing hepatocyte growth factor/scatter factor. *Proc Natl Acad Sci U S A*. 94:701-6.

Tan, P.B., and S.K. Kim. 1999. Signaling specificity: the RTK/RAS/MAP kinase pathway in metazoans. *Trends Genet*. 15:145-9.

Tanaka, T.S., S.A. Jaradat, M.K. Lim, G.J. Kargul, X. Wang, M.J. Grahovac, S. Pantano, Y. Sano, Y. Piao, R. Nagaraja, H. Doi, W.H. Wood, 3rd, K.G. Becker, and M.S. Ko. 2000. Genome-wide expression profiling of mid-gestation placenta and embryo using a 15,000 mouse developmental cDNA microarray. *Proc Natl Acad Sci U S A*. 97:9127-32.

Tatsumi, R., J.E. Anderson, C.J. Nevoret, O. Halevy, and R.E. Allen. 1998. HGF/SF is present in normal adult skeletal muscle and is capable of activating satellite cells. *Dev Biol*. 194:114-28.

Technology, C.S. 2002. Catalog & technical reference.

Thien, C.B., and W.Y. Langdon. 2001. Cbl: many adaptations to regulate protein tyrosine kinases. *Nat Rev Mol Cell Biol*. 2:294-307.

Thompson, J., X. Dolcet, M. Hilton, M. Tolcos, and A.M. Davies. 2004. HGF promotes survival and growth of maturing sympathetic neurons by PI-3 kinase- and MAP kinase-dependent mechanisms. *Mol Cell Neurosci*. 27:441-52.

Tonks, N.K. 1996. Protein tyrosine phosphatases and the control of cellular signaling responses. *Adv Pharmacol*. 36:91-119.

Tonks, N.K., and B.G. Neel. 1996. From form to function: signaling by protein tyrosine phosphatases. *Cell*. 87:365-8.

Toyonaga, T., O. Hino, S. Sugai, S. Wakasugi, K. Abe, M. Shichiri, and K. Yamamura. 1994. Chronic active hepatitis in transgenic mice expressing interferon-gamma in the liver. *Proc Natl Acad Sci U S A*. 91:614-8.

Trusolino, L., and P.M. Comoglio. 2002. Scatter-factor and semaphorin receptors: cell signalling for invasive growth. *Nat Rev Cancer*. 2:289-300.

Uehara, Y., O. Minowa, C. Mori, K. Shiota, J. Kuno, T. Noda, and N. Kitamura. 1995. Placental defect and embryonic lethality in mice lacking hepatocyte growth factor/scatter factor. *Nature*. 373:702-5.

Ullrich, A., and J. Schlessinger. 1990. Signal transduction by receptors with tyrosine kinase activity. *Cell*. 61:203-12.

Vande Woude G.F., J.M., Cortner J, Alvord G., Tsarfaty I., Resau J. 1997. Met/HGF: tumorigenesis, invasion and metastasis. *In* Plasminogen-related growth factors. Vol. 212. G.J. Bock GR., editor. West Sussex: John Wiley & Sons Ltd. 119-132.

Vastrik, I., B.J. Eickholt, F.S. Walsh, A. Ridley, and P. Doherty. 1999. Sema3A-induced growth-cone collapse is mediated by Rac1 amino acids 17-32. *Curr Biol*. 9:991-8.

Wakioka, T., A. Sasaki, K. Mitsui, M. Yokouchi, A. Inoue, S. Komiya, and A. Yoshimura. 1999. APS, an adaptor protein containing Pleckstrin homology (PH) and Src homology-2 (SH2) domains inhibits the JAK-STAT pathway in collaboration with c-Cbl. *Leukemia*. 13:760-7.

Wang, R., L.D. Ferrell, S. Faouzi, J.J. Maher, and J.M. Bishop. 2001. Activation of the Met receptor by cell attachment induces and sustains hepatocellular carcinomas in transgenic mice. *J Cell Biol*. 153:1023-34.

Waterman, H., M. Katz, C. Rubin, K. Shtiegman, S. Lavi, A. Elson, T. Jovin, and Y. Yarden. 2002. A mutant EGF-receptor defective in ubiquitylation and endocytosis unveils a role for Grb2 in negative signaling. *Embo J*. 21:303-13.

Weissman, A.M. 2001. Themes and variations on ubiquitylation. *Nat Rev Mol Cell Biol*. 2:169-78.

Wells, A., and L. Lillien. 2004. Attraction or repulsion: a matter of individual taste? *Sci STKE*. 5.

Wick, M., C. Burger, M. Funk, and R. Muller. 1995. Identification of a novel mitogen-inducible gene (mig-6): regulation during G1 progression and differentiation. *Exp Cell Res*. 219:527-35.

Worby, C., and B. Margolis. 2000. Positive versus negative signaling of LET-23: regulation through the adaptor protein, SEM-5. *Sci STKE*. 2000:PE2.

Xu, D., A. Makkinje, and J.M. Kyriakis. 2004. Gene 33 is an endogenous inhibitor of EGF receptor signaling and mediates dexamethasone-induced suppression of EGF function. *J Biol Chem*. 19:19.

Xu, D., A. Makkinje, and J.M. Kyriakis. 2005. Gene 33 Is an Endogenous Inhibitor of Epidermal Growth Factor (EGF) Receptor Signaling and Mediates Dexamethasone-induced Suppression of EGF Function. *J Biol Chem*. 280:2924-33.

Yang, X.M., J.G. Toma, S.X. Bamji, D.J. Belliveau, J. Kohn, M. Park, and F.D. Miller. 1998. Autocrine hepatocyte growth factor provides a local mechanism for promoting axonal growth. *J Neurosci*. 18:8369-81.

Yi, T., and J.N. Ihle. 1993. Association of hematopoietic cell phosphatase with c-Kit after stimulation with c-Kit ligand. *Mol Cell Biol*. 13:3350-8.

Yoon, C.H., J. Lee, G.D. Jongeward, and P.W. Sternberg. 1995. Similarity of sli-1, a regulator of vulval development in C. elegans, to the mammalian proto-oncogene c-cbl. *Science*. 269:1102-5.

Yu, T.W., and C.I. Bargmann. 2001. Dynamic regulation of axon guidance. *Nat Neurosci*. 4 Suppl:1169-76.

Zhang, Y.W., and G.F. Vande Woude. 2003. HGF/SF-met signaling in the control of branching morphogenesis and invasion. *J Cell Biochem*. 88:408-17.

# Guido Pantè*

*Curriculum Vitae*

July 2005

*Max-Planck Institute of Neurobiology
Department of Molecular Neurobiology
Am Klopferspitz 18a
82152 Munich-Martinsried
Germany

Phone: +49-89-8578 3187
Mobile: +49-160-98628464
Fax: +49-89-8578 3152
email: pante@neuro.mpg.de
www.neuro.mpg.de

## Personal Data

**First name:** Guido

**Last name:** Pantè

**Date and place of birth:** December 13, 1972, Torino, Italy

**Marital status:** unmarried

**Nationality:** Italian

**Other languages:** written and spoken English: excellent.

Written and spoken French: excellent. French primary school at the 'Centre culturel Franco-Italien', Torino, Italy.

German: basic knowledge

**Scientific interests:** Tyrosine kinases-mediated biological functions during mammalian development and cancer progression. Cell cycle and differentiation.

**Computer software:** Excellent knowledge of Adobe Photoshop and Illustrator, Microsoft Word, Excel, PowerPoint and Outlook.

**Present occupation and address:** Post doctorate fellow at the Max-Planck institute of Neurobiology (Department of Molecular Neurobiology, Am klopferspitz 18a, 82152 Martinsried (Munich), Germany.

# Academic studies and research work

**From April 2001 to July 2005:**

Ph.D. studies at the Max-Planck Institute for Molecular Neurobiology, Department of Molecular Neurobiology, Director Prof. Dr. Rüdiger Klein.

**Title of the Ph.D. thesis:** "Mitogen-inducible-gene-6 is an endogenous inhibitor of HGF/Met-induced cell migration and neurite growth**".**

**Grade:** *summa cum laude (21/7/2005)*.

**From November 2000 to April 2001:**

Visitor Scientist at the EMBL-European Molecular Biology Laboratory, Heidelberg, Germany. Dr. Rüdiger Klein laboratory.

**From March 1999 to October 2000:**

Telethon pre-doctoral fellowship. Research work in Carola Ponzetto's laboratory, Department of Biomedical Sciences and Oncology, University of Torino, Italy.

**March 1999:**

Degree in Biological Sciences, University of Torino, Italy.

Grade: 101/110

**From 1996 to 1998**

Experimental work for the thesis leading to the degree in Biological sciences: 'Analysis of myoblasts migration and proliferation in Met receptor signaling mutant mice', Department of Biomedical Sciences and Oncology, University of Torino, Italy. Supervisor Prof. Dr. Carola Ponzetto.

**From February to April 1998**

Work stage in Dr. Rüdiger Klein laboratory, EMBL-European Molecular Biology Laboratory, Heidelberg, Germany. Supervisor Dr. Flavio Maina.

# Publications and abstracts

*MITOGEN-INDUCIBLE-GENE-6 IS A NEGATIVE REGULATOR OF EPIDERMAL GROWTH FACTOR RECEPTOR-MEDIATED SKIN MORPHOGENESIS AND TUMOR FORMATION*

Ingvar Ferby, Oliver Kudlacek, **Guido Panté**, Axel Ullrich, Reinhard Fässler and Rüdiger Klein

Submitted to NATURE MEDICINE

*EXPRESSION OF A COILED-COIL PROTEIN 1, A NOVEL GENE DOWNSTREAM OF FGF2, IN THE DEVELOPING BRAIN*

Francesca Pellicano, Suzanne L. Inglis-Broadgate, **Guido Panté,** Wilhelm Ansorge, Tomoko Iwata .

In press in "Gene expression patterns"

*MITOGEN-INDUCIBLE-GENE-6 NEGATIVELY REGULATES HGF/MET-INDUCED CELL MIGRATION AND NEURITE BRANCHING*

**Guido Pantè**, Jane Thompson, Fabienne Lamballe, Tomoko Iwata, Ingvar Ferby, Francis A. Barr, Alun M. Davies, Flavio Maina, Rüdiger Klein.

In press in "Journal of Cell Biology"

*COUPLING MET TO SPECIFIC PATHWAYS RESULTS IN DISTINCT DEVELOPMENTAL OUTCOMES*

Flavio Maina, Guido Pantè, Francoise Helmbacher, Rosa Andrei, Annida Renvaktar, Alun M. Davies, Carola Ponzetto and Rüdiger Klein.

Molecular Cell 2001, 7, 1293-1306.

*MET SIGNALING MUTANTS AS A TOOLS FOR DEVELOPMENTAL STUDIES*

Carola Ponzetto, Guido Pantè, Chiara Prunotto, Alessandro Ieraci and Flavio Maina.

International Journal of Developmental Biology, 2000, 44, 645-653.

*TRANSCRIPTIONAL PROFILING OF HEPATOCYTE GROWTH FACTOR-STIMULATED CELLS*

Pantè G., Iwata T., Dolce L., Wabek E., Wagner M., Richter A., Ansorge W., and Klein R.
EMBL/Salk/EMBO conference on Oncogenes and Growth Control, Signaling and Cancer, Heidelberg April 20-23, 2002.

*TRANSGENIC MICE WITH INDUCIBLE TARGETED EXPRESSION OF SCATTER FACTOR IN MUSCLES*

Ponzetto C., Pantè G., and Prunotto C.
Telethon Congress, 15 November 1999.

*MUSCOLI NUOVI DI ZECCA GRAZIE ALLE BIOTECNOLOGIE*

Scienze (Italian translation of 'Science') 1999, 371, 82.

*HGF/MET: POSSIBLE INVOLVEMENT IN WAARDENBURG SYNDROME*

Carola Ponzetto, Antonio Schindler, Alessandro Ieraci, Guido Pantè, and Flavio Maina.
Keystone symposia on Molecular and Cellular Biology, Specificity in Signal Transduction, Lake Tahoe, Nevada 1-7 March 1998.

# References

Prof. Dr. Rüdiger Klein, director.
Department of Molecular Neurobiology, Max-Planck Institute of neurobiology. Am Klopferspitz 18a 82152 Munich-Martinsried, Germany.
Tel: +49-89-8578 3150
email: rklein@neuro.mpg.de

Prof. Dr. Carola Ponzetto
Group leader at the department of Anatomy, Pharmacology and Forensic Medicine, University of Torino, Corso Massimo d'Azeglio 52, 10126 Torino, Italy.
Tel: +39-0116707799
email: carola.ponzetto@unito.it

Dr. Flavio Maina
Group leader at the INSERM U382, Developmental Biology Institute of Marseille, Campus de Luminy, Case 907, 13288 Marseille Cedex 09, France.
Tel: +33-4-91269778
email: maina@ibdm.univ-mrs.fr